Aus dem Fachbereich Biophysik
Theoretische Medizin und Biowissenschaften
der Medizinischen Fakultät
der Universität des Saarlandes, Homburg/Saar

Impact of high glucose on functions of cytotoxic T lymphocytes

Dissertation zur Erlangung des Grades eines Doktors der Naturwissenschaften

der Medizinischen Fakultät

der UNIVERSITÄT DES SAARLANDES

2022

vorgelegt von: Wenjuan Yang

geb. am: 10.11.1989 in Shandong, China

Tag des Promotionskolloquiums: 06.07.2023

Dekan: Prof. Dr. M. D. Menger

Vorsitzender: Prof. M Sester

Berichterstatter: Prof. M. Hoth

Prof. L. Thurner

Contents

1. Abstract

Cytotoxic T lymphocytes (CTLs) are major players to eliminate aberrant cells such as tumor cells and infected cells. To kill their target cells, CTLs employ in most cases two mechanisms: cytotoxic protein containing lytic granules (LG) and Fas/FasL pathway. High levels of blood glucose, also termed hyperglycemia, is a typical symptom of diabetes mellitus. Although it is known that CTLs are involved in development of diabetes, to date, however, the functional impact of high glucose on CTLs and the corresponding mechanisms remain largely elusive. To address this question, primary human $CD8^+$ T cells were used, which were stimulated by CD3/CD28 beads and cultured in medium containing either high glucose (HG, 25 mM) or normal glucose (NG, 5.6 mM). I found that expression of cytotoxic proteins including perforin, granzyme A, granzyme B and FasL and LGs release remained unchanged in HG-cultured CTLs. Interestingly, TNF-related apoptosis-inducing ligand (TRAIL) was upregulated in CTLs by HG. With flow cytometry and inhibitors, I have identified that ROS and the PI3K-Akt-NFκB axis play an important role in the HG-induced TRAIL expression. In addition, TRAIL expressing CTLs can induce apoptosis of insulin-producing beta cells, which is significantly higher in the case of HG-CTLs compared to their counterparts cultured in NG. Further investigation shows that both metformin and vitamin D can reduce HG-enhanced expression of TRAIL in CTLs and coherently protect beta cells from TRAIL-mediated apoptosis by HG-cultured CTLs. This effect of metformin and vitamin D on down-regulation of TRAIL is also confirmed in CTLs isolated from patients with diabetes. Thus, this work reveals an antigen-independent

pathway regulated by HG to modulate CTL killing efficiency, suggesting a novel mechanism of CTL involvement in progression of diabetes and proposing a combination of metformin and vitamin D as a potentially promising strategy to protect beta cells of diabetic patients.

1. Zusammenfassung

Zytotoxische T-Lymphozyten (CTLs) spielen eine wichtige Rolle bei der Eliminierung abweichender Zellen wie Tumorzellen und infizierter Zellen. Um ihre Zielzellen abzutöten, wenden CTLs in den meisten Fällen zwei Mechanismen an: zytotoxisches Protein, das lytische Granula (LG) enthält, und den Fas/FasL-Weg. Hohe Blutzuckerwerte, auch Hyperglykämie genannt, sind ein typisches Symptom von Diabetes mellitus. Obwohl bekannt ist, dass CTLs an der Entwicklung von Diabetes beteiligt sind, bleiben die funktionellen Auswirkungen hoher Glukose auf CTLs und die entsprechenden Mechanismen bis heute weitgehend unklar. Um diese Frage zu beantworten, wurden primäre menschliche $CD8^+$ T-Zellen verwendet, die durch CD3/CD28-Kügelchen stimuliert und in Medium kultiviert wurden, das entweder hohe Glukose (HG, 25 mM) oder normale Glukose (NG, 5,6 mM) enthielt. Ich fand heraus, dass die Expression von zytotoxischen Proteinen, einschließlich Perforin, Granzym A, Granzym B und FasL und LGs-Freisetzung, in HG-kultivierten CTLs unverändert blieb. Interessanterweise wurde TNF-verwandter Apoptose-induzierender Ligand (TRAIL) in CTLs durch HG hochreguliert. Mit Durchflusszytometrie und Inhibitoren habe ich identifiziert, dass ROS und die PI3K-Akt-NFκB-Achse eine wichtige Rolle bei der HG-induzierten TRAIL-Expression spielen. Darüber hinaus können TRAIL-exprimierende CTLs die Apoptose insulinproduzierender Betazellen induzieren, die im Fall von HG-CTLs signifikant höher ist als bei ihren in NG kultivierten Gegenstücken. Weitere Untersuchungen zeigen, dass sowohl Metformin als auch Vitamin D die HG-verstärkte Expression von TRAIL in CTLs reduzieren und Betazellen kohärent vor TRAIL-

vermittelter Apoptose durch HG-kultivierte CTLs schützen können. Diese Wirkung von Metformin und Vitamin D auf die Herunterregulierung von TRAIL wird auch in CTLs bestätigt, die aus Patienten mit Diabetes isoliert wurden. Somit enthüllt diese Arbeit einen Antigen-unabhängigen Weg, der durch HG reguliert wird, um die CTL-Abtötungseffizienz zu modulieren, was auf einen neuen Mechanismus der CTL-Beteiligung am Fortschreiten von Diabetes hindeutet und eine Kombination aus Metformin und Vitamin D als potenziell vielversprechende Strategie zum Schutz von Betazellen von Diabetikern vorschlägt Patienten.

2. Introduction

2.1 Immune System: a masterpiece of nature

The immune system is a defense network covering our whole body, acting as a sophisticated force to protect our health day and night. The main threats to our health include disease-causing pathogens and tumor cells. Pathogens vary very much in the size, composition of surface molecules, mechanisms of invasion and replication. Tumor cells are also highly heterogenous in their origin and tumorigenic mutations. Nevertheless, the immune system can recognize invaded pathogens and transformed tumor cells to eliminate them, at least in most cases. This is an amazing masterpiece of nature. Human immune system is complex and same as all vertebrates. Humans possess two immune system arms: the innate immune system and the adaptive immune system. These two systems complement each other, cooperate and undertake different tasks.

2.2 The innate immune system

The innate immune system is responsible for non-specific immunity, is an immune system that a person has along with birth and the activity of which does not require priming of the pathogens or tumor cells. It can be found in plants, fungi and multicellular organisms. As a first line of defense, it responses fast with a wide range of action [1]. The innate immune system is made up of physical barriers, chemical barriers, complement system and innate immune cells [2] [3] [4]. Physical barriers include skin and mucous membranes. The skin is the largest organ of the body, covering almost the entire outer body surface [5] [6]. Mucous membranes cover breathing and digestive tracts. Together, they form a continuous, impassable physical barrier to block

pathogen entry [7]. Chemical barriers consist of those parts of the body in which potential pathogens can come into contact with host cells. The chemical barrier is composed of different proteins that belong to antimicrobial peptide (AMP) family. Proteins in the AMP family have the ability to clear bacteria and virus. In addition to these proteins, a variety of proteases and protease inhibitors that maintain proteolytic balance play an important role in the host and/or pathogen [8]. If pathogens manage to overcome physical and chemical barriers and enter the body, for example through wounds, innate immune cells will be recruited and undertake the job to fight the pathogens.

Innate immune cells encompass granulocytes, dendritic cells, monocytes, monocyte-derived macrophages and natural killer (NK) cells [9] [10]. Granulocytes encompass neutrophils, eosinophils, basophils. Following inflammation, granulocytes are recruited to sites of tissue damage or infection, where they are activated and perform their effector functions [11]. Dendritic cells are responsible for collecting and presenting pathogen-derived antigens to activate the adaptive immune cells [12]. Monocytes are the largest type of leukocyte in blood, which can differentiated to macrophages once enter tissues [13] [14]. Macrophages phagocytose invading pathogens and secrete antimicrobial and pro-inflammatory factors. Additionally, macrophages can uptake and degrade debris, dead cells and tumor cells [15] [16]. They play an important role in the homeostasis by phagocytes and have regulatory and repair functions [17]. Like Dendritic cells (DCs), macrophages can also serve as professional antigen presenting cells. They are essential for the activation of naive $CD4^+$ T cells. These innate cells can

have an extensive communication with effector $CD4^+$ T cells via peptide-loaded MHC-II surface expression or transfer, co-stimulatory and co-inhibitory molecules expression, and polarizing cytokines secretion [18] [19].

NK cells are specialized type of effector lymphocytes in the innate immune system, which possess intrinsic cytotoxicity and can also secret cytokines [20]. To kill their target cells, either tumor cells or infected cells, NK cells release cytotoxic proteins including perforin and granzymes or secret cytokines like granulocyte macrophage–colony-stimulating factor (GM-CSF), tumor necrosis factor-alpha (TNF-α) and interferon-alpha (IFN-α), as well as chemokines such as CCL1, CCL3, CCL4, CCL5, and CXCL8 (ref) to induce destruction of target cells [21] [22] [23].

There are also agents, mainly proteins, in plasma or tissue fluid, which can interfere with replication of pathogens or help to break down the invaders. One specialized proteins group termed complements which work with the innate immune system to target and clear the invading pathogens [24]. The other group is interferon (IFN). IFN-stimulated genes (ISGs) constitute the pillar in the innate immune system and are vital for the limiting replication and spread of intracellular and intercellular virus [25]. In addition, reactive oxygen species (ROS), mainly secreted by immune cells at the inflammation sites, also have antimicrobial effect, which can directly induce destruction of the invading microbes [26].

2.3 The adaptive immune system

The other branch of immune system is the adaptive immune system, also termed as acquired immune system. Contrary to the innate immune system, the adaptive system

identifies unique antigens derived from pathogens or tumor cells and produces antigen-specific immune responses [27]. Different from the almost immediate innate responses upon pathogen invasion, it takes 7-9 days for the adaptive immune responses to peak for the first exposure to the pathogen, as the adaptive immune cells need be primed, activated, and differentiated into effector cells, which proliferate to reach sufficient number to fight pathogens. When the pathogens are wiped out successfully, the majority of the effector cells undergo apoptosis, whereas some cells stay alive and differentiate into memory cells, serving as fast responder to fight the next invasion of the same pathogen [28] [29] [30] [31] [32] [33]. The adaptive immune cells include B cells and T cells [34]. B cells mediate humoral immune response and T cells mediate cellular immune response [35] [36]. B cells are responsible for producing antibodies in response to antigen recognition and also serve as professional antigen presenting cells to present antigens to T cells [37]. T cells, also known as T lymphocytes, are generated from in the bone marrow and mature in the thymus [38]. In the thymus, T cells go through a selection process where most developing T cells (called thymocytes) that recognize self-antigens are removed from the pool [39]. Each T cell clone possesses T cell receptors (TCRs) with specificity to a particular antigen [40]. The T cells, which survive during the thymic selection, mature to naive functional T cells. Afterwards, they leave the thymus for lymph nodes, ready to meet their cognate antigens [41] In lymph nodes, naive T cells can engage with antigen-presenting cells (APCs), which express major histocompatibility complexes (MHC) molecules to present antigen [42]. $CD4^+$ and $CD8^+$ T cells recognize antigens presented by MHC class II and class I molecules,

respectively. Upon engagement with antigen: MHC complexes, naive T cells are activated and differentiated into effector cells to exert effector function [43] [44].

2.3.1 Cytotoxic T lymphocytes

Cytotoxic T lymphocytes (CTLs) are effector $CD8^+$ T cells, which play a key role in killing virally infected cells and tumorous cells [45]. To search for their target cells, CTLs need to migrate through tissues and scan the cells they encounter. Once they encounter their target cells, cytotoxic T cells recognize the antigen: MHC I by their TCRs and an intimate contact is formed at the CTL-target contact interface, which is termed immunological synapse (IS) [46]. Then the killing machinery is oriented towards the IS to initiate destruction of target cells.

2.3.1.1 Migration and IS formation

The navigation and migration of CTLs is through peripheral tissues, which are complicated biological microenvironments. And extracellular matrix (ECM) is a key component of it [47]. For ECM, it is a three-dimensional network and collagen, as the main components, play important roles in the regulation of almost all cellular functions [48] [49]. In many cancers, the ECM becomes dense, stiff, and linearized near the tumors, creating a physical environment that facilitates the metastasis, invasion, and prognosis of cancer cells [47] [50]. In addition, the high-density matrix also induced the reduction of T cell proliferation, impairment of CTLs infiltrating into the target cell, as well as the diminished killing efficiency [51] [52]. Dr. Renping Zhao found that migration of CTLs was substantially impaired in dense collagen matrix, accompanied with the reduced killing efficiency of CTLs against tumor cells [47].

The cytoskeleton, which is consisted of actin filaments and microtubules, plays a critical role in the regulation of CTLs migration [53] [54]. During migration, the polymerization of actin drives T cells to produce protrusions at the leading edge [55]. The contraction of F-actin regulated by myosin yields force to revoke the uropod and then move T cells forwards [56]. In adhesion-dependent migration, the forces have to be transferred from the cell membrane to the matrix. This step is mainly mediated by adhesion molecules (integrins) [57].

Once CTLs recognize the matched antigens presented on the surface of target cells via an engagement of T cell receptors (TCRs), the activated TCRs will trigger a series of downstream signaling pathways to induce the tight contacts between T cells and target cells termed the immunological synapse (IS) [58]. Following T cell activation, the concentration of intracellular Ca^{2+} is markedly increased via Ca^{2+} influx. Ca^{2+} serves as an second messenger in T cells and is required for regulating the activation, proliferation, and effector functions [59]. In our lab, Dr. Xiao Zhou also found that the killing of CTLs against target cell is in a bell-shaped Ca^{2+} dependence, characterized by clearing up cancer cells at fairly low $[Ca^{2+}]_o$ (23–625 μM) and $[Ca^{2+}]_i$ (122–334 nM) [60].

2.3.1.2 Killing mechanisms

CTLs usually exert major killing mechanisms: lytic granules and Fas/FasL pathway. Lytic granules, also called cytotoxic granules, which contains cytotoxic proteins. Lytic granules are specialized lysosomes with an acidic pH value of around 5.5 [61] [62]. Different from classic lysosomes that are responsible for protein degradation, lytic

granules serve as one of the most efficient ammunition in CTLs to kill target cells [63]. Upon TCR activation, lytic granules are initially enlisted around the microtubule-organizing center (MTOC). During dynein-dependent transport, the granules migrate along microtubules toward the MTOC in the minus-end orientation [64]. Lysosome-associated membrane protein (LAMP)1/CD107a, as a marker of NK cell degranulation, influences the mobility of lytic granules and leads to reduced levels of perforin in the granules [65]. The cytotoxic content of lytic granules released into the cleft contains mainly pore-forming protein perforin and serine proteases granzymes [66]. Perforin forms pores on the plasma membrane of target cells in a calcium dependent manner. Studies showed that calcium is required for perforin to perform lytic and granzyme delivery function [67] [68].

Granzymes belong to serine protease family and expressed widely on CTLs and NKs. There exist at least 12 granzymes. Among of these, five granzymes have been found in humans: Granzyme A, B, H, K and M [69] [70] [71]. By far, granzymes A and B are the most exclusively studied members in the granzyme family. Granzyme A, the richest expressed granzyme in CTLs, can initiate perforin-dependent events leading to cell apoptosis. It can also induce apoptosis with granzyme B in an independent but coordinated manner [72] [73] [74]. Granzyme B is the most exclusively studied member in the granzyme family. It is a serine protease and traditionally well-known for its pro-apoptotic function in a perforin-dependent manner. This function underlies the ability of killing virus-infected target cells or tumor by cytotoxic T lymphocytes (CTLs) and natural killer (NK) cells [75]. Granzyme B entry into target cells is highly dependent

on perforin, perforin specifically prompts the cytoplasmic granzyme B to redistribute into the nuclei of dying cells, leading to DNA degradation and cell death [76] [77].

Fas/FasL pathway is another key killing machinery tightly regulated by TCR activation. FasL, belonging to tumor necrosis factor (TNF) superfamily, is normally stored in intracellular vesicles, which in some cases colocalize with perforin and in some cases not. Upon TCR activation, FasL-containing vesicles are transported towards the IS [78] and after fusion, FasL is integrated into plasma membrane of CTLs. Fas, also known as CD95, is found on target cell surface. It contains a death domain in the cytoplasmic region that is indispensable for inducing apoptosis [79]. Engagement of FasL with Fas induces recruitment of the Fas-associated death domain (FADD) and subsequent interaction with procaspase-8, ultimately leading to target cell apoptosis [80]. Interestingly, there is another rather unusual killing machinery employed by CTLs, which is independent of TCR activation: TRAIL (TNF related apoptosis inducing ligand). TRAIL could induce cell death by binding with its receptors and trigger cancer cell apoptosis but not normal cells [81] [82].

2.3.2 TRAIL

TRAIL, similar as FasL, also belongs to a member of TNF superfamily. TRAIL expression can be found on the surface of NK cells, T cells, macrophages and dendritic cells. Its most typical function is to induce the apoptosis including tumor, infected or transformed cells. There exist two forms of TRAIL: membrane TRAIL (mTRAIL) and soluble TRAIL (sTRAIL). Soluble secreted form of TRAIL can be obtained from membrane-bound TRAIL by cell surface cleavage. Both forms can be found in different

immune cells and regulated by different stimuli. Phytohemagglutinin (PHA) plus interleukin (IL-2) and lipopolysaccharide (LPS) could induce secretion of soluble TRAIL in T cells, B cells and monocytes. whereas IFN-β leads to both secretion of soluble TRAIL and enhancement of the surface-bound TRAIL in monocytes, but not in T cells [83]. TRAIL induces apoptosis by binding its death receptors. To bind with their receptors, TRAIL normally undergo oligomerization to form trimeric complexes [84].There are five different receptors: TRAIL-R1, -R2, -R3, -R4, and osteoprotogerin. TRAIL-R1 (DR4) and TRAIL-R2 (DR5) are death receptors, both of which contain complete cytoplasmic death domain at their cytoplasmic tail. Upon engagement with TRAIL, downstream signaling cascades will be activated including receptor oligomerization, DISC (death inducing signaling complex) formation, caspases activation and finally DNA fragmentation [85]. TRAIL-R3 (DR1) and TRAIL-R4 (DR2) are decoy receptors, as they lack truncated cytoplasmic domain, and thus cannot activate apoptotic signaling [86]. However, these decoy receptors can compete with death receptors to tune efficiency of TRAIL-mediated apoptosis. Osteoprotogerin is a soluble protein that may also act as a decoy/inhibitor by binding to TRAIL extracellularly [87]. Based on the fact that tumor cells are more sensitive to apoptosis induced by TRAIL, it is considered as a promising target to treat cancer [88]. Administration of TRAIL receptor (TRAIL-R) agonists or recombinant TRAIL are recognized as two main therapeutic approaches. And more interestingly, TRAIL-based therapeutic strategy shows toxicity to normal tissues when delivered systemically to animals and humans [89] [90].

Interestingly, TRAIL and its receptors have also been implicated in the development of diabetes and diabetes-associated complications [91]. It is reported that for diabetic nephropathy (DN), a major complication of diabetes, TRAIL was highly expressed in DN kidneys and was correlated with disease in the clinical and histologic severity. *In vitro*, both glucose and proinflammatory cytokines regulated TRAIL expression in the human proximal tubular cell line HK-2. TRAIL induced the apoptosis of tubular cell in a dose dependent manner. This effect was more pronounced in the presence of high levels of glucose and pro-inflammatory cytokines. It is proposed that TRAIL-induced cell death could play an important role in the progression of human DN [92]. Here there is a similar study showing that expression of TRAIL in glomerular and tubulointerstitial is increased in the model of DN. Additionally, a high-glucose microenvironment sensitizes renal tubular cells to TRAIL-induced apoptosis [93]. In addition, study also demonstrated that people diagnosed with T2DM and cardiovascular disease (CVD) had a higher ratio of OPG/TRAIL, compared with controls or people newly diagnosis with type 2 diabetes mellitus (Type 2 DM). It suggested that OPG/TRAIL ratio may predict cardiovascular disease in patients with Type 2 DM [94].

2.4 Glucose metabolism in T cells

Glucose plays a central role in energy consumption. The glucose cannot diffuse into the cell membrane, as it has a high molecular weight. Thus it needs glucose transporters to help its diffusion into the cell membrane [95]. Once the glucose enters into the cell via glucose transporters, the glucose can be utilized for energy releasing by oxidative phosphorylation or aerobic glycolysis [96]. The adaptive immune system's ability to

destroy tumors and pathogenic microorganisms is based on a complex set of signals that drive the activation and differentiation of T cell subsets. It has now been established that immune cell function and differentiation can be regulated by cellular metabolism [97]. It is evident that in the subsets of $CD4^+$ T cells, effector T cell and Th17 depend on aerobic glycolysis [98]. The research from Yin and colleagues showed that the oxidative phosphorylation is highly induced during the activation of $CD4^+$ T cells [99]. Emerging evidence also demonstrate that the differentiation and proliferation and cytokine production in T cells is strongly rely on their cellular metabolism [100] [101] [102] [103]. And glucose metabolism and access to glucose properly are essential for maintaining the effector function, particularly for the killing function in CTLs [104]. There is also study showing that the calcium influx elicited is reduced upon binding to target cell and CTL killing function is enhanced in an excessive glucose condition [105]. The reactive oxygen species (ROS) are generally referred to the free radicals and reactive molecules deriving from molecular oxygen [106]. ROS were deemed to arise almost entirely from mitochondrial metabolism [107]. However, more and more evidence demonstrate that a cellular enzyme named NADPH oxidase also generates lots of ROS in human [108]. It has been previously demonstrated that ROS act as mainly signaling molecules to regulate the regular physiological functions at cellular level. For example, ROS could prompt cell proliferation, differentiation and apoptosis, thereby inducing the process of natural aging [109] [110] [111]. Overexposure to UV radiation, improper diet and stimulant using can lead to increased production of free radicals [112]. Under physiological conditions, there is a balance between the

production and scavenging of free radicals in the body [113]. Overfull generation of free radicals can contribute to oxidative stress, causing damage at molecular and cellular level. ROS in vitro give rise to chemical modifications and destructive influence to proteins (aggregation), lipids (peroxidation) and nucleotides (DNA structure changing), contributing to the progress of free radical-mediated diseases [112]. Oxidative stress has extremely harmful effects on respiratory, circulatory and nervous systems [114] [115] [116]. Here, there is a review presenting some new concepts that damage caused by glucose in diabetes is by the increased generation of oxygen free radicals. ROS regulate various biological functions via stimulating the transduction signals, some of which are related with diabetes pathogenesis and complications [117] [118]. It is now increasingly clear that ROS play essential roles in the immune system and are closely related with many different aspects of immune response. For example, they are involved in host defense, interaction and activation the immune cell and immunosuppression [119] [120]. It has been demonstrated that addition of antioxidant could inhibit the T cell proliferation, activation and IL-2 receptor expression [121].

2.5 Diabetes

Diabetes mellitus, a metabolic disease featuring with high levels of blood glucose for a prolonged period [122]. Diabetes is a serious chronic disease; it has been listed one of the top ten causes of death in adults worldwide, with a marked increase of 9.3% of the world's population. That is, 463 million people had diabetes in 2019, and this number is estimated to go up to 10.9% by 2045 [123]. The symptoms of diabetes include frequent urination, excessive hunger or thirst and weight changes [124] [125] [126].

The most common types of diabetes are Type 1 diabetes mellitus (Type 1 DM) and Type 2 diabetes mellitus (Type 2 DM). Type 1 DM has been shown to be an autoimmune disease and CTLs make a big difference to disrupt pancreatic beta cells [127]. A rich body of evidence indicate that both $CD4^+$ helper and CTLs are key effectors in the development of Type 1 DM [128] [129]. Two sequential steps are involved in the onset of diabetes in anatomically distinct tissues. First, autoreactive T cells escaping the tolerance checkpoint are activated by antigen-presenting cells (APCs) which display the β-cell antigens in lymph nodes draining the pancreas (pLN) [130] [131]. At this stage, $CD4^+$ T cells is needed to activate $CD8^+$ T cells [132] [133]. Then activated CTLs penetrate the pancreas [134]. CTLs can destroy beta cells directly in an antigen-dependent manner [135]. In addition, autogenic antibody is also involved the development of Type 1 DM, subclinical period before Type 1 DM onset is featured by the being of autoantibodies (AAbs) targeted against islet-specific autoantigens [136]. For Type 2 DM, it is characterized by insulin resistance. There was growing evidence suggesting that adaptive immune system, especially T cells also play a critical role in the pathogenesis of Type 2 DM. Obesity, as a major pivotal risk factor for Type 2 DM-induced insulin resistance. Study by Shirakawa *et al*. showed that activated $CD4^+$ T cells ($CD4^+CD44^{hi}CD62L^{lo}$) was enhanced in the adipose tissue of obese mice [137]. $CD4^+$ helper T cells also play a pivotal role in Type 2 DM-associated complications, showing that inflammatory cytokines and activated T lymphocytes were improved in kidneys in Type 2 DM [138] [139]. For CTLs, along with other factors are also associated with the initiation and progression of Type 2 DM [140].

2.6 Vitamin D and metformin

Vitamin D, also referred to as calciferol, is a nutrient in our body, which is very important for building and keeping healthy bones [141]. We can obtain vitamin D from food, sun exposure and supplements. Many studies have shown that vitamin D regulates various functions in our body including bone metabolism, fighting cancer, blood pressure, cognitive health [142] [143] [144] [145]. In addition, vitamin D also plays an important role on the regulation of innate and adaptive immune systems [146]. This importance is proved by the finding that vitamin D receptor is expressed in almost all immune cells [147]. Vitamin D directly bind the vitamin D receptor on the antigen-presenting cell (APC) to exerts its regulation on T-lymphocytes. The effect of vitamin D on the T lymphocytes is dependent on the status of activation as they acquire higher vitamin D receptor concentrations upon activation [148]. Vitamin D could also inhibit the generation of Th1 cytokines (i.e., IL-2, IFN-γ), Th9 cytokines and Th17 cytokines (i.e. IL-17, IL-21) [149] [150] [151].

Epidemiological data show that vitamin D deficiency is linked with immune system deficits, increasing risk of infection, and susceptibility to autoimmune diseases such as Type 1 DM and Hashimoto's thyroiditis [148] [152]. For Type 1 DM, the destruction of β-cell is mediated by T cells, and vitamin D can protect beta cell and its function from autoreactive T cells-mediated infiltration within the pancreatic islets [153]. For hashimoto's thyroiditis (HT), vitamin D supplements intake orally could reduce the thyroid autoantibodies titers in women with postpartum thyroiditis treated with levothyroxine [154]. In summary, vitamin D plays an important role in the immune

function and we still have to learn more about the mechanisms by which vitamin D regulate the immune system.

Metformin is a composite derivative of guanidine, which is separated from the extract of the plant called *Galega officinalis* and it has significant antidiabetic effects [155]. Except for the consolidated role in Type 2 DM, emerging evidence in human has demonstrated that some split-new regulatory properties of metformin, such as kidney- and cardio- protection, antiproliferative, anticancer and antiaging effects [156] [157] [158] [159]. Furthermore, i*n vivo* and *in vitro* studies support the new hypothesis that metformin may exhibit immunomodulatory properties [160] [160]. Metformin also modulates the cellular functions including the development and maintenance of autoimmunity. Meanwhile, metformin is also involved in the recovery of immune homeostasis and amelioration of disease severity in autoimmune animal models [161]. Nath et al. investigated the effect of metformin on the experimental autoimmune encephalomyelitis (EAE), a multiple sclerosis (MS) which is mediated by T cells in the mouse model. In this work, they found that metformin treatment slowed the progression of disease, reduced the entry of inflammatory cells into the central nervous system (CNS), and also decreased the expression of cytokines such as IL-17, IL-6 and TNF-α [162]. Similarly, in a collagen-induced arthritis (CIA), a fully developed animal model of rheumatoid arthritis (RA), metformin can suppress systemic inflammation and synovitis. And it exerts bone protection by inhibiting the degradation of cartilage layer matrix, formation of osteoclast and apoptosis of chondrocyte [163]. Taken together, these findings above suggest that metformin paly an immunomodulatory role in T cell-

mediated autoimmunity and are capable of recovering the balance of tolerogenic and pathogenic T cell populations.

2.7 Goals

As described above, high glucose is a typical symptom of diabetes. CTLs play an important role in the pancreatic beta cell destruction and initiation and progression of diabetes. However, the impact of high glucose on CTL function is poorly understood. To address this question, the goal of this thesis is to understand how the functionality of CTLs changes in environment with high glucose. To reach this goal, the following aims were defined:

1. Is cytotoxic function of CTLs regulated by high glucose?
2. If yes, which steps are affected? Key events of cytotoxicity, such as expression levels of cytotoxic proteins, degranulation, migration, cytokine production, should be analyzed.
3. Investigate the underlying molecular mechanisms.

3. Materials and Methods

3.1 Antibodies and reagents

All chemicals are from Sigma-Aldrich (highest grade) unless otherwise mentioned. The following antibodies and reagents were purchased from BioLegend: Alexa 488 anti-human CD107a (LAMP-1) Antibody (Cat#328610, RRID:AB_1227504), APC-Cy7 anti-human CD3 antibody (Cat#300318, RRID:AB_314054), BV421 anti-human CD8 antibody (Cat#344748, RRID:AB_ 2629584), Alexa 488 anti-human Granzyme A antibody (Cat#507212, RRID:AB_528909), Alexa 647 anti-human perforin antibody (Cat# 308110, RRID:AB_ 493254), PE anti-human Fas-L antibody (Cat#306407, RRID:AB_2100664), PerCP anti-human CD3 antibody (Cat#300326, RRID:AB_2616610), BV421 anti-human CD3 antibody (Cat#300434, RRID:AB_10962690), APC antihuman CD253 (TRAIL) antibody (Cat#308210, RRID:AB_2564398), APC anti-mouse CD253 (TRAIL) Antibody (Cat#109310, RRID:AB_2721457), BV421 anti-mouse CD8a Antibody (Cat#100753, RRID:AB_2562558), PE anti-mouse CD3 Antibody (Cat#100206, RRID:AB_312663), PerCP anti-human CD25 antibody (Cat#356131, RRID:AB_2563591), APC anti-human CD62L antibody (Cat#304810, RRID:AB_ 314470), APC anti-human CD262 (TRAIL-R2) (Cat#307408, RRID:AB_ 2240691) and 7-AAD viability staining solution (Cat#420404). FITC anti-human CD69 antibody (Cat#11-0699-42, RRID: AB_10853975) was purchased from eBiosciences. FITC anti-human CD44 antibody was purchased from DAKO. Purified NA/LE mouse anti-human CD253 (RRID: AB_393955), BV421 mouse anti-human CD263 (TRAIL-R3) (Cat#744764, RRID:

AB_2742464) and Alexa647 mouse anti-human GLUT1 antibody (Cat#566580, RRID: AB_2869787) were purchased from BD Biosciences. Human TRAIL R1/TNFRSF 10A PerCP-conjugated antibody (Cat#FAB347C-100) and human TRAIL R4/TNFRSF 10D PE-conjugated antibody (Cat#FAB633P) were purchased from R&D Systems. NucView Caspase-3 enzyme substrate (Cat#10402) was purchased from Biotium. Idelalisib (Cat#S2226), MK-2206 (Cat#S1078) and Rapamycin (Cat#S1039) were purchased from Selleckchem. MG-132 (Cat#474787), N-acetyl-L-cysteine (NAC) (106425), Vitamin 1,25D3 (Cat#PHR1237), DMSO (Cat#D4540), Metformin hydrochloride (Cat#M0605000), H_2O_2 (Cat#31642) and Streptozotocin (Cat#572201) were purchased from Merck. Caffeic acid phenethyl ester (CAPE) (Cat#2743) was purchased from (R&D Systems). Mitoquinone (MitoQ) (Cat#10-1363) was purchased from Biotrend. Cellular ROS Assay Kit (Cat#ab113851) was purchased from Abcam. Calcipotriol (Cat#2700) was purchased from TOCRIS. Protein transport inhibitor (Cat#554724) was purchased from BD.

3.2 cell culture

3.2.1 cell lines

For the preparation of cell lines, there are cell culture team in our lab. Cora Hoxha, Gertrud Schäefer, Kathrin Förderer and Sandra Janku are responsible for the split and culture of suspension and adherent cells. In my work, suspension cell line Raji and adherent cell line human pancreatic beta cell line 1.4E7 were used. The steps they take to process the cells are as follows: Raji cells were cultured in RPMI-1640 medium (ThermoFisher Scientific) supplemented with 10% FCS and 1% Penicillin-

Streptomycin and the cells were split on Monday (1:6), Wednesday (1:6), and Friday (1:8). Human pancreatic beta cell line 1.4E7 (Cat# EC10070102) was purchased from Merck and cultured in RPMI-1640 medium containing 2 mM glutamine, 1% Penicillin-Streptomycin plus 10% FCS and were split on Monday (1:6) and on Friday (1:5). The cell was conducted as follows: (1) Check the growth status of the cells with microscopy. (2) Remove the old medium from the flask and rinse the cells with D-PBS gently. (3) Add 2 ml of pre-warmed Trypsin-EDTA solution to cells and incubate for 2 min at room temperature (RT). (4) Check if the cells are detached and bang the side of flask with hand gently to ensure the cells detached thoroughly. (5) Add fresh medium with usually an equal volume of the Trypsin (to inactivate the activity of trypsin). (6) Add fresh medium to a new flask and add the corresponding portion of the trypsinized cells to it. Raji and 1.4E7 cells were cultured at 37 °C with 5% CO2.

3.2.2 PBMC preparation

Our technician Carmen Hässig was responsible for the isolation of PBMCs. PBMCs from healthy donors were prepared from the leukocyte-reduction system (LRS) chamber as follows: (1) LSM 1077 (Lymphocyte Separation Medium 1077) should be always placed at RT in dark. (2) Add 15-17 ml LSM 1077 medium to a leucosep tube and centrifuge at 1000 g for 30 sec. (3) Clamp the LRS chamber vertically on a stand, cut the tubing at both marked points using sterilized scissors (70% EtOH) and put the lower tubing in the prefilled leucosep tube. (4) Connect a 20 ml syringe with HBSS (hose, yellow tip, combifix adapter) with the upper tubing and flush material in the chamber into the leucosep tube. (5) Fill up the leucosep tube with HBSS up to 50 ml.

(6) Keep 1 drop of the elute in a 3 cm dish in HBSS and examine the morphology of erythrocytes under a microscope. (7) Centrifuge at 450 g for 30 min at RT (22 °C) (Note: brake:0 acc:1, Gradient centrifugation, handle with care). (8) Aspirate the upper yellowish layer, transfer the leukocyte ring into a 50 ml falcon tube (approx. 8 ml), then fill the tube with HBSS up to 50 ml (the leukocyte ring can also be transferred directly with a 5 ml pipette). (9) Centrifuge at 250 g for 10 min at RT (Note: brake:9, acc:9). (10) Discard the supernatant and add 1-3 ml of erythrocyte lysis buffer (155 mM NH_4Cl, 10 mM $KHCO_3$, 0.1 mM EDTA, pH = 7.3) to resuspend the pellet very carefully and keep at RT for 60-120 sec (depending on pellet size). (11) Add HBSS up to 50 ml to stop the erythrocyte lysis. (12) Centrifuge at 130 g for 10 min at RT (Note: brake:9, acc:9). (13) Discard the supernatant and add 20 ml of pre-chilled PBS/0.5% BSA. (13) Count the cells and keep the cells on ice for further use.

3.2.3 $CD8^+$ T cells preparation and stimulation

Our technician Carmen Hässig was also responsible for the isolation of primary human $CD8^+$ T cells with Human $CD8^+$ T Cell isolation Kits (Miltenyi Biotec) followed by the manufacturer's instruction. Primary human $CD8^+$ T cells were cultured in AIMV medium (ThermoFisher Scientific) at the density of 3×10^6 cells/ml at 37 °C with 5% CO_2 overnight. Then these cells were stimulated with human T-activator CD3/CD28 beads (Cat#11132D ThermoFisher Scientific) at a density of 1.5×10^6 cells/ml with the cell to bead ratio of 1:0.8 and cultured in DMEM medium containing either normal (5.6 mM, NG, Cat#31885-023) or high glucose (25 mM, HG, Cat#41966-029) (ThermoFisher Scientific) for 3 days unless otherwise mentioned. On day 2, to maintain

the glucose concentration, half of medium was removed and supplemented with fresh medium plus recombinant human IL-2 (100 U/ml, Miltenyi, Cat#130-097-748). Glucose levels was examined using "Contour Next Sensoren" test strips (SMS Medipool). If cells were cultured longer than three days, we added supernumerary glucose (stock concentration: 889.5 M) into the medium every two days to reimburse the consumption of glucose. All cells were cultured at 37 °C with 5% CO_2.

3.3 Regent preparation

Metformin (stock solution: 100 mM) and NAC (stock solution: 100 mM) were dissolved in ddH_2O. The other reagents were dissolved in DMSO including Vitamin D (stock solution: 50 mM), Idelalisib (stock solution: 50 mM), MK-2206 (stock solution: 10 mM), Rapamycin (stock solution: 10 mM), CAPE (stock solution: 50 mM), MitoQ (stock solution: 10 mM).

3.4 Degranulation assay

To assess degranulation, primary human $CD8^+$ T cells were stimulated with human T-activator CD3/CD28 beads in NG (5.6 mM) or HG (25 mM) medium for three days. The protocol of SEA/SEB-pulsed target cells is as follows: (1) Take out 0.5×10^6 of Raji cells and centrifuge at 200 g for 5 min at RT. (2) Remove the supernatant and resuspend in 100 µl AIMV medium. (3) Place the cells in a 96-well plate, then add 1 µl SEA and 1 µl SEB into the medium. (4) Incubate the cells at 37 °C with 5% CO_2 for 30 min. For the degranulation assay, SEA/SEB-pulsed Raji cells were settled with activated $CD8^+$ T cells mentioned above at a ratio of 1:1 in 100 µl of medium in the presence of protein transport inhibitor (GolgiStop, 1:200, BD) for 4 hours at 37 °C with 5% CO_2.

Afterwards, the cells were stained with BV421 anti-human CD8 antibody (1:50) to distinguish target cells from $CD8^+$ T cells and Alexa 488 conjugated anti-human CD107a antibody (1:50) for 30 min at 4 °C in dark. Then the samples were analyzed with flow cytometry.

3.5 Flow cytometry

To stain surface molecules, at least 0.5×10^6 cells were used. The cells were first centrifuged at 250 g for 5 min at RT, then supernatants were removed and the pellets were washed twice with 500 µl PBS/0.5% BSA. Afterwards, the cells were stained with the corresponding antibodies for 30 min at 4 ℃ in dark. Finally, the cells were washed twice with 500 µl PBS/0.5% BSA and resuspended in 100 µl of PBS/0.5% BSA for FACS analysis. When additional intracellular staining required, after surface staining, the cells were fixed in pre-chilled 4% PFA for 15 min at RT and then permeabilized for 10 min in PBS/0.5% BSA containing 0.1% saponin and 5% FCS, followed by antibody staining in permeabilizing solution for 45 min at RT in dark. Then the cells were washed twice with 500 µl of PBS/0.5% BSA prior to FACS analysis. Data were acquired with a FACSVerse flow cytometer (BD Biosciences) and were analyzed by FlowJo v10 (FLOWOJO, LLC).

3.6 Apoptosis assay

To assess 1.4E7 cell apoptosis, NucView® 488 Caspase-3 Substrate (Biotium) was used. Co-culture day 3 activated $CD8^+$ T cell with 1.4E7 at an E:T ratio of 20:1 in 300 µl of NG (5.6 mM) or HG (25 mM) medium in a 96-well plate for 4, 8 and 12 hours. Transfer the cells to a 1.5 ml EP tube, wash twice with 500 µl of PBS/0.5%BSA. Stain cells with

BV421-CD3 antibody (1:50) in 50 µl of PBS/0.5%BSA for 30 min at 4℃° in dark. Wash the cells twice with 500 µl of PBS/0.5%BSA. Add 0.5 µl of substrate solution (stock concentration: 1 mM) to 100 µl of cell suspension in PBS/0.5%BSA and mix gently but thoroughly. Incubate the cells at RT for 30 min in dark. After staining, wash cells twice with 500 µl of PBS/0.5%BSA. Add 150 µl of PBS/0.5%BSA to resuspend the cells. Analyze data by flow cytometry in the green detection channel (excitation/emission: 485 nm / 515 nm).

3.7 Multiplex cytokine assay

To determine the cytokines released by activated $CD8^+$ T cells, primary human $CD8^+$ T cells were stimulated with CD3/CD28 activator beads in NG (5.6 mM) or HG (25 mM) for 3 days. Then cells were collected by centrifuging with 1000 g at 4 °C for 30 min. The supernatants were aliquoted in 100 µl and stored at -80 °C. The pre-set CD8/NK panel (BioLegend) was used and all samples were performed by LEGENDplex™ bead-based immunoassays kits according to the manufacturers' instructions. Two sets of beads are used in the human CD8/NK panel. The smaller beads include 6 bead populations and the larger beads include 7 bead populations. According to the size and internal fluorescent dye of the beads, this panel can detect 13 analytes simultaneously. For the assay preparation step, we should prepare 1× wash buffer, protein standards and samples. There are three points to be noted in this step. Firstly, the 20× wash buffer should be equilibrated to RT beforehand and mixed the salts into solution. Secondly, the standard should be mixed and kept it for 10 min at RT. Thirdly, cell culture supernatant should avoid multiple (>2) freeze-thaw cycles, and the sample can be tested

without dilution, as the sample concentration varies a lot. For the assay procedure step, a V-bottom or a filter plate is used. There are several remarks: (1) All reagents should be brought at RT before use. (2) Always keep the plates upright to avoid losing the beads. (3) The plates should be protected from light. (4) Protein standards and the samples should be performed in duplicate and arranged as suggested (vertically on the plate) for easy data acquisition and analysis. After that, we can start the experiment, the details are as follows: (1) Load 50 µl the standard and samples into the plate as listed in the table. (2) Vortex the mixed beads for 30 sec and add 25 µl of beads into the plate. Note: the mixed beads should be shaked intermittently to avoid settling. (3) Seal the plate with a plate sealer and cover it with an aluminium foil to avoid light. Then put the plate on a plate shaker for 2 hours at RT. Note: the shaking speed should be adjusted in an optimal condition to guarantee a thorough mix of beads with other reagents. (4) Centrifuge the plate at 250 g for 5 min. (5) Remove the supernatant avoiding agitating the beads. (6) Wash the plate with 200 µl of wash buffer, repeat the steps 4 and 5. (7) Add 25 µl of detection antibody into each well. (8) Seal the plate with a plate sealer. and cover it with an aluminium foil to avoid light. Then put the plate on a plate shaker for 1 hour at RT. (9) Add 25 µl of SA-PE into each well. (10) Seal the plate with a plate sealer and cover it with an aluminium foil to avoid light. Then put the plate on a plate shaker for 30 min at RT. (11) Repeat the steps 4 and 5. (12) Wash the plate (200 µl wash buffer/well), repeat the steps 4 and 5. (13) Add 150 µl of wash buffer to resuspend the beads. (14) Analyse the samples using the flow cytometry. Data were quantified using BioLegend's LEGENDplex™ data analysis software.

3.8 Diabetic mouse model

C57BL/6N mice were prepared by Prof. Leticia Prates Roma's group. Leticia Prates Roma and Susanne Renno take on the task of preparation of diabetic mouse model. To induce the diabetic mouse model, we firstly weighted the mice and then injected streptozotocin intraperitoneally into the mice for five consecutive days (50 mg/kg per day). After that, the person in charge housed these mice until day 21. During this period, we obtained blood samples from the mice tail vein and tested the blood glucose levels every day using "Contour Next Sensoren" test strips (SMS Medipool). If blood glucose level exceeded 250 mg/dL one week after injection, we determined the mice as diabetes. At day 21, mice were killed by cervical dislocation. The chest of mice was open and then spleen was obtained. After that, the mice splenocytes were isolated from the spleen. The details are in the following: (1) Add 20 ml cold PBS/0.5%BSA/2mM EDTA in a peri dish and place a 70 μM cell strainer in it. (2) Put the spleen in peri dish as soon as possible after the removal of spleen from mice. (3) Cut the spleen into small pieces and put the sliced spleen in the cell strainer. (4) Grind the spleen by a piston of a 2 ml syringe through a 70 μm cell strainer. (5) Wash the cell strainer with pre-chilled PBS/0.5%BSA/2mM EDTA until homogenised spleen has been rinsed from the cell strainer. (6) Transfer the rinsed splenocytes to a 50 ml falcon tube. (7) Wash the petri-dish with cold PBS/0.5%BSA/2mM EDTA and fill the falcon tube with PBS/0.5%BSA/2mM EDTA up to 50 ml. (8) Centrifuge the splenocytes for 8 min at 240 g and 4 °C. (9) Discard the supernatant, add 1 ml erythrocyte lysis buffer and carefully resuspend the pellet. (10) Incubate the pellet for 1 min at RT. (11) After that,

fill the falcon with PBS/0.5%BSA/2mM EDTA to 50 ml to stop erythrocyte lysis. (12) Count the splenocytes with Z2. (13) Centrifuge the cells with at 240 g for 8 min at 4 °C. Then the isolated splenocytes were stimulated with mouse T-activator CD3/CD28 beads (ThermoFisher Scientific, Cat#11453D) in NG (5.6 mM) or HG (25 mM) medium at the density of 1.5 x 10^6/ml in 500 µl for three days in presence of human IL-2 (20 U/ml, Miltenyi) and 50 µM of beta-Mercaptoethanol.

3.9 Microarray and analysis

Caroline Diener and Martin Hart are responsible for carrying out Microarray. Eckart Meese helped with the result interpretation. The steps they process are as follows: Primary human $CD8^+$ T cells stimulated with CD3/CD28 activator beads in NG (5.6 mM) or HG (25 Mm) medium for three days were used. Total RNA was picked up with miRNeasy Mini Kit (Qiagen) followed by the manufacturer's instructions. The RNA was quantified by NanoDrop 2000c Spectrophotometer (ThermoFisher Scientific). RNA quality was evaluated by RNA Integrity Number value using an Agilent 2100 Bioanalyzer instrument and the RNA 6000 Nano analyser from Agilent Technologies (Santa Clara). All samples had an RIN value of 10, indicating a good quality for the total RNA. In total 100 ng of RNA was used for microarray. Microarray data were analysed by Andreas Denger and Volkhard Helms. Briefly, Linear Models for Microarray Data (limma) R package was utilized to analyse the Agilent microarray data for differential expression. Firstly, they perform background correction (NormExp) and quantile normalization for the samples, respectively. From the dataset, they removed juxtaposed probes for background correction, probes with no associated gene symbols,

and genes that were categorized as unexpressed by Agilent feature extraction software for at least 22 of the 24 arrays. After the filtering step, the dataset includes 22,658 transcripts totally, which corresponds to 15,360 genes. For the analysis of differential expression analysis, they fitted a linear model to each individual sample. Then they calculated the linear model between samples in NG (5.6 mM) or HG (25 mM) conditions. A t-test was used for the identification of differentially expressed genes. The calculation of associated *p*-values for each gene and adjustment of multiple testing were performed by the empirical Bayes method and the Benjamini-Hochberg method, respectively. If the adjusted *p*-value of genes were below 0.05, then the gene was categorized as differential expression (DE) for a given contrast. Among the DE genes, gene annotations were enriched using the limma package.

3.10 Seahorse assay

To determine the oxidative phosphorylation and glycolysis, the seahorse assay was carried out by Leticia Soriano-Baguet and Dirk Brenner from Luxembourg Institute of Health. Primary human $CD8^+$ T cells were stimulated either in NG (5.6 mM) or HG (25 mM) medium for three days. At day 3, the activated $CD8^+$ T were seeded in pre-warmed DMEM medium at a cell density of 3×10^5 cells/well and kept for 45 min to 1 hour at 37 °C without CO_2 prior to the assay. The extracellular acidification rate (ECAR) and oxygen consumption rate (OCR) were tested by Leticia Soriano Baguet with the XF Glycolytic Stress Test and XF Cell Mitochondrial Stress Test kits, respectively.

3.11 Preparation of PBMC from diabetic patients

To investigate the clinical relevance of TRAIL regulation, we cooperated with the

Department of Internal Medicine II at the University Medical Centre in Homburg, Saarland, Germany. Frederic Küppers and Grigorios Christidis were responsible for collecting blood samples from diabetic patients and healthy individuals. The test for diabetes is according to the present diagnostic criteria from the American Diabetes Association-ADA. And healthy samples were tested in the light of a HbA1c < 5,7% on the day of the blood collection. All subjects obtained the written informed consent prior to the blood sampling collection, strictly accordance with the procedure described in the ethical approval of the ethic committee of the medical association of Saarland (Ethic Vote Nr: Ha 84/19). After getting the collected blood samples, all samples were tested the blood glucose level by "Contour Next Sensoren" test strips (SMS Medipool). After that, the isolation of PBMCs from patients and healthy controls was carried out as described in 3.2.2. The isolated PBMCs were stimulated with human CD3/CD28 activator beads (cell to bead, 1:0.8) and cultured in DMEM containing NG (5.6 mM) or HG (25 mM) for three days at the density of 3×10^6/ml, with additional recombinant human IL-2 (100 U/ml, Miltenyi) at 37 °C with 5% CO_2.

3.12 Intracellular ROS detection

For the detection of ROS production, DCFDA (dichlorofluorescein diacetate)-Cellular ROS Assay Kit (Abcam) was used. Primary human $CD8^+$ T cells were stimulated in NG (5.6 mM) and HG (25 mM) medium with CD3/CD28 activator beads for 6 hours in the presence of recombinant human IL-2 (100 U/mL, Miltenyi). After stimulation, cells were washed twice with 500 µl of PBS/0.5% BSA and stained with antibody against CD8 for 30 min at 4 ℃ in dark. In between, prepare 1× staining buffer and a

working DCFDA solution. For 50 ml of 1× Buffer, add 5 ml of 10× Buffer with 45 ml ddH_2O and mix gently and thoroughly. After that, combine 1 µl of 20 mM DCFDA solution with 1 ml of 1× Buffer. The final concentration is 20 µM. After staining, cells were washed twice with 500 µl of PBS/0.5% BSA and incubated with 20 µM of DCFDA for 30 min at 37 °C in dark. Finally, the samples were analysed directly by flow cytometry analysis without washing and were quantified with FlowJo v10 (FLOWOJO, LLC).

3.13 H_2O_2 treatment

To determine whether ROS is involved in the TRAIL expression, we treated cells with H_2O_2. H_2O_2 (stock concentration: 9.8 M) was diluted with 1× PBS. Primary human $CD8^+$ T cells were stimulated in NG (5.6 mM) and HG (25 mM) medium with CD3/CD28 activator beads in the presence of different concentrations of H_2O_2 indicated in the figure legends (1, 3, or 10 mM) and kept at 37 °C with 5% CO_2. For the control group, the cells were treated with 1× PBS. As H_2O_2 is unstable, H_2O_2 was added to the culture medium every 24 hours.

3.14 Quantitative RT-PCR

The mRNA expression analysis was performed by Gertrud Schäfer as described before [164]. Primary human $CD8^+$ T cells were stimulated with CD3/CD28 activator beads for three days in NG (5.6 mM) and HG (25 mM) medium. After stimulation, the cells were treated as follows: (1) Centrifuge the cells in a sterile tube with 1000 rpm at 4 °C for 5 min and discard the supernatant. (2) Add ice-cold, sterile D-PBS to wash cells, centrifuge the cells with 1000 rpm at 4 °C for 5 min and discard as much the supernatant

as possible. (3) Add 500 µl TRIzol reagent to lyse the cell pellets. (4) Cell pellets were stored at -20 ℃ before use. Total RNA was extracted from activated $CD8^+$ T cells using TRIzol reagent followed by the user guide (ThermoFisher Scientific, SKU#A33251). Afterwards, reverse transcription of isolated RNA to complementary DNA (cDNA) was done. Relative expression of gene was carried out by qRT-PCR by CFX96Real-TimeSystemC1000 Thermal Cycler (Bio-Rad Laboratories). We used TBP (TATA box-binding protein) as a housekeeping gene used for the normalizing target genes. Primer sequences that have been used are listed as follows (forward/reverse): TBP (5'-CGGAGAGTTCTGGGATTGT-3'/5'-GGTTCGTGGCTCTCTTATC-3'), GZMA (5' TTGGGGCTCACTCAATAACC 3'/5' TGGTTCCTGGTTTCACATCA 3'), GZMB (5' GAGACGACTTCGTGCTGACA 3'/5' CTGGGCCTTGTT GCTAGGTA 3'), FASLG (5' GCACACAGCATCATCT TTGG 3'/5' CAAGATTGAC CCCGGAAGTA 3'). For perforin (NM_005041 and NM_001083116), the primer sequence was forward 5′ ACTCACAGGCAGCCAACTTT 3′ and reverse 5′ CTCTTGAAGTCAGGGTGCAG 3′ as referred in [165]. Pre-designed primers for TRAIL (QT00068957) and Glut1 (QT00079212) were purchased.

3.15 CTL viability assay

To determine the effect of vitamin D and metformin treatment on the CTLs viability, 7-AAD viability staining was performed. 7-AAD (7-amino-actinomycin D) is fluorescent chemical compound with a high DNA affinity, which can be excited by 488 nm and detected by the PE-Cy®5/PerCP channel. Primary human $CD8^+$ T cells were stimulated with CD3/CD28 activator beads in NG (5.6 mM) or HG (25 mM) medium

in the presence of vitamin D and metformin for three days. After that, the cells were stained as follows: (1) Centrifuge the cells at 250 g for 30 min at RT. (2) Discard the supernatant and add 500 µl of PBS/0.5% BSA to resuspend the cells. (3) Repeat the steps 1 and 2. (4) After washing twice, stain the cells with CD8 antibody at 4 ℃ for 30 min in dark. (5) Wash cells with 500 µl of PBS/0.5% BSA twice. (6) Resuspend the cells in 500 µl of PBS/0.5% BSA and then add 5 µl of 7-AAD staining solution (per million cells). (7) Incubate the cells for 10 min at RT in dark. (8) Data was acquired by flow cytometry without washing and analysed by FlowJo v10 (FLOWOJO, LLC).

3.16 Statistical analysis

Statistical analysis was carried out by GraphPad Prism 6. For two-group comparisons, two-tailed paired/unpaired Student's t-test was used. For multiple-group comparisons, one-way or two-way ANOVA was performed followed by Bonferroni's test. All data are presented as mean ± SD if not mentioned otherwise. All *p* values were shown in the figures.

4. Results

In our previous work, Dr. Zhu Jie found that the killing efficiency was increased in HG-cultured CTLs compared to their counterparts in NG. I followed up this project and investigated the underlying mechanisms. I first focused on the canonical killing mechanisms employed by CTLs to destroy target cells, namely lytic granules (LGs) and Fas/FasL pathways. No difference was identified in these two classical pathways (cytotoxic protein expression and degranulation). CTL Migration and cytokine release was also not altered by HG. Finally, TRAIL was identified to be the molecule responsible for HG-enhanced CTL killing efficiency. ROS and PI3K/Akt/NFκB are involved in regulating increased TRAIL expression induced by HG. I also found that metformin and vitamin D reduced HG-enhanced TRAIL expression on CTLs and therefore protected apoptosis of pancreatic beta cells mediated by HG-CTLs.

4.1. CD107a expression is not altered by HG

To investigate whether the killing machinery is changed by HG, firstly, I explored the impact of HG on releasing of LGs using degranulation assay. To this end, we stimulated negatively isolated primary human $CD8^+$ T cells with CD3/CD28 T cell activator beads in the medium presence of NG (5.6 mM) or HG (25 mM) for three days, then we examined CD107a expression on the surface of CTLs by FACS. CD107a has been identified as a degranulation marker of NKs and activated $CD8^+$ T cells [166]. The recognition and killing of tumour cells by cytotoxic lymphocytes, such as $CD8^+$ T lymphocytes and NK cells, is primarily through the secretion of immune lytic particles. During this process, the granule membrane is fused with the cytoplasmic membrane of

effector cells, which results in lysosome-associated proteins exposed to the surface, such as CD107a [167]. From our results, we found that there was no difference of CD107a expression between and NG- or HG-cultured CTLs **(Figure 1A-C)**.

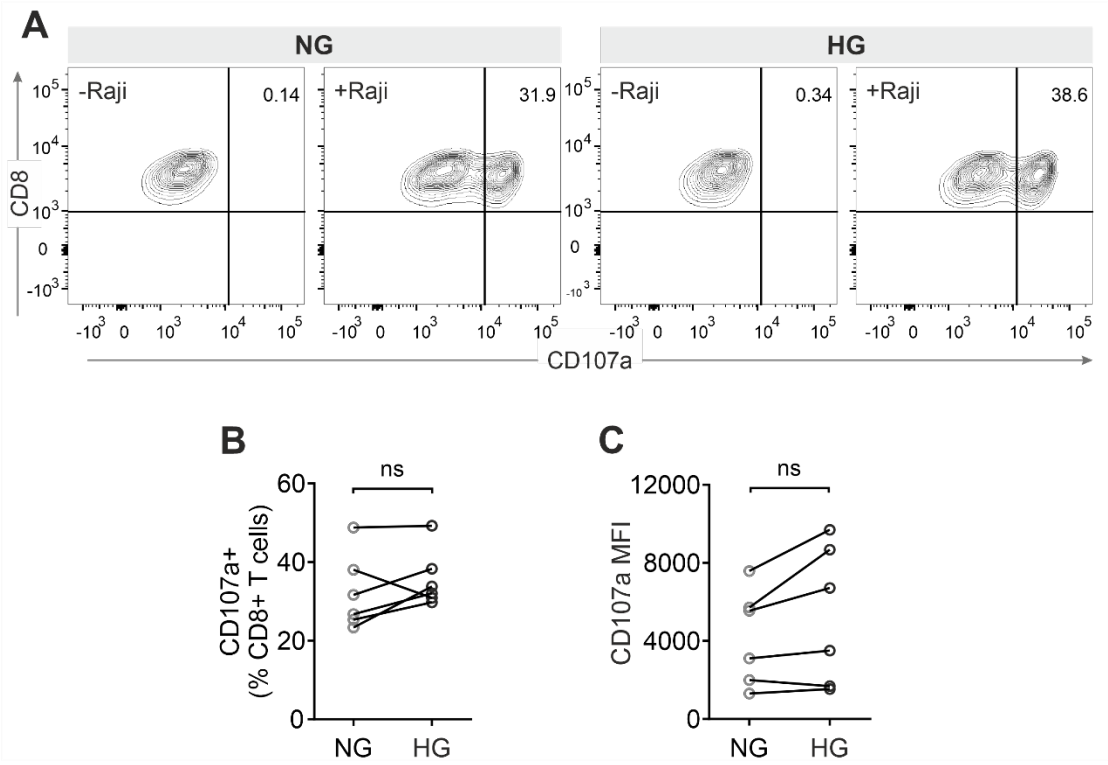

Figure 1. CD107a expression was not altered by HG. Primary human $CD8^+$ T cells were stimulated with CD3/CD28 activator beads in NG (5.6 mM) or HG (25 mM) medium for three days. Then $CD8^+$ T cells were incubated with SEA/SEB-pulsed Raji cells for 4 hours. Afterwards, degranulation assay was carried out to determine the expression of CD107a on CTLs. One representative donor is shown in (**A**) and the quantification is shown in (**B, C**) (n = 6 donors from three independent experiments). MFI, Mean fluorescence intensity. Data were analysed by two-tailed paired Student's t test. * $p < 0.05$; ns, not significant. Figure and legend modified from [104].

4.2. HG does not affect LGs pathway

Subsequently, we analysed cytotoxic proteins expressionincluding perforin, granzyme A (GzmA) and granzyme B (GzmB). The results showed that at the mRNA level perforin and GzmB were not changed by HG, but GzmA was moderately down-regulated in HG-cultured CTLs **(Figure 2A-C)**. At the protein level there was also no difference of perforin expression between HG and NG, whereas a slightly reduction of

GzmA in HG-cultured CTLs **(Figure 2D-G)**, which is in a good agreement with the data at the mRNA level. Nevertheless, the reduced GzmA level would not contribute to HG-enhanced CTL killing.

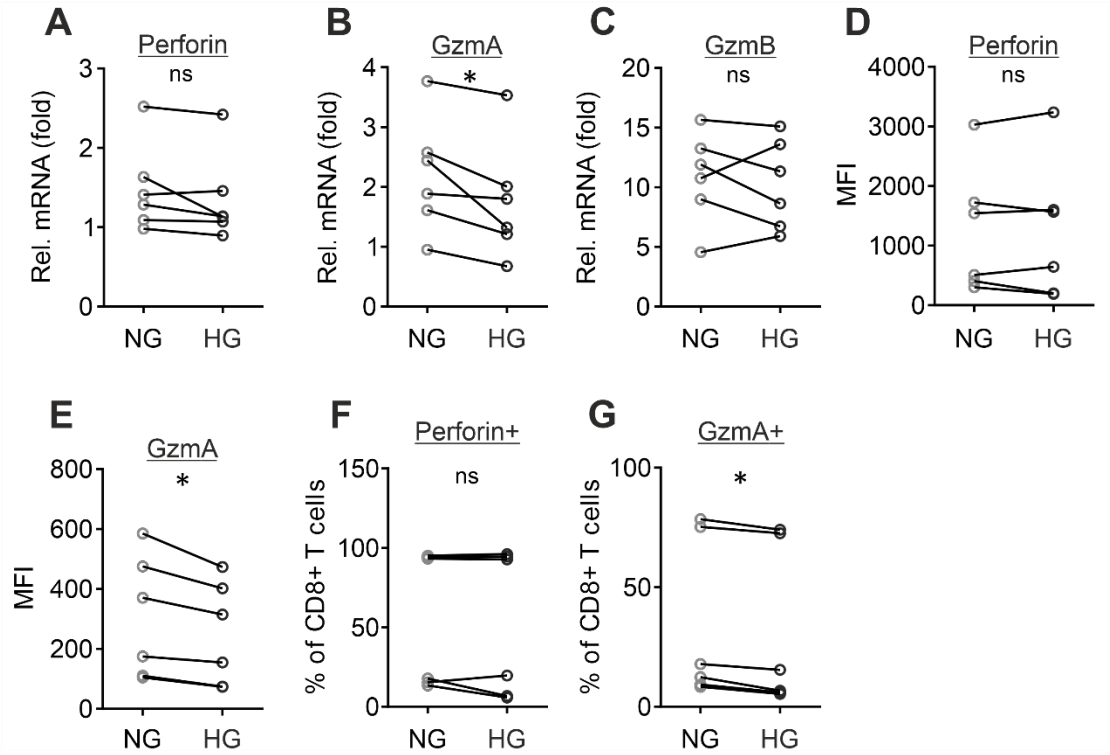

Figure 2. HG does not affect the LGs pathway. Primary human $CD8^+$ T cells were stimulated with CD3/CD28 activator beads for three days in the medium with high or normal glucose. Then cytotoxic proteins expression was determined by quantitative PCR and flow cytometry. Expression of cytotoxic proteins at the mRNA level (**A-C**) (n = 6 donors from three independent experiments) and at the protein level (**D-G**) (n = 6 donors from three independent experiments). MFI, Mean fluorescence intensity. All data were analysed by two-tailed paired Student's t test. * $p < 0.05$; ns, not significant. Figure and legend modified from [104].

4.3. HG does not influence Fas/FasL pathway

Next, we examined the Fas/FasL pathway. We found that at the mRNA level the expression of FasL was up-regulated in HG-cultured CTLs **(Figure 3A)**, but at the protein level it remained unchanged **(Figure 3B, C)**. Taken together, these results suggest that the HG-enhanced CTL killing is not attribute to the canonical CTL killing machineries, i.e., LGs and Fas/FasL pathway.

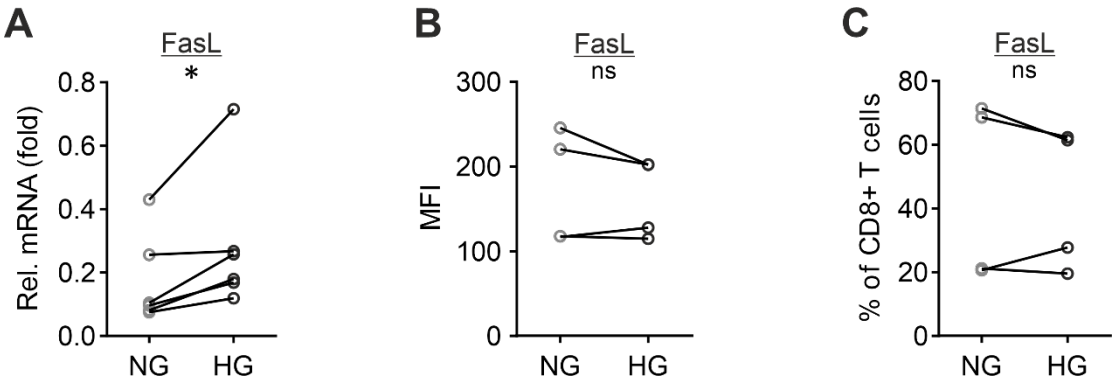

Figure 3. HG does not influence the Fas/FasL pathway. Primary human $CD8^+$ T cells were stimulated with CD3/CD28 beads for three days in the medium with high or normal glucose. Then cytotoxic proteins expression was determined by quantitative PCR and flow cytometry. Expression of FasL at the mRNA level (**A**) (n = 6 donors from three independent experiments) and at protein level (**B, C**) (n = 4 donors from two independent experiments). MFI, Mean fluorescence intensity. Data were analysed by two-tailed paired Student's t test (**A-J**). * $p < 0.05$; ns, not significant. Figure and legend modified from [104].

4.4. HG does not alter cytotoxic proteins and cytokines release

Since LGs and Fas/FasL pathway were not changed by HG, next I examined whether the release of cytotoxic proteins and cytokines was altered in CTLs by HG. A bead-based multiplex cytokine assay was used, which can measure up to 13 analytes from the same samples at the same time. This assay can overcome Enzyme-linked immunosorbent assay (ELISA). ELISA is a most widely used and effective method for the measurement of proteins or cytokines, but is not well suitable for high throughput multiplex analyses [168]. This multiplexing assay allows for time/cost economy and makes sure that all of measurements are carried out under the same conditions [169]. The assay is composed of six main cytotoxic granules including GzmA, GzmB, perforin, granulysin, soluble FasL and soluble Fas, and seven key cytokines released by CD8 cells including IFNγ, IL-2, IL-4, TNFα, IL-6, IL-10 and IL-17A. Primary human $CD8^+$ T cells were stimulated with CD3/CD28 T cell activator beads in NG (5.6 mM) or HG (25 mM) for three days. Then cells were collected by centrifuging with 1000 g at 4 °C for 30 min. Afterwards, the supernatants were aliquoted and stored at -80 °C before

testing. As shown in **Figure 4**, there was no difference identified in concentration of cytotoxic proteins or cytokines in the supernatant between NG- or HG-cultured CTLs. These data suggest that the enhanced killing capacity in HG-CTLs is not due to altered release of cytokines or cytotoxic proteins.

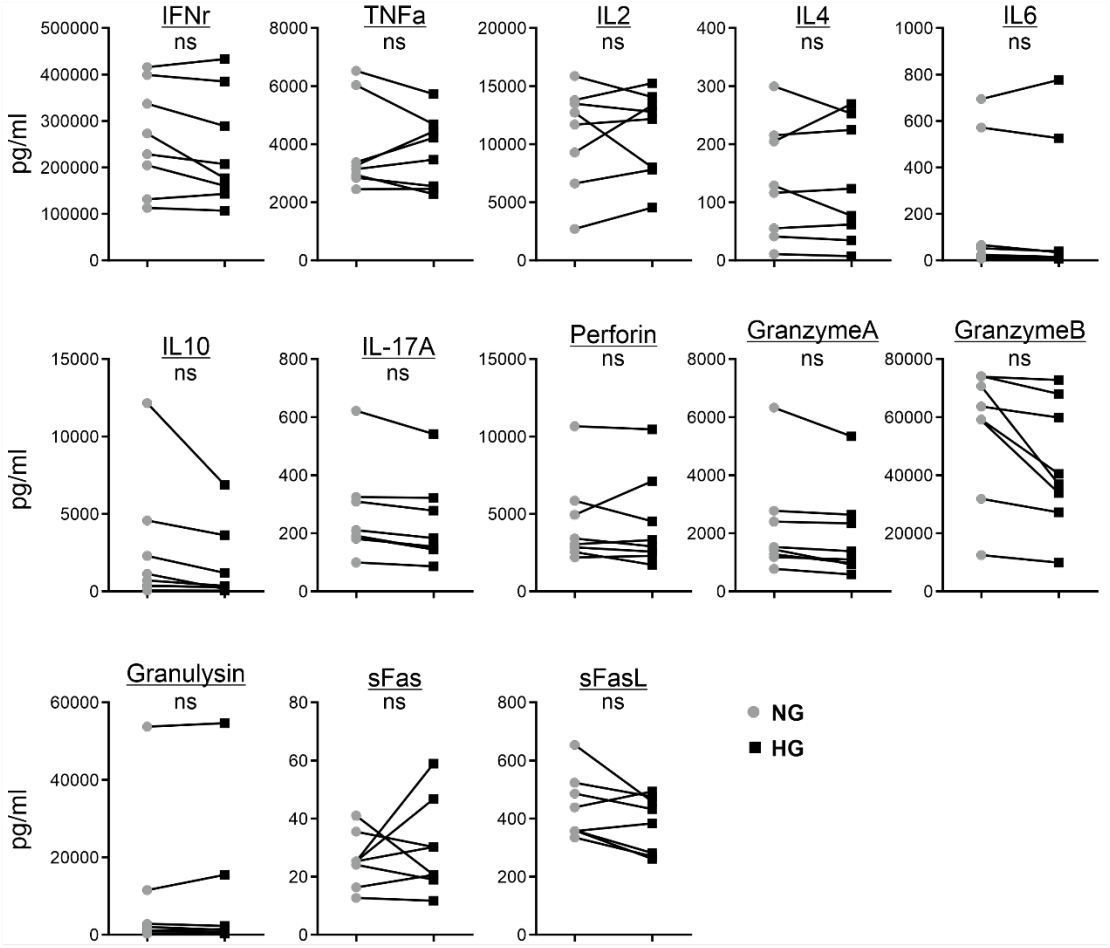

Figure 4. Release of cytokines and cytotoxic proteins in CTLs. Negatively isolated primary human $CD8^+$ T cells were stimulated by CD3/CD28 activator beads for three days in medium with NG or HG. Supernatants were collected and stored at -80 °C until it was used for experiments. Then the bead-based multiplex assay was carried out to analyse the cytokines production and n = 8 donors from four independent experiments. Data were analysed by two-tailed paired Student's t test. Figure and legend modified from [104].

4.5. TRAIL is up-regulated in environments with high glucose

The next coming question is if HG does not affect LGs and Fas/FasL pathway, which molecules are responsible for HG-enhanced CTL killing. I turned my focus to TRAIL pathway. TRAIL has a similarity with as FasL and is also a part of TNF superfamily. It

has been shown that TRAIL is a potent apoptotic inducer in various cancer cells *in vitro* and effectively restricts the growth of tumour *in vivo* without disrupting the normal tissues [170]. In negatively isolated primary human $CD8^+$ T cells stimulated with CD3/CD28 T cell activator beads in NG (5.6 mM) or HG (25 mM) for three days, TRAIL expression was determined using quantitative PCR and flow cytometry. We found that TRAIL was substantially enhanced in HG-cultured CTLs compared to that of in NG-cultured CTLs at the level of mRNA **(Figure 5A)**. Concomitantly, we also identified that both the total TRAIL expression **(Figure 5B, C)** and surface TRAIL expression **(Figure 5D-F)** were substantially increased in HG-cultured CTLs at the protein level. To test whether high glucose also elevates TRAIL expression *in vivo*, I used a diabetic mouse model. In this model, streptozotocin was injected into C57BL/6N mice, which secrete more insulin than that of the C57BL/6J substrain responding to glucose in vitro [171]. Blood glucose level higher than 250 mg/dL was considered diabetic. Interestingly, we found that compared to control CTLs, diabetic CTLs displayed significantly enhanced level of TRAIL expression **(Figure 5G, H)**, which is in a good agreement with our observation with primary human $CD8^+$ T cells stimulated *in vitro*. Furthermore, the blood glucose level was positively correlated with the TRAIL expression **(Figure 5I)**. In addition, we also examine the clinical relevance of the regulation of TRAIL in environments with high glucose in diabetic patients. Frederic Küppers and Grigorios Christidis at Internal Medicine II, University Hospital Saarland collected the blood from patients diagnosed with diabetes and healthy individuals. Heathy individuals were recruited as the control group. Then we isolated

PBMCs from the patients and analysed the TRAIL expression in freshly CTLs. Interestingly, we found that there is a positive correlation between TRAIL expression and blood glucose level of diabetic patients **(Figure 5J)**. These results showed that the expression of TRAIL in CTLs could be induced and even up-regulated under environments with high glucose.

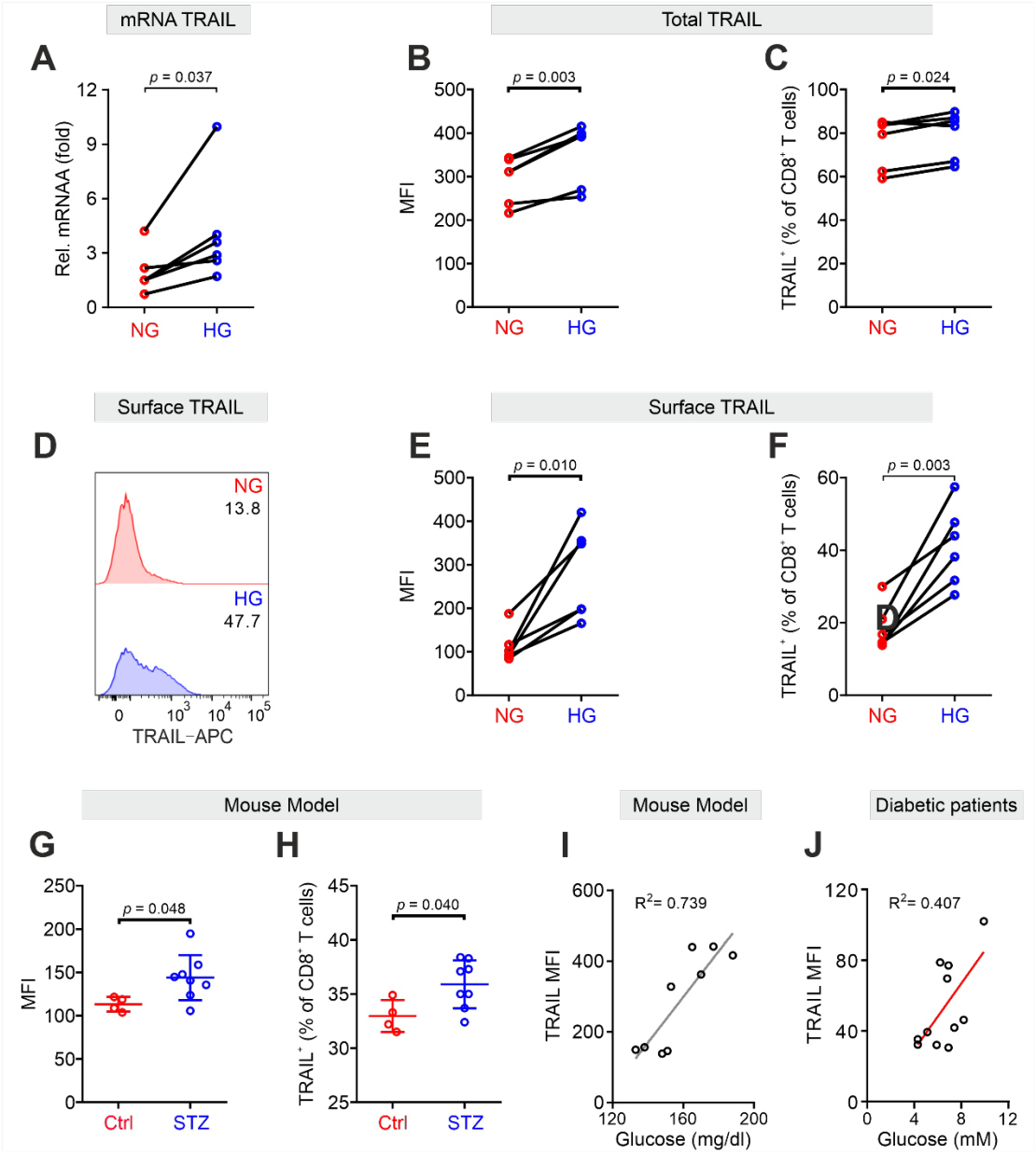

Figure 5. Expression of TRAIL in CTLs was up-regulated under environments with high glucose. Primary human $CD8^+$ T cells were stimulated with CD3/CD28 antibody-coated beads for three days in NG (5.6 mM) or HG (25 mM) medium. **(A)** TRAIL expression in CTLs at mRNA level was quantified by qRT-PCR (n = 6 donors from three independent experiments). **(B-F)** Total and surface TRAIL

expression in CTLs at protein level were determined by flow cytometry, respectively. CTLs were stained with antibody against CD8 and TRAIL after permeabilization **(B, C)** or without permeabilization **(D-F)**. **(D)** One representative donor out of six. Quantification of Total TRAIL **(B, C)** (n = 6 donors from three independent experiments) and surface TRAIL in CTLs **(E, F)** (n = 6 donors from three independent experiments). **(G, H)** TRAIL expression is increased in diabetic mice. Mouse splenocytes were isolated from STZ-induced diabetic mice or controls, then cells were stained with PE-mCD3, BV421-mCD8, and APC-mTRAIL for flow cytometry analysis (Ctrl = 4, STZ mice = 8). **(I)** TRAIL expression in CTLs from mice is positively correlated with the blood glucose levels. **(J)** Positive correlation of TRAIL expression in freshly isolated $CD8^+$ T cells and the blood glucose levels from 11 diabetic patients. MFI, mean fluorescent intensity. Data were represented as Mean ± SD. Data were analyzed by two-tailed paired Student's t test (**A, B, C, E, F**), two-tailed unpaired Student's t test (**G, H**), trendline analysis (**I**), Person's correlation coefficient analysis (**J**). The connecting lines are the data from the same donor. Figure and legend modified from [172].

4.6. TRAIL expression in diabetic CTLs was higher than that of in healthy CTLs

For the healthy individuals and diabetic patients collected from Internal Medicine II , University Hospital Saarland, we isolated PBMCs and stimulated with CD3/CD28 antibody-coated beads in the medium with HG or NG for three days . Then we anaysed TRAIL expression by flow cytometry. After stimulation, we identified that compared to TRAIL expression in healthy individuals, the TRAIL expression was markedly increased in diabetic CTLs for both NG and HG environments **(Figure 6A-C)**. Notably, we also found that the expression of TRAIL in CTLs from diabetic patients in NG medium has a comparable level with the expression of TRAIL in CTLs from healthy CTLs in HG medium. Additionally, we also identified that there was no difference of TRAIL expression in diabetic CTLs between type I and type II diabetes **(Figure 6D, E)** or between males and females **(Figure 6F, G)** and no correlation with the age **(Figure 6H-K)**.

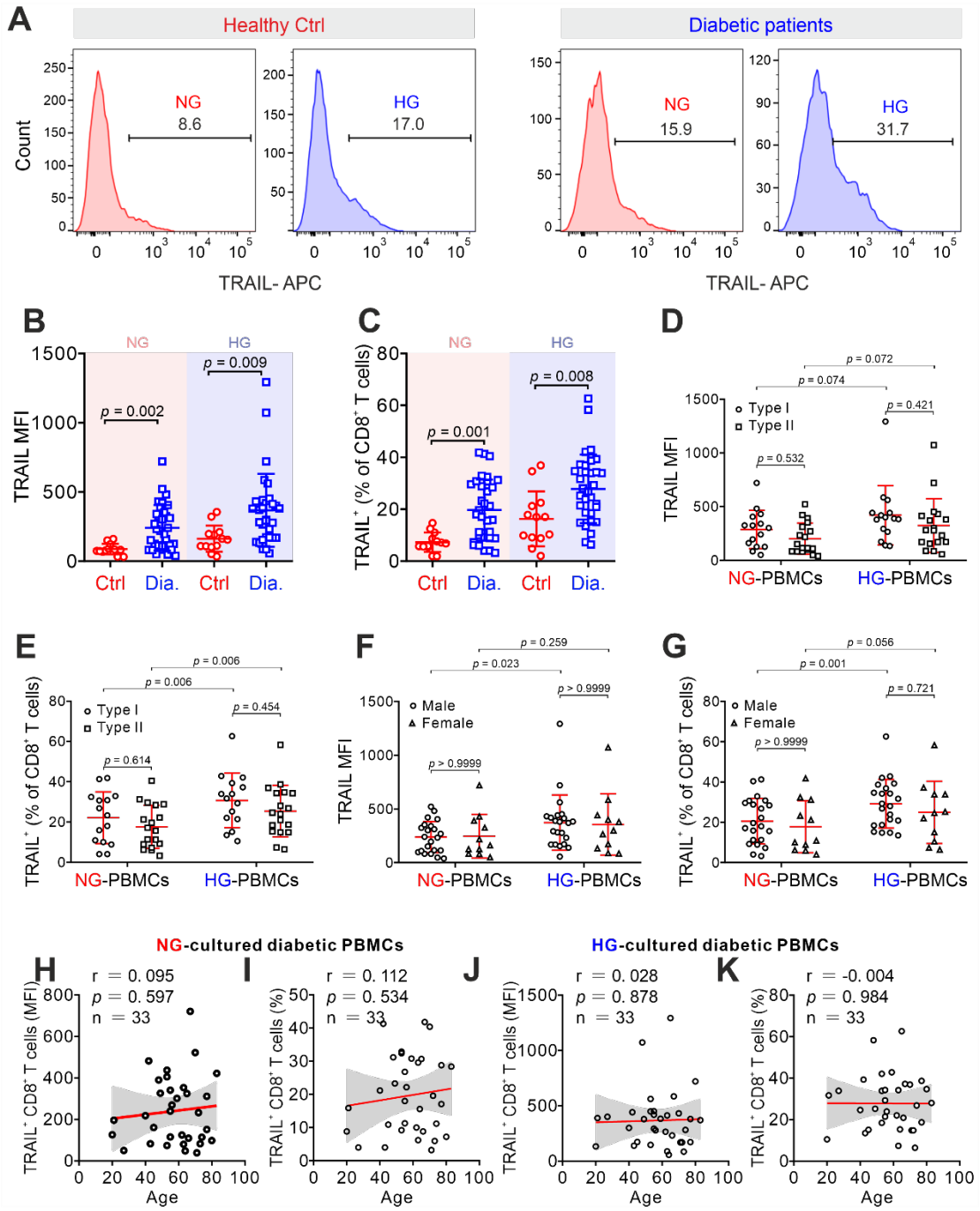

Figure 6. TRAIL expression was markedly increased in diabetic CTLs for both NG and HG environments. PBMCs were isolated from diabetic patients or healthy individuals and then stimulated with CD3/CD28 T cell activator beads in NG (5.6 mM, pink shade) or HG (25 mM, blue shade) medium for three days. TRAIL expression was analysed by flow cytometry (Ctrl, n = 13 from thirteen independent experiments; diabetic patients, n = 33 from twenty-four independent experiments). One representative donor from either group is shown in **(A)**. **(B, C)** Quantification of TRAIL expression in healthy controls and diabetes. No correlation of TRAIL expression with diabetic types **(D**, **E)**, genders **(F**, **G)**, or age **(H-K).** MFI, mean fluorescent intensity. Data were represented as Mean ± SD. Data were analysed by two-tailed unpaired Student's t test **(B, C),** two-way ANOVA with Bonferroni's multiple comparison test **(D-G),** Person's correlation coefficient analysis **(H-K).** Figure and legend modified from [172].

4.7. TRAIL-R2 was mainly expressed in pancreatic beta cells

Since TRAIL is an apoptosis inducing surface molecule, we next explored whether TRAIL is responsible for HG-enhanced CTL killing. It is reported that treating with soluble TRAIL results in pancreatic beta cell apoptosis [173]. Here we ultilized human pancreatic beta cell line 1.4E7 as target cell, which is derived from electrofusion of human primary pancreatic islets with a human pancreatic ductal carcinoma cell line PANC-1. Before conducting a killing assay, we examined the expression of TRAIL receptors on the surface of 1.4E7 beta cell line. We found that among the four TRAIL receptors, only TRAIL-R2 which can induce apoptosis was mainly expressed in 1.4E7 beta cell line **(Figure 7)**.

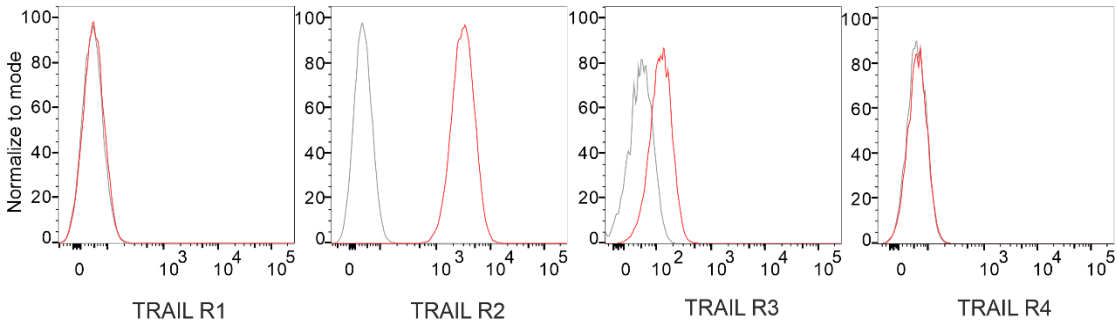

Figure 7. TRAIL receptors expression in 1.4E7 beta cells. Pancreatic beta cell 1.4E7 were stained with antibody against TRAIL-R1, -R2, -R3 and R4. Data were analysed by flow cytometry. Gray: unstained controls. Figure and legend modified from [172].

4.8. HG-cultured CTLs enhance killing capacity against beta cells

To examine CTL killing, primary human $CD8^+$ T cells were stimulated with CD3/CD28 activator beads for three days and then incubated with 1.4E7 beta cells for various time points (4, 8, and 12 hours). The harvested cell mixture was well resuspended and stained with antibodies against CD3. Only singlets were selected and CTLs were separated from 1.4E7 beta cells based on CD3 expression **(Figure 8A)**. Quantification of caspase-3 activity in beta cells shows that apoptosis of beta cells can be induced by CTLs and

this CTL-mediated apoptosis was significantly enhanced by HG **(Figure 8B-G)**.

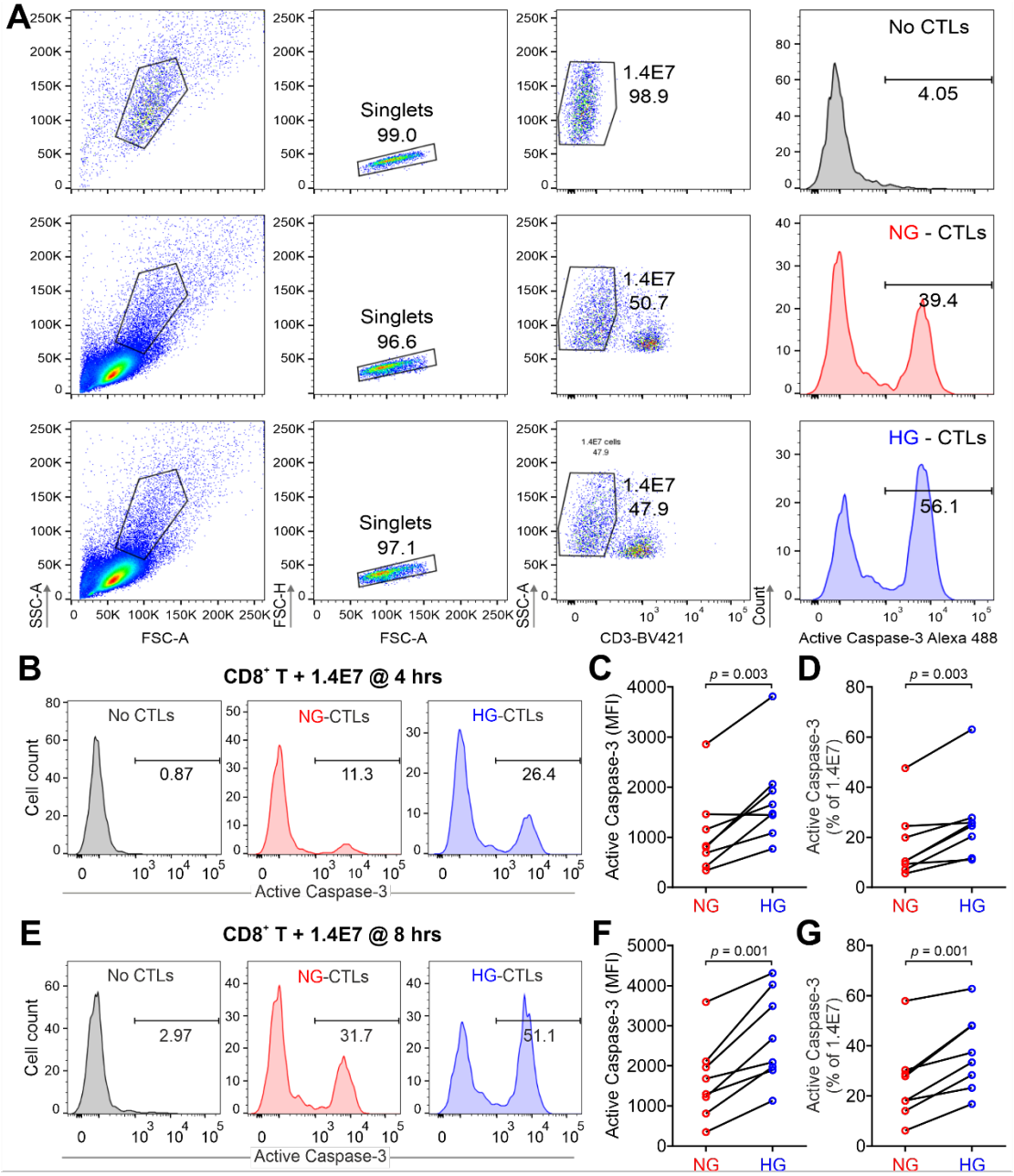

Figure 8. HG-cultured CTLs enhance killing capacity against beta cells. (**A**) Gating strategy for apoptosis assay of 1.4E7 beta cells at 12 hour. (**B-G**) Primary human $CD8^+$ T cells were stimulated with CD3/CD28 beads for three days in NG (5.6 mM) or HG (25 mM) medium. Afterwards, beta cells 1.4E7 were incubated with CTLs with effector to target ratio of 20:1 for 4 hrs (**B-D**), 8 hrs (**E-G**) or 12 hrs (**A**). Then cells were stained with antibody against CD3 to gate beta cells. Assessment of caspase-3 activity as a readout for analysing CTL-induced beta cells apoptosis. Representative donors at 4 hrs and 8 hrs shown in **B** and **E**, respectively. Quantification of caspase-3 activity at 4 hrs (**C, D**) and 8 hrs (**F, G**) (n = 8 donors from five independent experiments). Data were analysed by two-tailed paired Student's t test (**C, D, F, G**). All connecting lines are data from the same donor. Figure and legend modified from [172].

4.9. TRAIL expression is positively correlated with the apoptosis of pancreatic beta cell

Based on the findings that HG-cultured CTLs enhance killing capacity against beta cells. We next want to know whether there exists correlation between the TRAIL expression and beta cell apoptosis. In short, primary human $CD8^+$ T cells were stimulated with CD3/CD28 T cell activator beads for three days in NG (5.6 mM) or HG (25 mM) medium. Afterwards, we analysed TRAIL expression by flow cytometry. We then analysed the correlation by pearson's correlation coefficients. Interestingly, the results showed that the beta cells apoptosis is positively correlated with the TRAIL expression in CTLs at all three time points examined (**Figure 9A-F**).

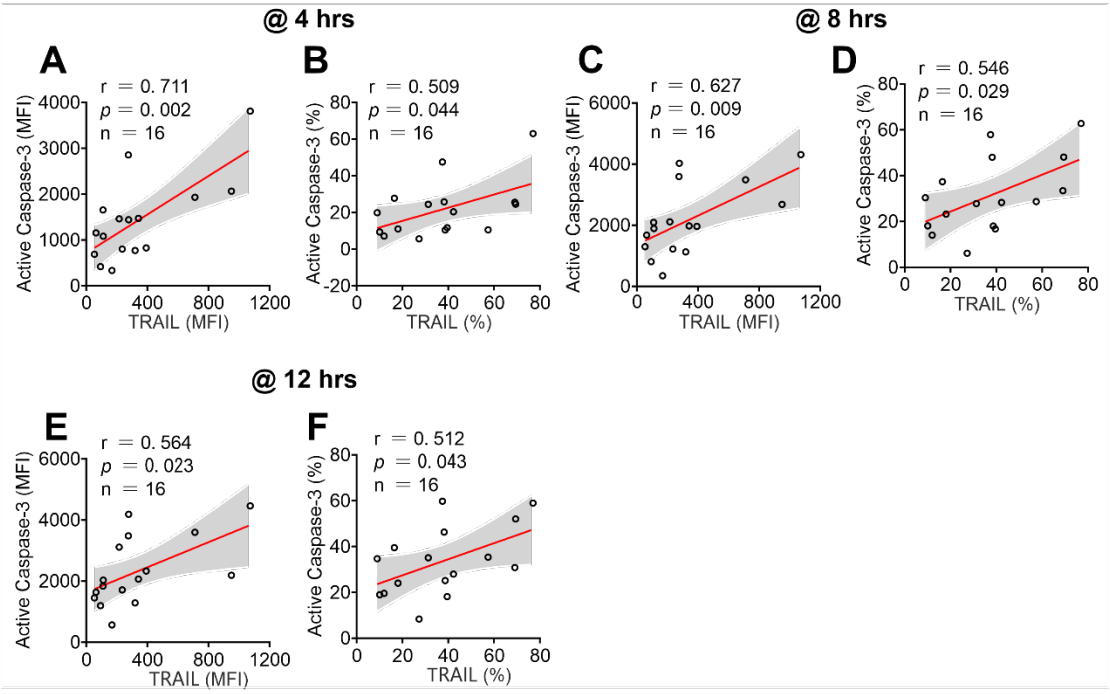

Figure 9. Correlation of TRAIL expression with beta cells apoptosis. Caspase-3 activity is tested at 4 hr **(A, B),** 8 hr **(C, D)** and 12 hr **(E, F)**, respectively. Results are from 16 donors from five independent experiments. MFI, mean fluorescent intensity. Data were analysed by Pearson's correlation coefficients**.** Figure and legend modified from [172].

4.10. CTLs-induced beta cell apoptosis is TRAIL-dependent

To further test whether apoptosis of beta cells is in a TRAIL-dependent manner, we

broke TRAIL function using TRAIL inhibitor. We analysed caspase-3 activity and found that blockade of TRAIL function indeed reduced the beta cell apoptosis for HG-cultured CTLs **(Figure 10A-C)**. Taken together, these results show that HG-CTLs induce enhancement in TRAIL-mediated apoptosis of pancreatic beta cells.

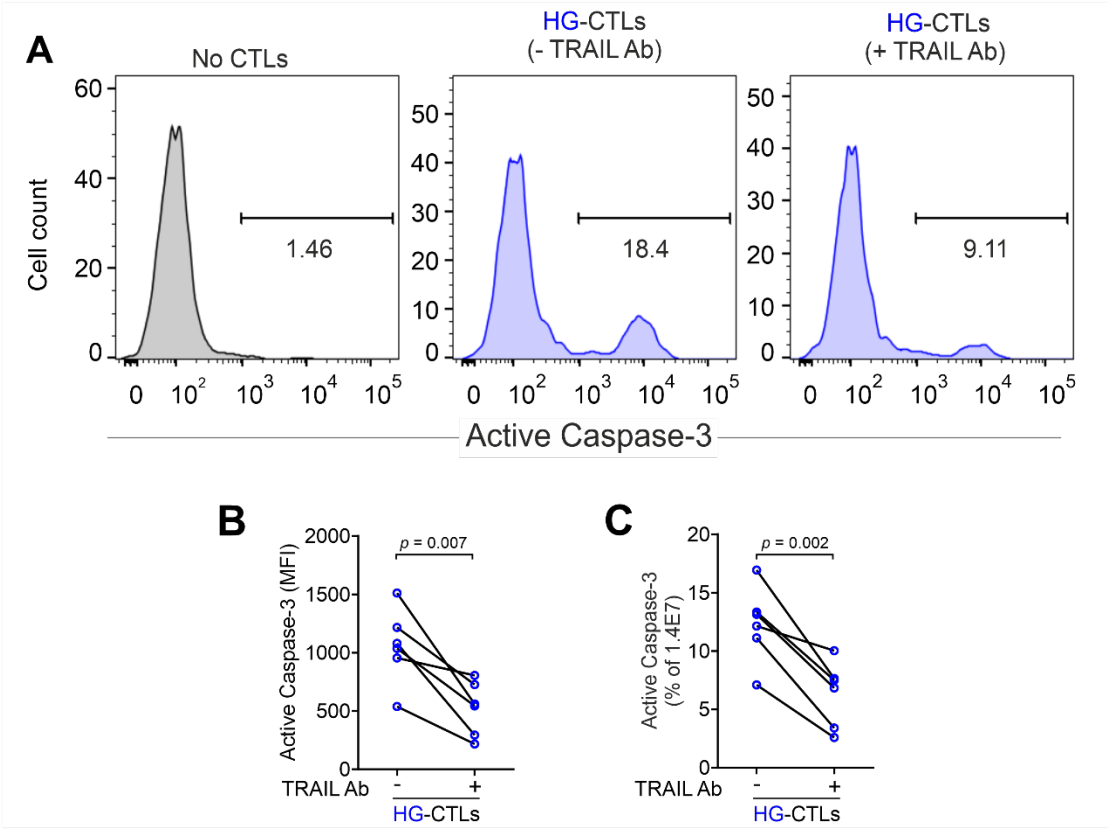

Figure 10. Apoptosis of beta cell induced by CD8$^+$ T cells is TRAIL dependent. CTLs were incubated with 1.4E7 cells in the presence or absence of TRAIL inhibitor (50 µg/ml) for 4 hours and caspase-3 activity was analysed by flow cytometry. One representative donor out of six donor is shown in **A** and the quantification is shown in **B** and **C** (n = 6 donors from two independent experiments). MFI, mean fluorescent intensity. Data were analysed by two-tailed paired Student's t test **(B, C)**. All connecting lines are the data from the same donor. Figure and legend modified from [172].

4.11. Glucose metabolism was reprogrammed by high glucose

The upcoming question is how TRAIL expression in CTLs is enhanced by HG. To address this question, we first examined T cell metabolism, as the effector functions of CTLs are reported to be regulated by glucose metabolism. Glucose metabolism includes oxidative phosphorylation and glycolysis, which can be determined by the oxygen

consumption rate (OCR) and the extracellular acidification rate (ECAR), respectively. Results from seahorse assay showed that both OCR and ECAR were enhanced in HG-cultured CTLs compared to their counterparts cultured in NG **(Figure 11A-F)**, indicating an increase in oxidative phosphorylation and glycolysis in CTLs by HG culture.

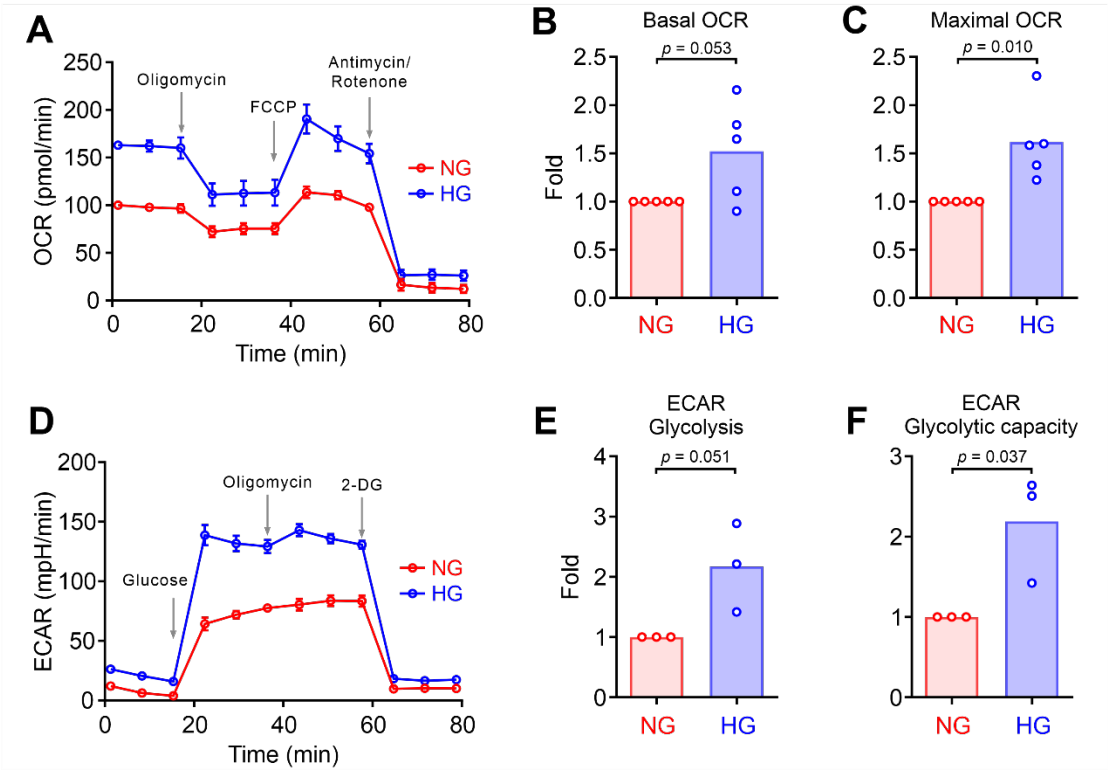

Figure 11. Glucose metabolism was reprogrammed by high glucose. Primary human $CD8^+$ T cells were stimulated with CD3/CD28 T cell activator beads for three days in NG (5.6 mM) or HG (25 mM) medium. Oxidative phosphorylation **(A-C)** and glycolysis **(D-F)** of CTLs were determined by seahorse assay. After obtaining of OCR in basal conditions, purified $CD8^+$ T cells were added into oligomycin, mitochondrial disintegrant FCCP and antimycin/rotenone. **(A)** One representative donor for oxidative phosphorylation. Basal OCR **(B)** were analysed and Maximum OCR **(C)** were assessed after FCCP decoupling, respectively (n = 5 from two independent experiments). Purified $CD8^+$ T cells were injected sequential compounds glucose, oligomycin and 2-DG to measure glycolysis, glycolytic capacity. **(D)** One representative donor for glycolysis. Glycolysis **(E)** after addition of glucose and glycolytic capacity **(F)** was measured following by injection of oligomycin, respectively (n = 3 from two independent experiments). All data were analysed by two-tailed unpaired Student's t test. Figure and legend modified from [172].

4.12. Neither mTOR nor glucose transporters contribute to the reprogrammed metabolism in CTLs by HG

Since mTOR is shown to be an important regulator for glycolysis in T cells, we postulated that the key molecules which are involved in glycolysis such as mTOR and glucose transporters would be involved in HG-enhanced TRAIL expression in CTLs. To test this postulation, we examined phosphorylate subunit of mTOR at Ser2448 mTORC1 and mTORC2, which indicates the activity of mTOR [174]. Surprisingly, no difference in phosphorylation at Ser2448 in CTLs was detected between NG- and HG-cultured PBMCs **(Figure 12A-C)**. To further examine the involvement of mTOR in HG-enhanced expression of TRAIL in CTLs, we abrupted mTOR activity functionally with rapamycin, a specific inhibitor for mTOR during stimulation of $CD8^+$ T cells. We found that even at the highest rapamycin concentration (600 nM), the MFI was not statistically significant in rapamycin-treated HG-CTLs in spite of slight increase in the percentage of $TRAIL^+$ CTLs relative to their counterparts in NG **(Figure 12D-F)**. Next, we examined glucose transporters expression in NG- and HG- cultured CTLs and started with glucose transporter 1 (Glut1), a main member of glucose transporters. We found that at the mRNA level expression of Glut1 was down-regulated in HG-CTLs **(Figure 12G)**, but no difference was identified at the protein level **(Figure 12H, I)**. In addition, membrane Glut1 also remained unchanged in HG-CTLs **(Figure 12J, K)**. Our results indicate that the reprogrammed metabolism in CTLs by HG is not attribute to mTOR molecules and glucose transports.

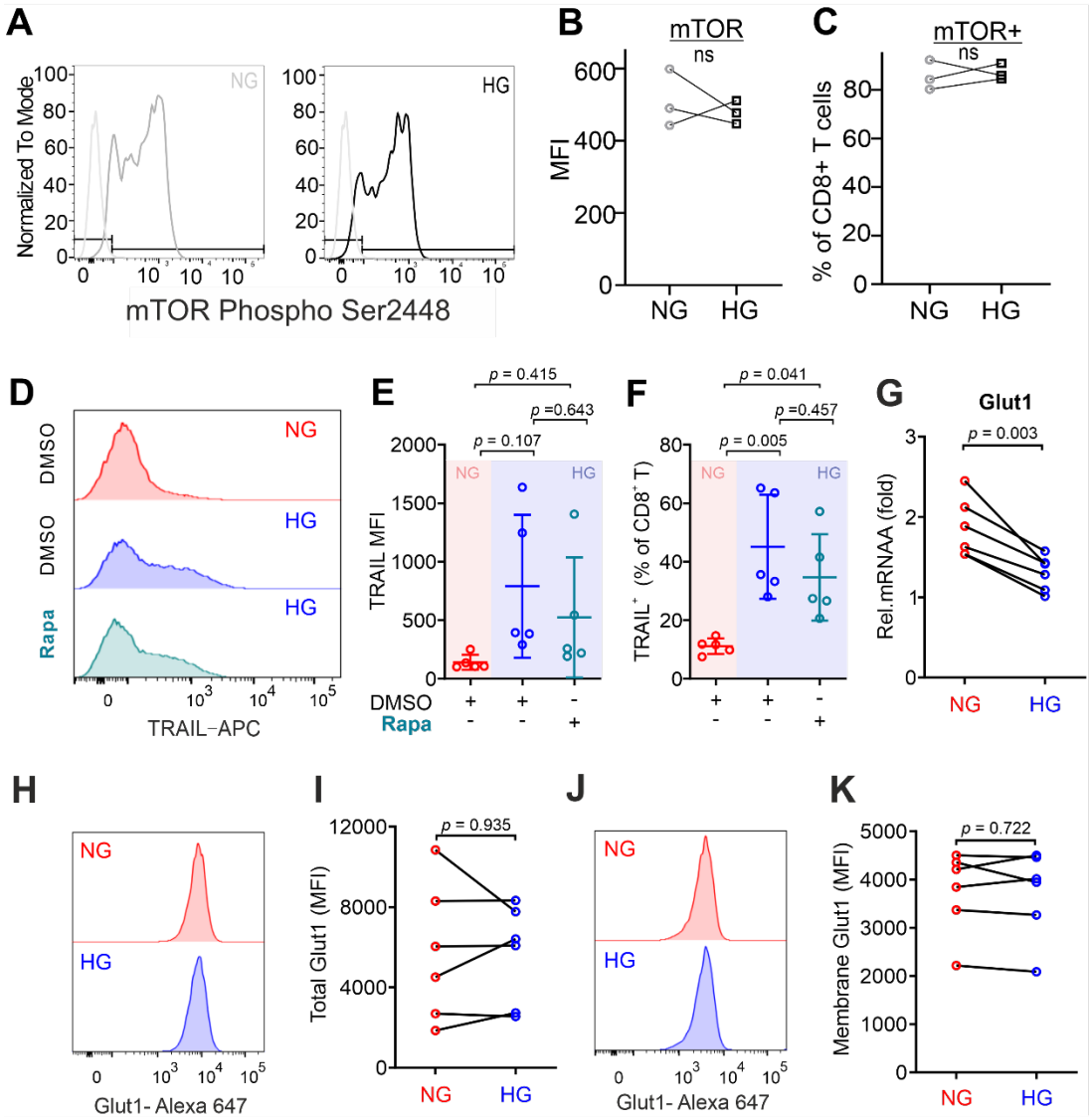

Figure 12. Neither mTOR nor glucose transporters contribute to the reprogrammed metabolism in CTLs by HG. (A-C) Human PBMCs were stimulated with CD3/CD28 T cell activator beads in NG- or HG medium for three days. Then cells were stained with antibody against CD3, CD8 and PhosphoPair mTOR (Ser2448). One representative donor is shown in **(A)** and quantification is shown in **(B, C)** (n = 3 donors from two independent experiments). **(D-F)** mTOR is not involved in HG-enhanced TRAIL expression in CTLs. Primary human $CD8^+$ T cells were stimulated with CD3/CD28 antibody-coated activator beads for three days in NG (5.6 mM) or HG (25 mM) in presence or absence of mTOR inhibitor Rapamycin (600 nM, n = 5 donors from three independent experiments). Representative donor is shown in **(D)** and quantification is shown in **(E, F)**. **(G-K)** Glucose transporter is not changed by HG. Primary human $CD8^+$ T cells were stimulated with CD3/CD28 beads for three days in NG (5.6 mM) or HG (25 mM) medium. **(G)** Expression of Glut1 in CTLs at the mRNA level was quantified by qRT-PCR (n = 6 donors from three independent experiments). **(H-K)** Determination of total and membrane Glut1 in CTLs at the protein level by flow cytometry. **(H, J)** One representative donor showing the total **(H)** and membrane Glut1 **(J)** in CTLs. **(I, K)** Flow cytometric analysis of total **(I)** (n = 6 from four independent experiments) and membrane Glut1 **(K)** (n = 6 from three independent experiments). Data represent Mean ± SD and were analysed by two-tailed paired Student's t test **(B, C, G, I, K)** or one-way ANOVA with Bonferroni's multiple comparison test **(E, F)**. Figure and legend modified from [172].

4.13. Glucose transports are not affected by HG in CTLs in microarray data

To have an in-depth understanding of genes influenced by HG, we analysed transcriptomes between NG-cultured CTLs and HG-cultured CTLs (**Data are not shown here**). We first analysed all glucose transporters expression. The results showed that SLC2A1/Glut1, SLC2A3/Glut3 and SLC2A14/Glut14 were mainly expressed in CTLs, and the expression of Glut1 was moderately down-regulated in HG-cultured CTLs compared with the expression of Glut1 in NG-cultured CTLs **(Figure 13)**, which is consistent with what we observed from quantitative PCR **(Figure 12G)**. The difference in Glut3/SLC2A3 and Glut14/SLC2A14 is marginal. Thus, from the figure 12 and figure 13, we can conclude that glucose transports are unlikely to be responsible for HG-enhanced TRAIL expression in CTLs.

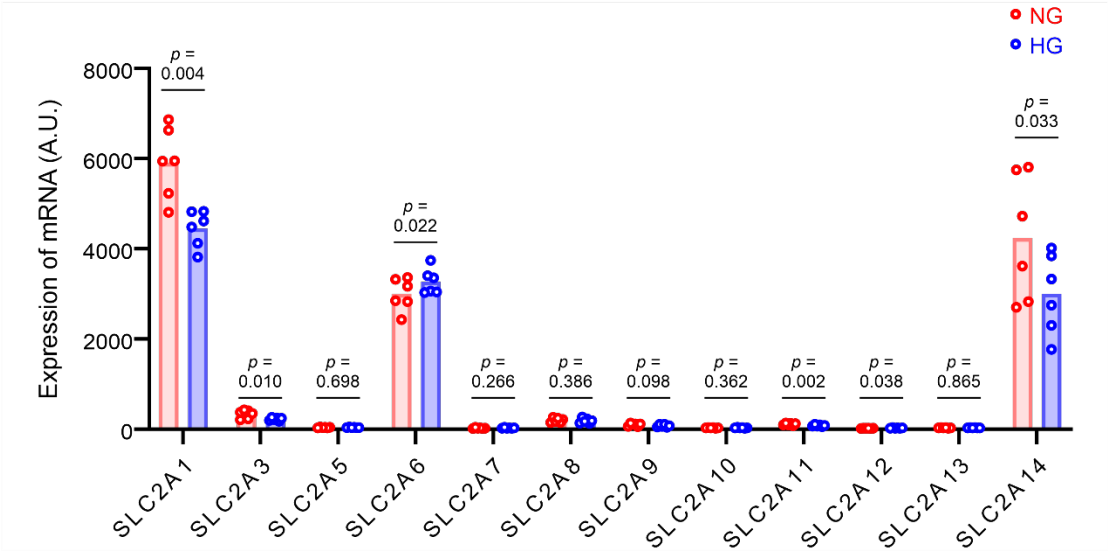

Figure 13. Glucose transporters expression in the Microarray data. The transcriptomics data of glucose transporters expression at the mRNA level, n = 6 from five independent experiments and two independent microarray analyses. A.U. represents arbitrary units. Data represent Mean ± SD and were analyzed by two-way ANOVA with Bonferroni's multiple comparison test. Figure and legend modified from [172].

4.14. ROS is likely to be involved in HG-induced TRAIL expression in CTLs

Regarding the enriched GO terms, the cellular metabolism changed significantly. We compared the samples of HG- to NG- CTLs and found that many genes related with metabolic processes are substantially altered. Among these genes, there are totally 58 are significantly upregulated and 47 are significantly down-regulated (**Data are not shown fere**). Furthermore, 6 genes that are annotated with the ROS metabolism are significantly deregulated (**Data are not shown here**). Additionally, ROS is also an important by-product of oxidative phosphorylation and glycolysis, we next investigated the possible role of ROS in HG-regulated TRAIL expression in CTLs. We detected ROS production using DCFDA [175]. DCFDA is a fluorogenic dye that measures reactive oxygen species (ROS) activity within the living cells. Once DCFDA diffuse into the cell, it can be deacetylated to a non-fluorescent compound by cellular esterases. The compound is then oxidized by ROS into DCF, which is extremely fluorescent and can be detected by fluorescent spectroscopy with excitation / emission at 485 nm / 535 nm. In our results, we found that upon activation, HG-cultured CTLs produced more ROS than their counterparts in NG **(Figure 14A, B)**. These findings suggest that ROS may be involved in HG-regulated CTL function. To further explore the role of ROS in HG-enhanced TRAIL expression, we stimulated primary human $CD8^+$ T cells with CD3/CD28 antibody-coated beads in addition of different concentrations of H_2O_2, a relatively stable form of ROS. Interestingly, we found that compared to the control group, with 1 μM H_2O_2 treatment, the percentage of $TRAIL^+$ CTLs was increased in

NG-CTLs, but the MFI is statistically not significant. With 3 μM H_2O_2 treatment, both percentage of $TRAIL^+$ CTLs and MFI were elevated in NG-CTLs. While with 10 μM H_2O_2 treatment, the percentage of $TRAIL^+$ CTLs and MFI were also increased, but statistically not significant **(Figure 14C-E)**. Whereas neither percentage of $TRAIL^+$ CTLs nor MFI was remained changed by H_2O_2 treatment in HG-CTLs. These results imply that HG-enhanced TRAIL expression is likely via the enhanced ROS in CTLs.

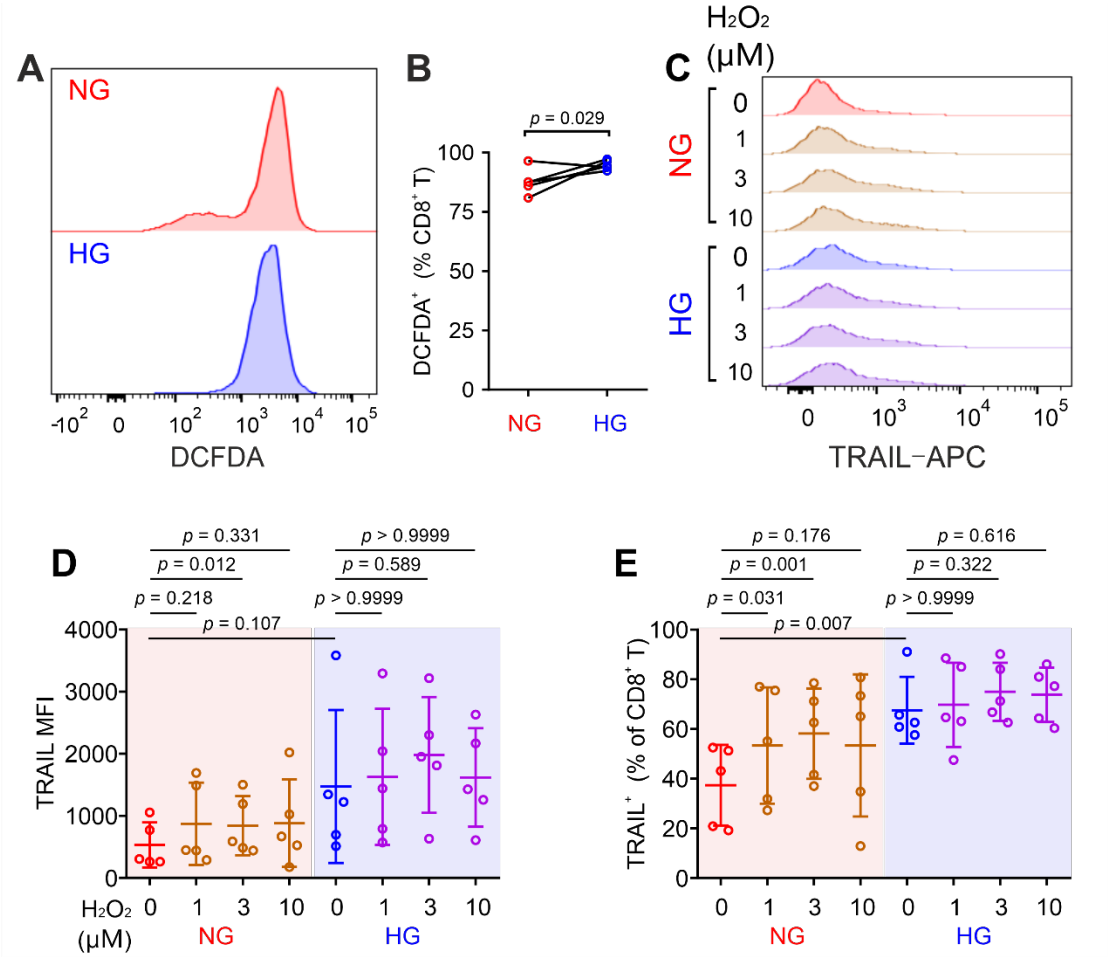

Figure 14. ROS was likely to be involved in HG-enhanced TRAIL expression in CTLs. (A, B) Determination of ROS production at 6 hours after CD3/CD28 activator beads stimulation by cellular ROS assay-DCFDA. One representative donor is shown in **(A)** and quantification is shown in **(B)** (n = 5 donors from three independent experiments). **(C, D)** H_2O_2 treatment increases the expression of TRAIL in NG-cultured CTLs. Primary human $CD8^+$ T cells were stimulated with CD3/CD28 antibody-coated beads in presence of indicated concentration of H_2O_2 for three days. One representative donor is shown in **(C)** and quantification is shown in **(D, E)** (n = 5 from three independent experiments). Results are represented as Mean ± SD. Data were analysed by two-tailed paired Student's t test **(B)** or one-way ANOVA with Bonferroni's multiple comparison test **(D, E)**. Figure and legend modified from [172].

4.15. Abruption of mitochondrial-produced ROS does not influence the TRAIL expression in HG-CTLs

As shown in Figure 14, TRAIL expression was upregulated in HG-cultured CTLs in the presence of ROS. We supposed that ROS play an essential role in TRAIL expression. To verify this hypothesis, we used ROS scavengers mitochondrial targeted antioxidant MitoQ to treat the $CD8^+$ T cells for three days and tested TRAIL expression by flow cytometry. As shown in figures, when mitochondrial produced ROS was removed by MitoQ in HG-CTLs, the TRAIL expression did not significantly alter **(Figure 15A-C),** suggesting that mitochondrial ROS is not involved in the HG-induced TRAIL expression in CTLs.

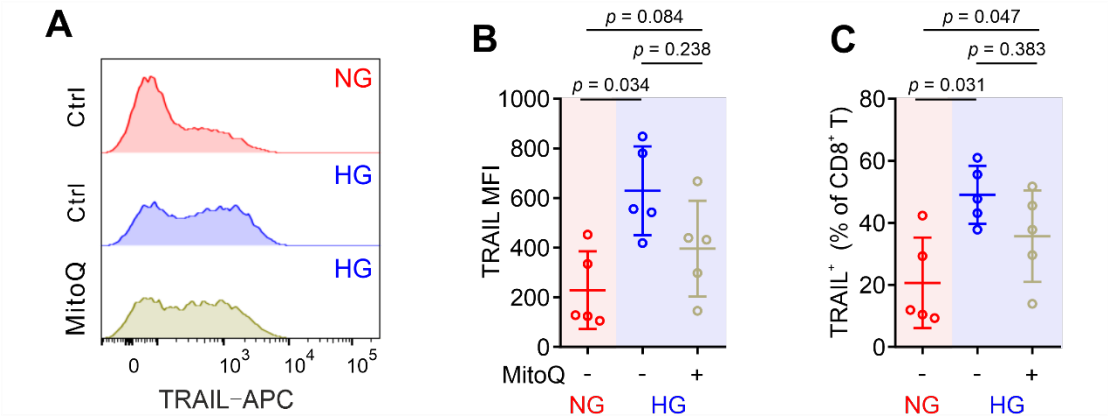

Figure 15. Abruption of ROS production in mitochondrial does not inhibit TRAIL expression in HG-CTLs. Primary human $CD8^+$ T cells were stimulated with CD3/CD28 T cell activator beads for three days in presence of MitoQ (0.4 µM, n = 5 from three independent experiments). Representative donor is shown in **(A)** and quantification of TRAIL expression is shown in **(B, C)**. Results are represented as Mean ± SD. Data were analyzed by one-way ANOVA with Bonferroni's multiple comparison test **(B, C)**. Figure and legend modified from [172].

4.16. Removement of cytosolic ROS inhibit the TRAIL expression in HG-CTLs

We next tested whether cytosolic ROS is involved in the TRAIL expression in CTLs. We used ROS scavengers NAC (N-acetyl-L-cysteine) which has a general inhibition

effect. As shown in figures, when ROS production produced in cytosol was inhibited by NAC, TRAIL expression was significantly reduced in HG-CTLs to the level of TRAIL expression in NG-CTL **(Figure 16A-C)**. Thus, we suggest that cytosolic ROS plays a major role in HG-enhanced TRAIL expression in CTLs.

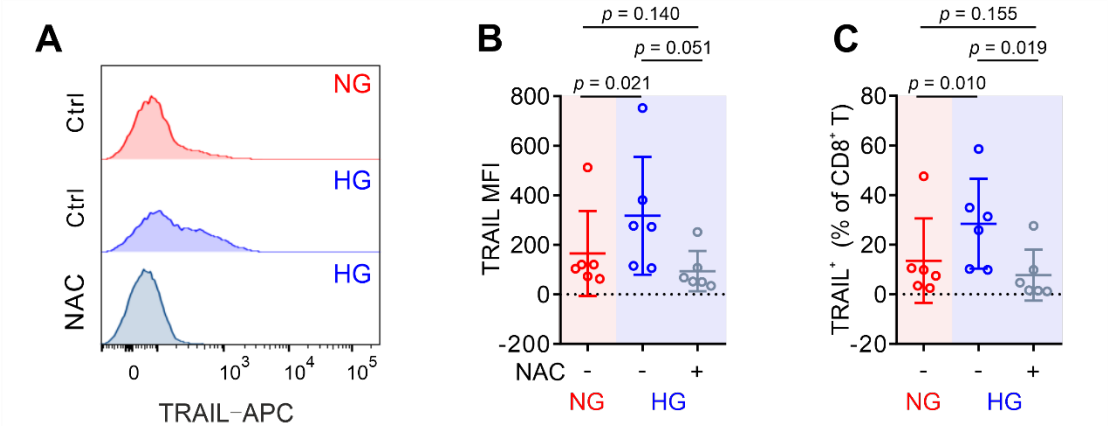

Figure 16. Abruption of cytosolic ROS production inhibit TRAIL expression in HG-CTLs. Primary human $CD8^+$ T cells were stimulated with CD3/CD28 antibody-coated beads for three days in presence of NAC (10 mM, n = 6 donors from three independent experiments). Representative donor is shown in **(A)** and quantification of TRAIL expression is shown in **(B, C)**. Results are represented as Mean ± SD. Data were analyzed by one-way ANOVA with Bonferroni's multiple comparison test **(B, C)**. Figure and legend modified from [172].

4.17. TRAIL is associated with "positive regulation of IκB kinase/NFκB signalling"

To further explore whether other molecules are also involved in regulating TRAIL expression in CTLs by HG, we did an analysis for the KEGG pathway in view of transcriptome data **(Figure 17A)**. This analysis showed 11 genes that were significantly up-regulated, and KEGG pathway *apoptosis* annotated TRAIL (synonym name TNFSF10) in HG samples **(Data are not shown here)**. In the top10 GO terms which is influenced by HG, TRAIL is associated with "IκB kinase/NFκB signalling" and "apoptotic process", both of which are involved in positive regulation **(Figure 17B)**.

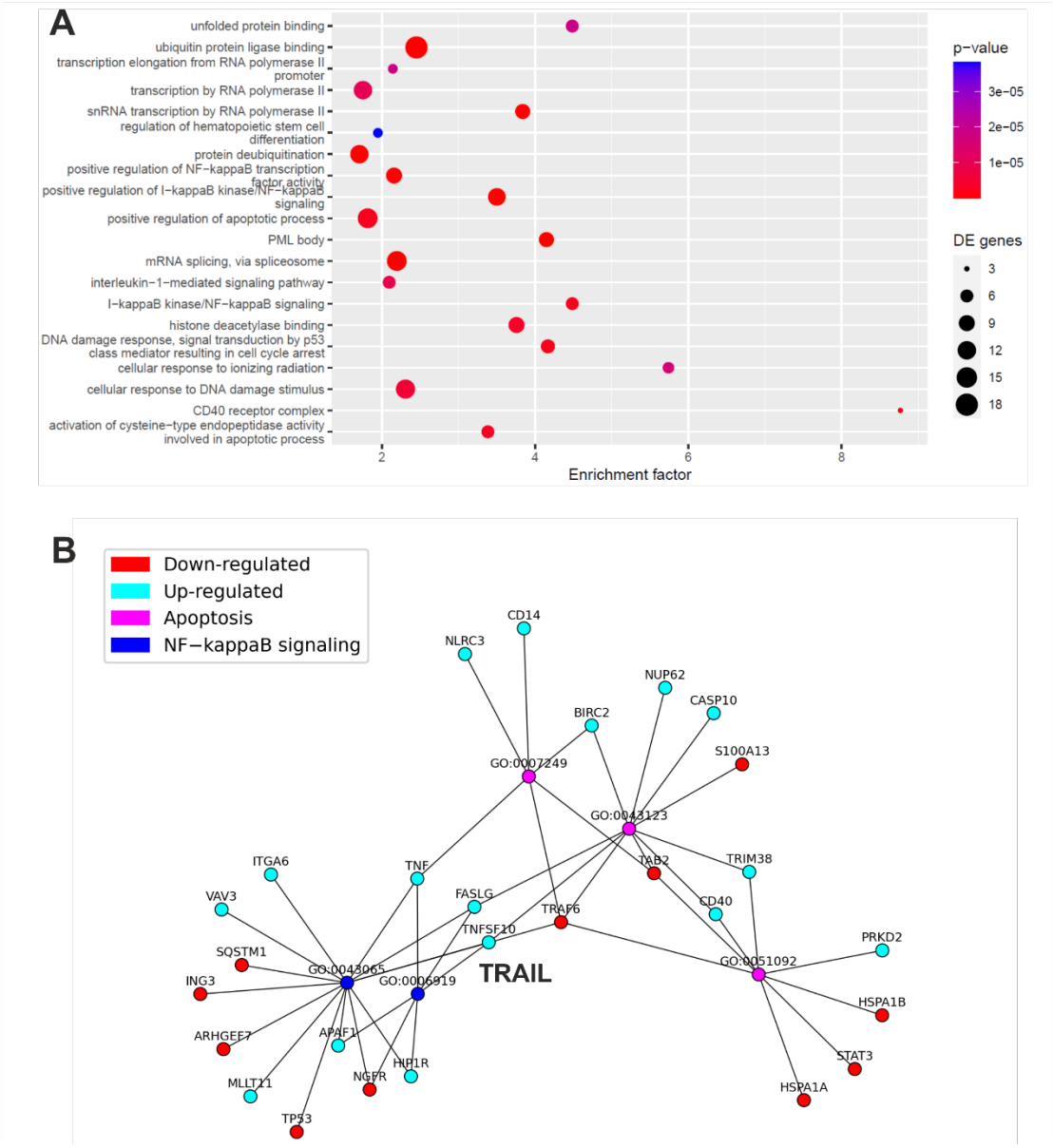

Figure 17. TRAIL is associated with "IκB kinase/NFκB signalling" and "apoptotic process"**. (A)** Comparison of enriched KEGG pathways between NG and HG conditions. **(B)** 10 most significantly enriched/exhausted Gene ontology terminology under HG and NG medium. Determination for the enrichment was carried out by the *pathfindR* package. A sub-network of human protein-protein interplay network was established that included only significantly differential expressed genes. The enrichment factor for an annotation is computed as the fraction of proteins in the sub-network with this annotation relative to the entire network. Figure and legend modified from [172].

4.18. HG-induced TRAIL expression in CTLs is regulated by NFκB pathway

Additionally, it also reported that high glucose is involved in inflammation via NF-kB signalling pathway [176]. We then tested whether NFκB is involved in HG-enhanced

TRAIL expression in CTLs. Primary human CD8$^+$ T cells were stimulated with CD3/CD28 antibody-coated beads with NFκB specific inhibitor CAPE treatment. We found NFκB activity inhibition by its corresponding inhibitor significantly reduced expression of TRAIL in HG-CTLs compared to vehicle-treated cells **(Figure 18A-C)**. This effect was verified by the other NFκB inhibitor MG-132 **(Figure 18D-F)**. These results suggest that NFκB is essential for TRAIL expression in CTLs.

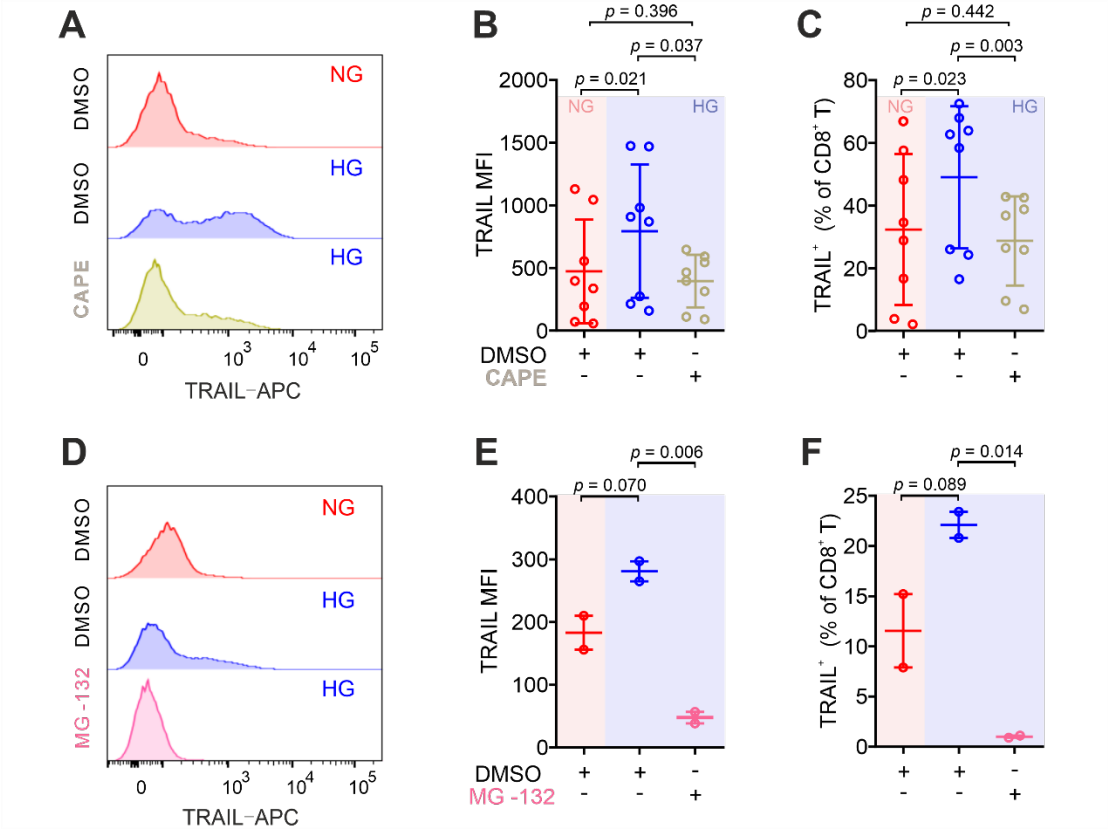

Figure 18. Enhancement of TRAIL in CTLs by HG is regulated by NFκB pathway. Primary human CD8$^+$ T cells were stimulated with CD3/CD28 T cell activator beads for three days in NG (5.6 mM) or HG (25 mM) with NF-κB specific inhibitor CAPE treatment (**A-C**, 5 μM, n = 8 donors from three independent experiments), MG-132 (**D-F**, 250nM, n = 2 donors from one independent experiments). Representative donors for CAPE, MG-132 are shown in **A** and **D**, respectively. Quantifications for CAPE and MG-132 are in **B, C and E, F**, respectively. Data are represented as Mean ± SD and *p* values were assessed by one-way ANOVA with Bonferroni's multiple comparison test. Figure and legend modified from [172].

4.19. TRAIL expression is regulated by PI3K/Akt pathway

Functions of NFκB can be regulated through PI3K-Akt pathway [177]. We therefore

block PI3K activity using PI3Kδ inhibitor idelalisib. We found that disruption of PI3K function decreased the TRAIL expression **(Figure 19A-C)**. We next investigated the the downstream molecule of PI3K: Akt. We blocked Akt activity using its inhibitor MK-2206, and we found that abruption of Akt function abolished the expression of TRAIL in HG-CTLs **(Figure 19D-F)**. Taken together, our results demonstrated that PI3K/Akt and NFκB pathway regulated HG-enhanced TRAIL expression in CTLs.

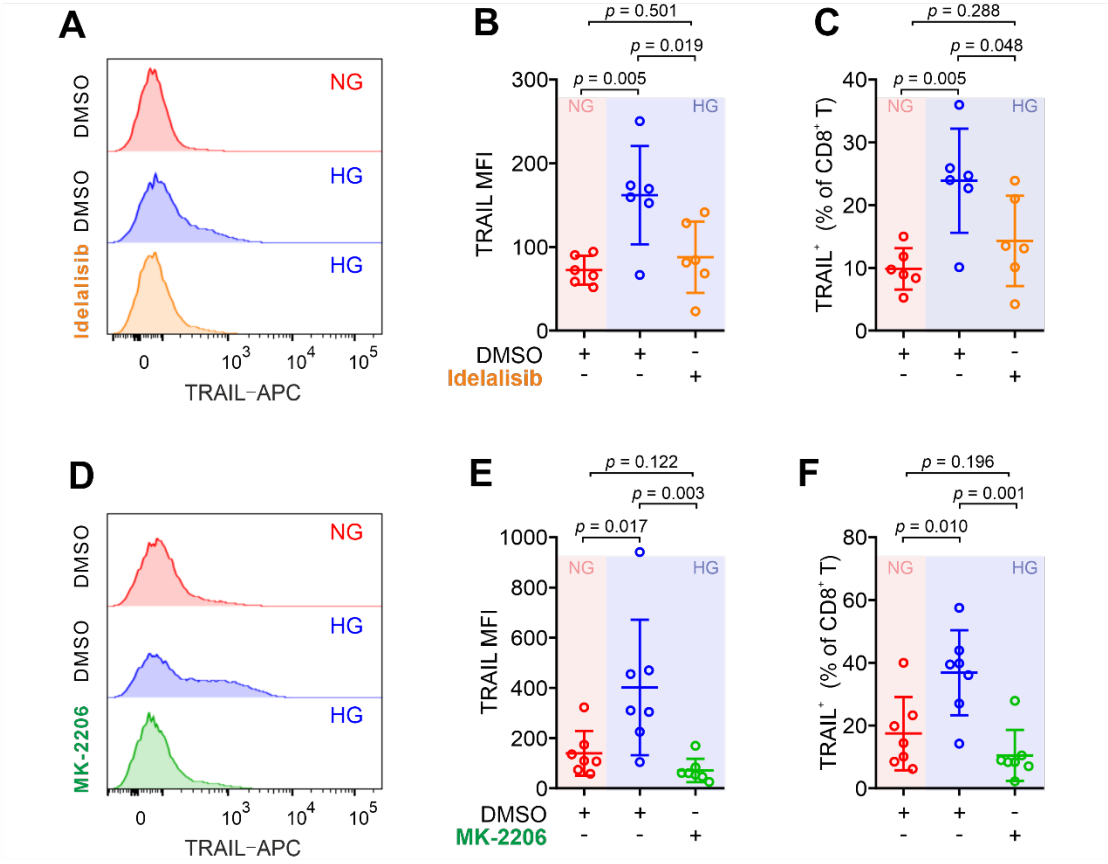

Figure 19. Enhancement of TRAIL in CTLs by HG is regulated by PI3K/Akt pathway. Primary human $CD8^+$ T cells were stimulated with CD3/CD28 activator beads for three days in NG (5.6 mM) or HG (25 mM) in presence or absence of PI3K inhibitor Idelalisib (**A-C**, 300 nM, n = 6 donors from three independent experiments) or Akt inhibitor MK-2206 (**D-F**, 200 nM, n = 7 donors from four independent experiments). Representative donors for Idelalisib and MK-2206 are shown in **A** and **D**, respectively. Quantifications for Idelalisib and MK-2206 are shown in **B, C** and **E, F**, respectively. Data are represented as Mean ± SD and *p* values were assessed by one-way ANOVA with Bonferroni's multiple comparison test. Figure and legend modified from [172].

4.20. Metformin down-regulate HG-induced TRAIL expression

Since HG-enhanced TRAIL expression could induce the destruction of human pancreatic beta cell as shown above **(Figure 8)**, we sought for possible therapeutical approaches to reduce TRAIL expression to protect pancreatic beta cells. We first examined the effect of metformin on the regulation of TRAIL in CTLs. Primary human $CD8^+$ T cells were stimulated with addition of metformin for three days. And we tested TRAIL expression by flow cytometry. Our data showed that metformin can substantially decreased HG-enhanced TRAIL expression in CTLs in a dose-dependent manner (**Figure 20A-C**). This result suggest that metformin can protect pancreatic beta cells from TRAIL-mediated apoptosis.

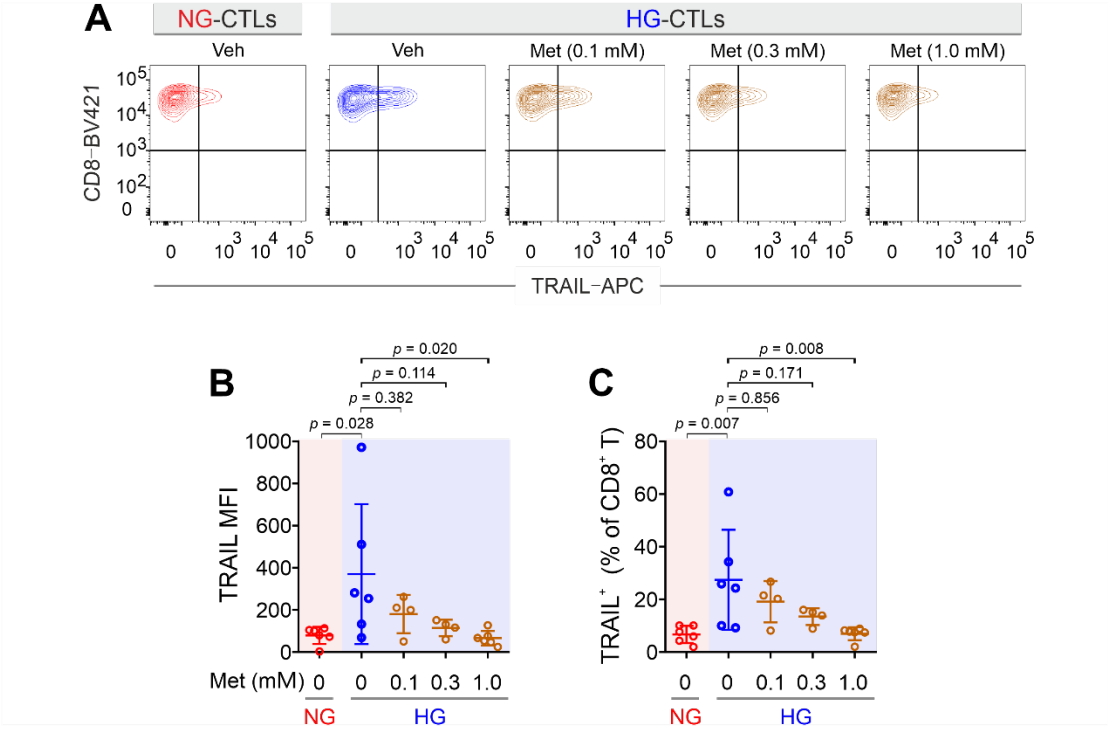

Figure 20. Metformin down-regulate the HG-induced TRAIL expression in CTLs. Primary human $CD8^+$ T cells were stimulated with CD3/CD28 beads for three days in presence of metformin (met) with indicated concentrations mentioned above. TRAIL expression was analyzed by flow cytometry. Representative donor is shown in **A**. Quantification is shown in **B, C** (n = 4-6 donors from four independent experiments). Data are represented as Mean ± SD and *p* values were assessed by one-way ANOVA with Bonferroni's multiple comparison test. Figure and legend modified from [172].

4.21. HG-inducd TRAIL expression in CTLs could be down-regulated by vitamin D

In addition to metformin, vitamin D has also been reported to be associated with glucose metabolism [178] [179], protection of pancreatic beta cells [180], diabetes [181]and HG-regulated cell functions [182]. We then tested if vitamin D has a similar effect on the TRAIL regulation in CTLs. To this end, we stimulated primary human $CD8^+$ T cells with CD3/CD28 activator beads in NG (5.6 mM) or HG (25 mM) medium with treatment of different concentration of 1,25 D3 for three days, and analysed TRAIL expression by flow cytometry. The results showed that the enhancement of TRAIL expression by HG in CTLs was markedly down-regulated by 1,25D3 in a dose-dependent manner **(Figure 21A-C)**. Our data suggest that vitamin D pathway plays a vital role in regulation of HG-enhanced TRAIL expression in CTLs. Calcipotriol (Cal), a man-made vitamin D analogue, has a high affinity with vitamin D receptor. There exist some big functional similarities between Cal and the natural vitamin D3 at the cellular level. Cal shows dual functions in pancreatic cancer, showing anti-tumour activity but also suppress T cell effector function [183]. In our work, we also want to know the impact of Cal on the regulation of TRAIL expression in CTLs. we stimulated primary human $CD8^+$ T cells with CD3/CD28 activator beads in NG (5.6 mM) or HG (25 mM) medium in the addition of different concentration of Cal for three days and analysed TRAIL expression by flow cytometry. Interestingly, we found that nanomolar concentration of Cal was sufficient to reduce the enhancement of TRAIL expression induced by HG in CTLs **(Figure 21D-F)**.

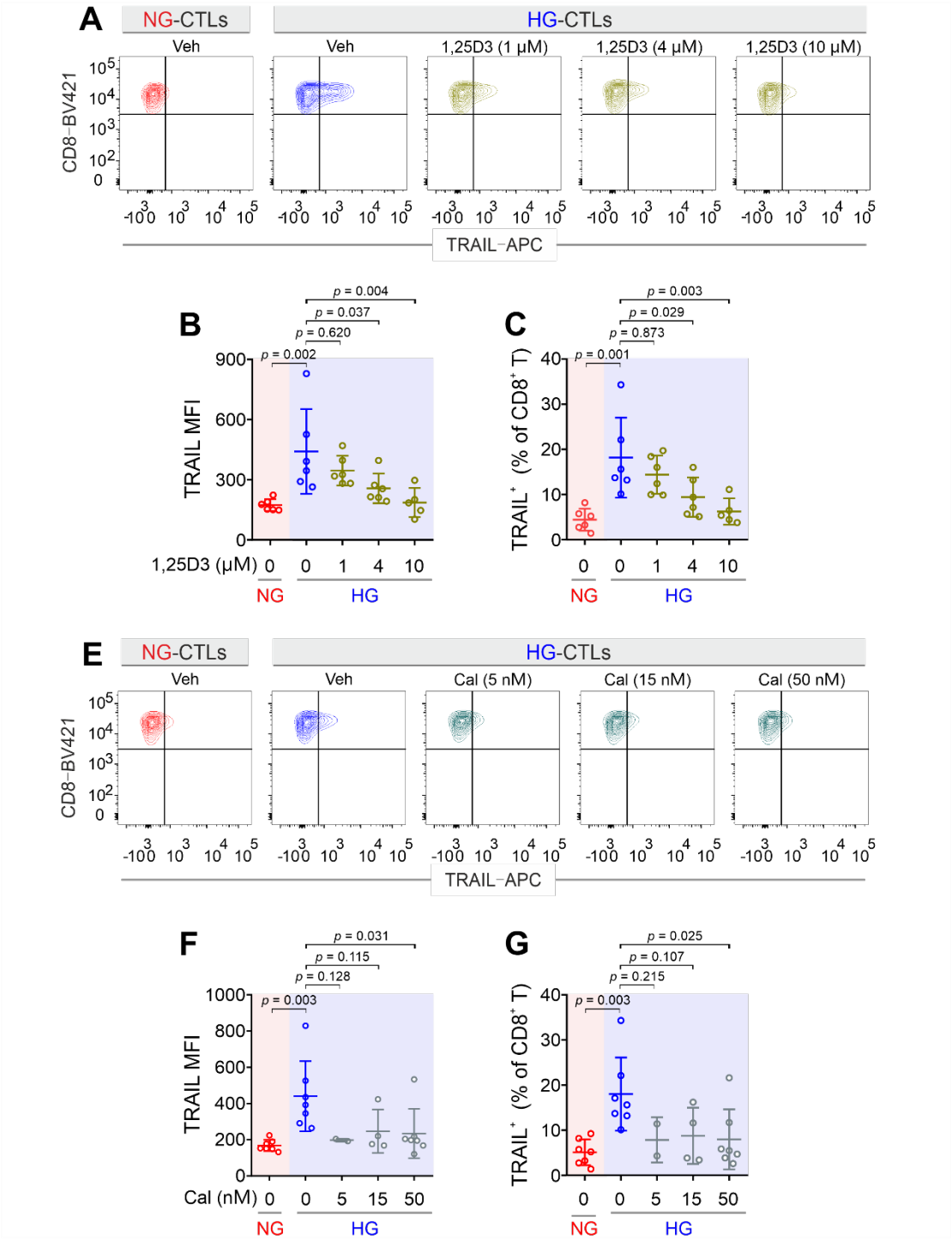

Figure 21. Vitamin D down-regulate the HG-induced TRAIL expression in CTLs. Primary human CD8$^+$ T cells were stimulated with CD3/CD28 beads for three days with treatment of vitamin D (1,25 D3) or calcipotriol (Cal) at indicated concentrations shown above. Expression of TRAIL was evaluated by flow cytometry. (**A-C**) The enhancement of TRAIL by HG in CTLs could be reduced by vitamin D (n = 5-6 donors from four independent experiments). (**D-F**) Treatment of calcipotriol decreased the expression of TRAIL induced by HG (n = 2-7 donors from four independent experiments). Representative donors are shown in **A** and **D**. Quantifications are shown in **B, C** and **E, F**, respectively. Data are represented as Mean ± SD and *p* values were assessed by one-way ANOVA with Bonferroni's multiple comparison test. Figure and legend modified from [172].

4.22. Combination of metformin and vitamin D could further down-regulate TRAIL expression in CTLs

Since metformin and vitamin D could reduce the enhancement of TRAIL expression by HG in CTLs, we next tested if they could function synergistically. We stimulated primary human $CD8^+$ T cells with CD3/CD28 activator beads in the medium of NG (5.6 mM) or HG (25 mM) in the presence of the intermediate concentration of met (0.3 mM) and 1,25 D3 (4 µM), as the decreasing of TRAIL expression was moderate in both conditions **(Figure 20/21B, C)** and analysed TRAIL expression by flow cytometry. Interestingly, we found that combination of metformin and vitamin D could further down-regulate HG-enhanced TRAIL expression in CTLs **(Figure 22A-C)**.

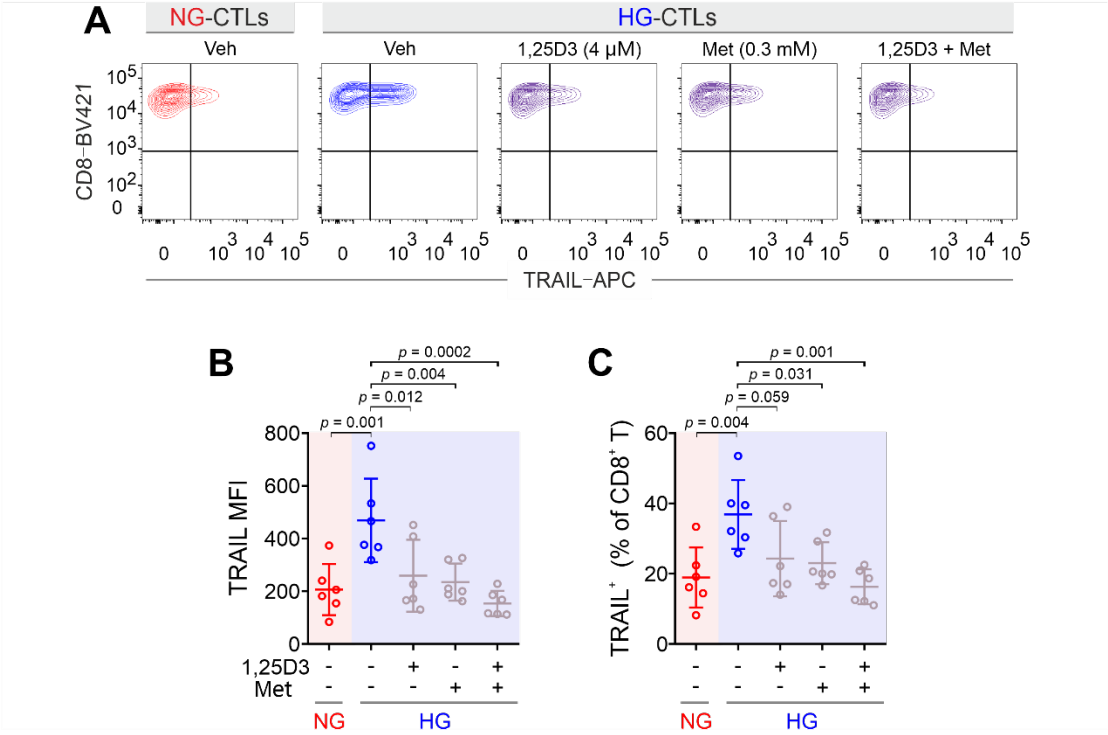

Figure 22. Combination of metformin and vitamin D down-regulate the HG-induced TRAIL expression in CTLs. Primary human $CD8^+$ T cells were stimulated with CD3/CD28 beads for three days with metformin and vitamin D treatment at indicated concentrations. TRAIL expression was analyzed by flow cytometry. Representative donor is shown in **A**. Quantification is shown in **B, C** (n = 6 donors from four independent experiments). Data are represented as Mean ± SD and *p* values were assessed by one-way ANOVA with Bonferroni's multiple comparison test. Figure and legend modified from [172].

4.23. T cell activation and cell viability was not affected by metformin and vitamin D treatment

We next analysed whether vitamin D or/ and metformin treatment could affect T cell activation or viability. T cell activation marker includes CD25, CD69, CD62L and CD44. CD25, the alpha chain of IL-2 receptor, is identified as the most renowned activation marker on the cell surface. It is expressed on resting memory and regulatory T cells. Its expression is enhanced within 24 hours after stimulation and maintains elevated state for a few days [184]. CD69 is a classical early activation marker [185]. CD62L, also termed L-selectin, play a critical role in the trafficking of T cell [186]. CD44 is an outstanding activation marker and can distinguish effector and memory T cells from the naïve [187]. We examined these mentioned-above activation marker expression in $CD8^+$ T cells after stimulation and treatment with metformin or/ and vitamin D for three days by flow cytometry. The results showed that treatment of metformin and vitamin D does not affect the T cell activation (**Figure23A-E**). We next also want to get knowledge of whether vitamin D or/ and metformin treatment influence the activity of $CD8^+$ T cells per se. we used 7-Aminoactinomycin D (7-AAD) assay. 7-AAD is a DNA dye that can distinguish live, apoptotic, and dead cells by flow cytometry. Primary human $CD8^+$ T cells were stimulated in presence of indicated concentrations of metformin or/ and vitamin D for three days. And we stained cells with 7-AAD staining solution and analysed the 7-AAD using flow cytometry. From the data, we found that the activity of $CD8^+$ T cells were not affected by treatment of metformin or/ and vitamin D.

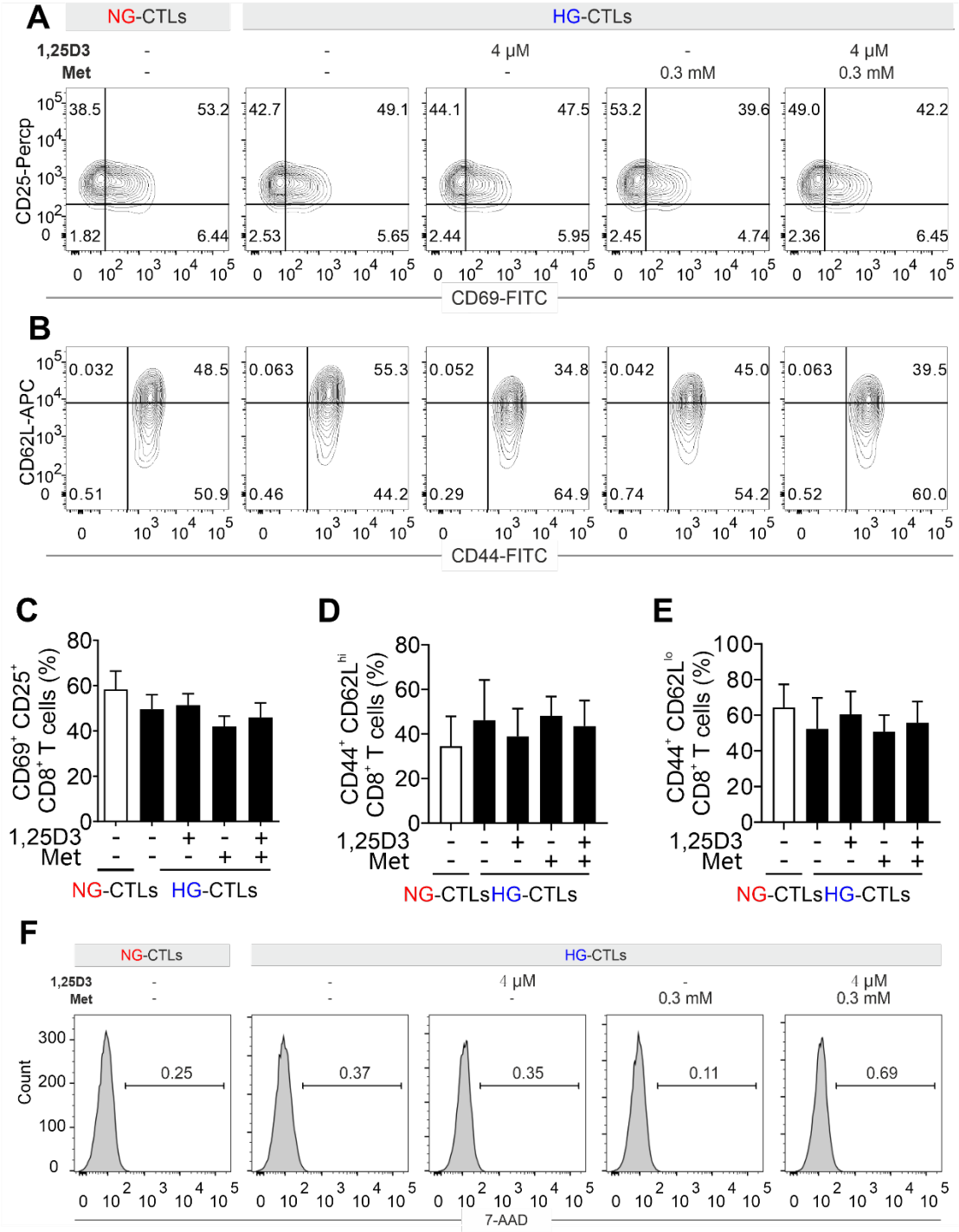

Figure 23. T cell activation and cell viability was not affected by metformin and vitamin D. Primary human CD8$^+$ T cells were stimulated with CD3/CD28 activator beads for three days in addition of vitamin D, metformin, or combination of vitamin D and metformin at indicated concentrations. **(A-E)** Assessment of the activation of CD8$^+$ T cells by staining activation marker (n = 3-4 donors). **(F)** Determination of CD8$^+$ T cells apoptosis by staining 7-AAD. Data are represented as Mean ± SD. All data were analyzed by one-way ANOVA with Bonferroni's multiple comparison test. Figure and legend modified from [172].

4.24. Combination of metformin and vitamin D could also reduce TRAIL expression in CTLs from healthy individuals

Additionally, we also examined the regulation of metformin and vitamin D on TRAIL expression in CTLs from healthy individuals. Isolated PBMCs were stimulated with CD3/CD28 activator beads in the NG or HG medium for three days. TRAIL expression was determined by flow cytometry. The data showed that the expression of TRAIL in CTLs from health was reduced by 1,25D3 (**Figure 24A, B**), met **(Figure 24C, D)** in a dose-dependent manner. And combination of met and 1,25D3 could further reduce the expression of TRAIL in CTLs from healthy individuals (**Figure 24E, F**).

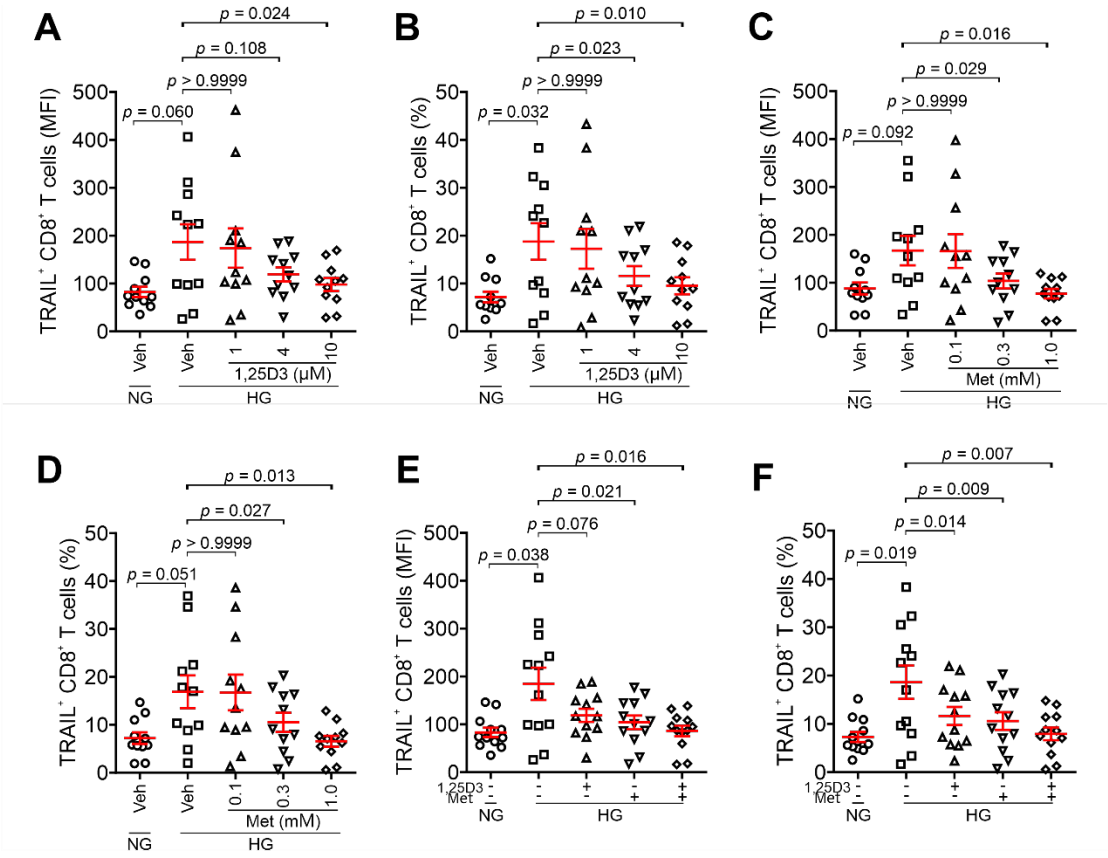

Figure 24. Vitamin D and/or metformin down-regulate HG-induced TRAIL expression in CTLs from healthy individuals. PBMCs isolated from healthy individuals were stimulated with CD3/CD28 beads in presence of vitamin D (1,25D3, **A**, **B**), metformin (Met, **C**, **D**), Met (300 μM) and/or 1,25D3 (4 μM) **(E, F)** for three days. TRAIL expression was assessed by flow cytometry. Data are represented as Mean ± SEM. All data were analysed by one-way ANOVA with Bonferroni's multiple comparison test.

4.25. Metformin and vitamin D could protect pancreatic beta cells from TRAIL-mediated apoptosis

The data we discussed above showed that metformin and/or vitamin D could down-regulate the HG-enhanced TRAIL expression both in CTLs and CTLs from healthy individuals. And the finding in **Figure 8** also demonstrated that high glucose enhanced the killing capacity against pancreatic beta cell, which is in a TRAIL-dependent manner. Based on these two findings above, we next want to know if metformin or vitamin D could protect pancreatic beta cells from TRAIL-mediated apoptosis. In order to do this, we stimulated primary human $CD8^+$ T cells with CD3/CD28 activator beads in the presence of metformin and/or 1,25D3 for three days. Then CTLs were incubated with 1.4E7 beta cells for different time points: 4, 8, and 12 hours, without metformin or vitamin D to avoid the possible potential effect on beta cell per se. After that, the cells were stained with CD3 and caspase-3 substrate and apoptosis of pancreatic beta cells was determined by caspase-3 activity with flow cytometry. From our data, we found that metformin and vitamin D could reduce the TRAIL-mediated beta cell apoptosis at the indicated timepoints **(Figure 25A-D)**. In summary, our results suggest that metformin and vitamin D could protect beta cells apoptosis from HG-induced $TRAIL^{high}$ CTLs *in vitro*.

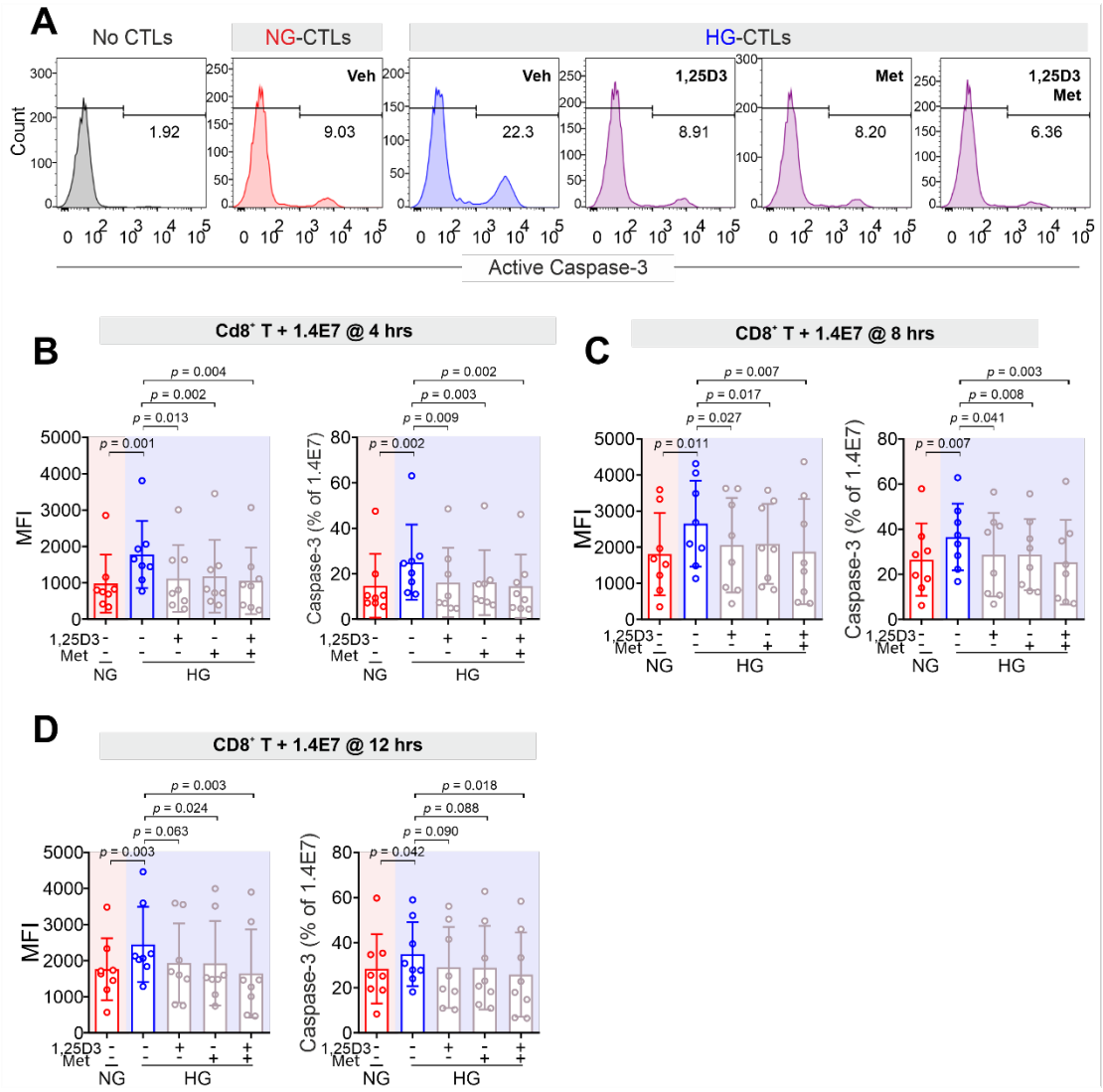

Figure 25. Metformin and vitamin D could protect TRAIL-mediated beta cells apoptosis. Primary human $CD8^+$ T cells were stimulated with CD3/CD28 activator beads for three days with treatment of metformin (met), vitamin D, or combination of metformin and vitamin D with indicated concentrations. Apoptosis of beta cells was determined by activity of caspase-3. **(A)** One representative donor showing the apoptosis of beta cells at 4 hours. (**B-D**) Quantification of apoptosis of beta cells at 4 hour **(B)** (n = 8 donors from six independent experiments), 8 hours **(C)** (n = 8 donors from seven independent experiments) and 12 hours **(D)** (n = 8 donors from six independent experiments). Results are represented as Mean ± SD. One-way ANOVA with Bonferroni's multiple comparison test was applied for statistical analysis. Figure and legend modified from [172].

4.26. Metformin and Vitamin D can also regulate TRAIL expression in diabetic CTLs from the patients

Next, we tested whether metformin and vitamin D can also regulate the expression of TRAIL in diabetic CTLs from the patients. We isolated PBMCs from the diabetic

patients and stimulated with CD3/CD28 beads in NG or HG medium for three days in the addition of indicated concentrations of vitamin D (1,25D3), Calcipotriol (Cal), metformin (Met), or Metformin (300 µM) and/or 1,25D3 (4 µM) and analysed the TRAIL expression by flow cytometry. The results showed that the expression of TRAIL in diabetic CTLs was reduced by 1,25D3 (**Figure 26A, B**), Cal (**Figure 26C, D**) and metformin (**Figure 26E, F**) in a dose-dependent manner. And the combination of metformin and 1,25D3 could further reduce the expression of TRAIL in diabetic CTLs (**Figure 26G**).

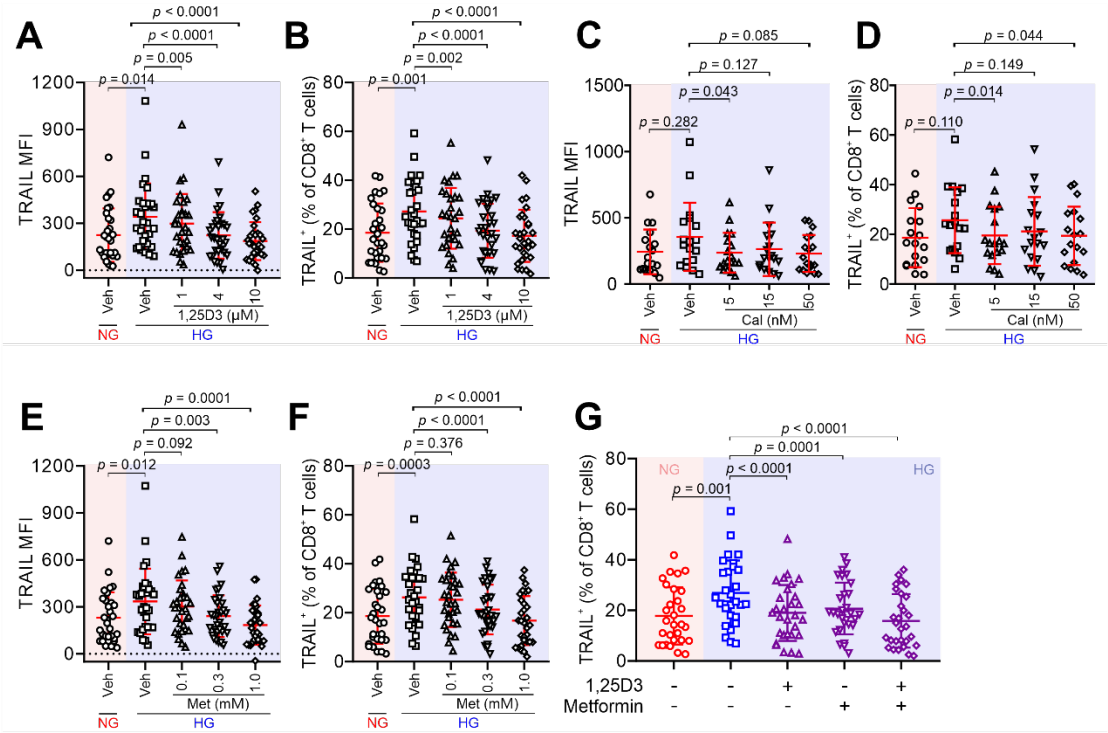

Figure 26. Metformin and vitamin D down-regulate the expression of TRAIL in CTLs from diabetic patients. PBMCs were isolated from diabetic patients and stimulated with CD3/CD28 T cell activator beads with treatment of vitamin D (1,25D3, **A, B**), Calcipotriol (Cal, **C, D**), metformin (Met, **E, F**), or Metformin (300 µM) and/or 1,25D3 (4 µM) (**G**) for three days in NG (5.6 mM, pink shade) or HG (25 mM, blue shade) medium. TRAIL expression was assessed by flow cytometry. Data are represented as Mean ± SD (1,25D3 n = 30; Cal n = 18; Met n = 31; Met and/or 1,25D3 n = 29 from 21, 14, 23, 21 independent experiments). All *p* values were assessed by one-way ANOVA with Bonferroni's multiple comparison test. Figure and legend modified from [172].

4.27. Medicine taking itself can affect the regulation of metformin or 1,25 D3 on TRAIL expression in CTLs

Considering some diabetic patients have already taken medicine, we next analysed whether medicine taking itself can affect the regulation of metformin or 1,25 D3 on the TRAIL expression. The patients from the Internal Medicine II, University Hospital Saarland can be divided into three groups: 6 patients have taken vitamin D (1,25D3), 9 patients have taken metformin (Met), and 18 patients have not taken any vitamin D and metformin. As described above, the PBMCs were isolated from these diabetic patients and stimulated by CD3/CD28 activator beads in HG or NG for three days in the presence of indicated concentrations of vitamin D (1,25D3) and metformin (Met). Then TRAIL expression was analysed by flow cytometry. Interestingly, we found that CTLs from diabetic patients not taking any metformin or vitamin D showed marked upregulation of TRAIL under HG conditions (**Figure 27A**), while CTLs from the patients taking metformin showed no difference in TRAIL expression between NG-cultured and HG-cultured CTLs (**Figure 27B**). CTLs from diabetic patients taking vitamin D moderately enhanced TRAIL expression under HG conditions (**Figure 27C)**. For the no metformin and vitamin D taking and only metformin taking group, culturing the diabetic CTLs in HG with metformin treatment further reduced TRAIL expression (**Figure 27D, E**). Likewise, for the no metformin and vitamin D taking and only vitamin D taking group, culturing diabetic CTLs with vitamin D treatment in HG could down-regulated TRAIL expression (**Figure 27F, G**). These findings demonstrate that the HG-enhanced TRAIL expression in CTLs from diabetic patients can be down-regulated by

metformin and vitamin D treatment.

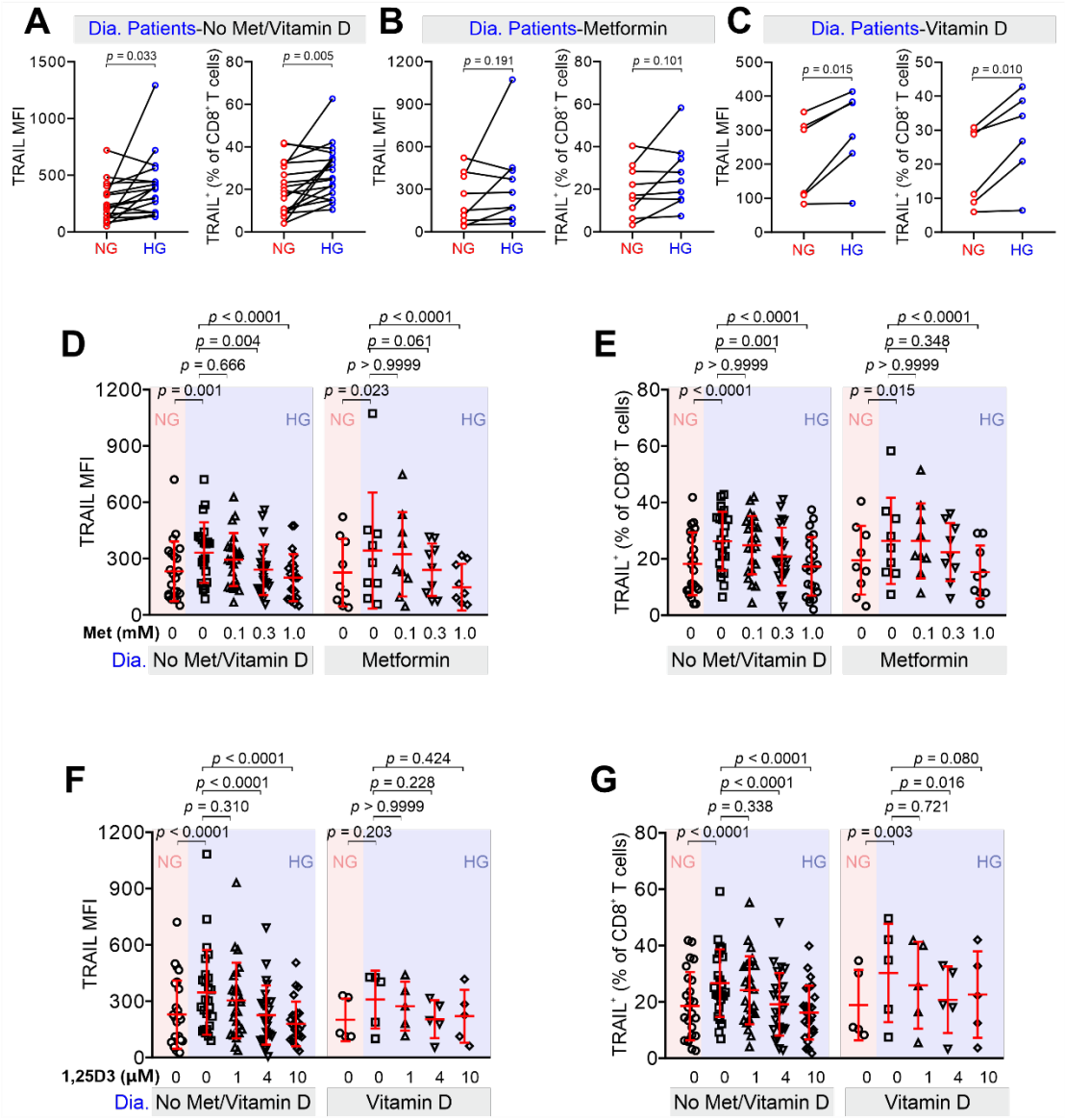

Figure 27. Medicine taking itself can affect the regulation of metformin or 1,25 D3 on the TRAIL expression. Diabetic patients were divided into three groups based on if metformin or vitamin D was taken. PBMCs were isolated from these diabetic patients and stimulated by CD3/CD28 activator beads in HG or NG for three days in the presence of indicated concentrations of vitamin D (1,25D3) and metformin (Met). Then TRAIL expression was analysed by flow cytometry. Data are represented as Mean ± SD. All *p* values were analysed by one-way ANOVA with Bonferroni's multiple comparison test (**A-C**) or two-way ANOVA with Bonferroni's multiple comparison test (**D-G**). Figure and legend modified from [172].

5. Discussion

This work is focused on the regulation of HG on functions of CTLs. And our study demonstrated that HG did not alter the LGs and Fas/FasL pathway. Interestingly, we found that TRAIL expression in CTLs was upregulated by HG *in vitro* and *in vivo*. ROS and PI3K/Akt/NFκB axis are involved in HG-induced enhancement of TRAIL expression in CTLs. $TRAIL^{high}$ CTLs induced the apoptosis of pancreatic beta cells. Metformin and vitamin D could reduce the increased TRAIL expression induced by HG, which therefore further protected pancreatic beta cells apoptosis mediated by $TRAIL^{high}$ CTL in HG.

For diabetes, CTLs play a pivotal and indispensable role in the development and progression of Type 1 DM. Autoimmune CTLs, which recognize self-antigen on beta cells, destroy the insulin-producing pancreatic beta cell through the effector functions, resulting in beta cell destruction, insulin deficiency and hyperglycemia. CTLs, as well as other factors, are also involved in its initiation and development of Type 2 DM. Up to date, the investigations about the role of CTLs in diabetes are mostly focused on the effect of islet autoreactive T cells on Type 1 DM. The impact of HG on CTL functions per se is still not well understood. Previous work from our lab shows that target recognition-induced calcium influx is reduced in HG-cultured CTLs [105]. Dr. Jie Zhu from our group found that HG could enhance the cytotoxicity of CTLs induced by TCR engagement. I found that cytotoxic proteins expression including granzymes, perforin and FasL are not altered by HG. There is also no difference of degranulation and cytokine release between HG and NG group. Migration of CTLs is also not affected by

HG. Interestingly, enhancing extracellular Ca^{2+} concentration diminishes the difference in killing efficiency between NG- and HG-CTLs [104], indicating that Ca^{2+} is involved in HG-enhanced CTL killing induced by TCR. Of note, since the different killing efficiency between NG-cultured and HG-cultured CTLs is not abolished by adding extracellular Ca^{2+}, other mechanisms must also be involved in HG-enhanced CTL killing.

In this work, I have revealed TRAIL as a major mechanism to mediate HG-enhanced CTL cytotoxicity. Besides the apoptotic capacity of TRAIL to cancer cells, TRAIL has also been supported that is involved in the development of diabetes and obesity [188]. TRAIL induce cell apoptosis by ligation with its receptors. In humans, there are four TRAIL receptors including TRAIL-R1, -R2, -R3 and -R4. TRAIL-R1 and -R2 belong to death receptors, which contains cytoplasmic death domain and can induce the cell death. TRAIL-R3 and -R4 are knowns as decoy receptors, which lack of death domain and cannot induce cell apoptosis. The death receptors are highly expressed in many tissues such as adipose, pancreas, kidney, heart. We then examined the TRAIL receptors expression in 1.4E7 pancreatic beta cell. And our results showed that of the four TRAIL receptors, only TRAIL-R2 was mainly expressed in 1.4E7 beta cell. We further tested the TRAIL-mediated cell apoptosis using 1.4E7 beta cell. The results showed that HG-induced enhancement of TRAIL increased apoptosis of pancreatic beta cells. Our findings indicated that CTL-induced destruction of pancreatic beta cells is in a TRAIL-dependent manner. Blockade of TRAIL expression in CTLs may protect pancreatic beta cells from death.

Whether decreasing of TRAIL expression in CTLs could keep beta cells from destruction, or diabetic progression is reduced by TRAIL deficiency? Feeding TRAIL/ApoE double knockout strain mice a high fat diet significantly increased their fasting glucose level compared with TRAIL- or ApoE- mice. Injection of sTRAIL intraperitoneally in mice fed a high-fat diet decreased beta cell damage. Why systemic blockade of TRAIL could deteriorate the progression of diabetes? Strong evidence shows that TRAIL plays an essential role in suppressing the diabetogenic T cells functions, which can recognize the autoantigen on beta cells, causing them to be destroyed. For example, in NOD mice, ablation of TRAIL increased the proliferation of metastatic diabetogenic T cells. Consequently, blockade of TRAIL systematically cannot protect beta cells.

Studies showed that TRAIL expression in T cells could be induced by type I interferons (IFNs, e.g., IFN-α and IFN-β). However, we did not find the difference of IFN-α and IFN-β between HG- and NG-cultured CTLs from the microarray data. It indicated that interferons were not responsible for the enhancement of TRAIL expression by HG in CTLs. More interesting, convincing studies showed that IFN-α play a key role in the initiation of Type 1 DM. IFN-α signaling blocking protect beta cell from destruction by CTLs at prediabetes stage in a mouse model. Therefore, we supposed that before the elevated blood glucose caused by the clinical disease, TRAIL expression could be induced by IFN-α, which resulted in the progression of diabetes.

The cells use glucose to generate energy including oxidative phosphorylation and glycolysis. In addition, it has shown that aerobic glycolysis plays an important role in

the functions of T cells. In our work, we found that OCR and ECAR were increased in HG-cultured CTLs. Some key regulatory pathways in T cells have been reported to modulate the cell metabolic process. The naive $CD8^+$ T cells utilize IL-7 signaling pathway to mediate basal oxidative phosphorylation and glycolysis. After activation, the metabolism of $CD8^+$ T cells is reprogrammed, manifested by enhanced levels of the glycolytic flux. This enhancement in glycolysis attributes to the upregulation of Glut1 on $CD8^+$ T cells owing to AKT activation by CD28 co-signaling and TCR. The induction of MYC by AKT-dependent mTOR signaling can also trigger the glycolytic upregulation in $CD8^+$ T cells [189]. In oligodendrocyte precursor cells, the glucose uptake and lactate release were increased under high-glucose condition [190].

Glucose is transported into the cells by glucose transporters (Glut) [191]. Glut1 is strongly upregulated upon immune cell activation. Inhibition and loss of Glut1 hampered the proliferation and function of T cells [192]. For example, Glut1 expression is elevated in activated murine $CD4^+$ T cells to benefit glucose glycolysis [193]. In human T cells, it is reported that Glut1 is enhanced in beads-activated T cells. However, our results here showed that expression of Glut1 was not altered at protein level and even a slightly down-regulation at the mRNA level in HG-cultured CTLs. Our microarray data also supported that the Glut expression was not affected by HG. These results indicated that glucose transporters were unlikely responsive target proteins to HG-induced metabolic reprogramming in CTLs.

Of note, our microarray data show that apart from Glut1/SLC2A1, Glut3/SLC2A3, and Glut14/SLC2A14 are the predominantly expressing members among all known glucose

transporters. Glut3/SLC2A3 is shown an upregulation of mRNA level in an activation-dependent manner in human $CD4^+$ T cells, and is further increased when infection with HIV-1 [194]. Studies also suggested Glut3 play an essential role in the effector function of Th17 cells [195]. High expression of Glut3 in immune T cells indicate that Glut3 response to infection or inflammatory disease as a metabolic checkpoint. Glut14/SLC2A14 is related with inflammatory bowel disease [196]. And among immunotherapy with checkpoint inhibitor patients, Glut14 was significantly upregulated in responder patients' T-cell population [197]. These findings suggest that Glut 14 may function as a metabolomic biomarkers in inflammatory disease or immune checkpoint inhibitor therapy.

ROS, a set of derivatives molecular oxygen produced by a normal aerobic metabolism. ROS production is mainly harbored in mitochondria. High glucose triggered elevated level of ROS can lead to mitochondrial dysfunction [198]. Lactate, as a ROS generator, itself can influence the ROS production. In skeletal muscle, lactate-induced upregulation of ROS can lead to autophagy [199]. In addition, acute or chronic hyperglycemia in diabetes also increases ROS production and activates beta-cell apoptosis [117]. In keratinocytes, augmented ROS levels induced by a high glucose environment leads to mitochondrial dysfunction and apoptosis via stress signaling pathways [198]. High glucose exacerbates the pathogenesis of inflammation or autoimmunity, which is mediated by mitochondrial generated ROS in Th17 cells [200]. Our results here showed that HG could increase ROS production in CTLs. And treatment with H_2O_2 enhanced expression of TRAIL in NG-cultured CTLs.

Interestingly, inhibition of cytosolic ROS production of this process by NAC can significantly suppress TRAIL expression in HG-cultures CTLs. However, blockade of mitochondrial ROS by its scavengers did not influence TRAIL expression in CTLs. Taken together, these data demonstrate that cytosolic ROS rather than mitochondrial ROS is indeed involved in HG-induced TRAIL expression in CTLs. This suggests that Th17 cells and CTLs may use difference regulatory mechanisms to response the high glucose environment.

Interestingly, numerous studies have demonstrated that ROS, as an upstream regulator, could activate PI3K/AKT signaling pathway as well as NFκB pathway. In addition, it is reported that high glucose could also activate PI3K/Akt signaling pathway in vascular smooth muscle cells. Based on these findings, we investigate the regulation PI3K/Akt pathway on TRAIL expression in CTLs. We found that blockade of PI3K/AKT function by their corresponding inhibitors abrupted the HG-induced TRAIL expression in CTLs. For the downstream regulator of mTOR and NFκB, we also showed that inhibiting the mTOR and NFκB activity influenced the expression of TRAIL in HG-cultured CTLs. From these results, we can conclude that PI3K/AKT and NFκB pathway is involved in HG- upregulated TRAIL expression in CTLs.

Vitamin D has a close link with to the initial of insulin resistance in diabetes. Vitamin D reduces inflammation, which is involved in inducing insulin resistance [201]. In addition, vitamin D has an important effect on the functions of immune system. Epidemiological data show that vitamin D deficiency is linked to immune functioning deficits, such as an increasing risk of infection and a susceptibility to autoimmune

disease [147]. In particular, the vitamin D receptor which was induced by initial TCR signaling play an essential role in increasement of phospholipase gamma1, which plays a key role in the activation of T cells and the differentiation of Treg/T17 cell [202] [203]. Additionally, vitamin D speeds up the conversion of Th cells from proinflammatory to anti-inflammatory status by epigenetic remodeling [204]. Interestingly, vitamin D could also keep the elevated Ca^{2+} and ROS in a normal resting level during diabetes. Based on these findings above, we hypothesize that vitamin D could reduce the HG-enhanced expression of TRAIL by diminishing the ROS production in CTLs. Our results here demonstrated that the HG-enhanced TRAIL expression could be downregulated by vitamin D in a dose dependent manner. Remarkably, during my experiments, I noticed that CTLs harvested in winter were mostly sensitive to high glucose, whereas the responsive donors decreased in summer.

In addition, vitamin D is also linked to other autoimmune diseases like multiple sclerosis (MS) and Rheumatoid arthritis (RA) [205]. MS is a potentially disabling brain and spinal cord disease caused by the attacked protein myelin. And studies showed that there are multiple beneficial immunomodulatory effects of vitamin D supplementation on the MS patients [206]. RA mainly affects joints, resulted from your body's own tissues being attacked by your immune system. The prevalence of vitamin D deficiency in patients with RA is highly associated with disease severity [207]. Interestingly, TRAIL is also shown to be involved in progression of MS and RA [208] [209]. Our findings that vitamin D-regulated TRAIL expression in CTLs could play a role in ameliorating the progression of MS and RA.

Metformin, as we all know, is the first line medicine to treat Type 2 DM. Studies showed that addition of metformin could reduce insulin dose requirement in the insulin therapy for the adolescents, pediatrics with Type 2 DM [210]. Additionally, emerging evidence *in vivo* and *in vitro* suggest that metformin also has immune-modulatory properties, manifesting a powerful contributor to anticancer and antiaging features [211] [159]. For example, metformin enhances the antitumor efficiency of CTLs by blocking the inhibitory checkpoint of PD-L1 which expressed on the surface of tumor cells. Additionally, metformin has anti-aging effect by activating AMPK pathway which as a target for aging inhibition. In addition, *in vitro* experiments using MS-1 cell line reveal that metformin ameliorates HG-induced MS-1 cell injury by reducing oxidative stress, suppressing apoptosis and accelerating proliferation. And maybe this protective role of metformin is mediated through the activation of FXR [212]. Our work here demonstrated that metformin diminishes HG-induced upregulation of TRAIL in CTLs. The underlying mechanisms still need further investigation. mTOR, a well-defined target for metformin is excluded as inhibition of mTOR by rapamycin does not alter TRAIL expression in HG-CTLs. We postulate that ROS could be responsible as a molecule target for the regulation of metformin on TRAIL expression in CTLs. HG-induced ROS production promoted TRAIL expression in CTLs, and metformin could diminish this HG-enhanced TRAIL expression. The regulatory effect of metformin may mediate by inhibiting ROS production under HG conditions.

The impact of combination of vitamin D and metformin has been tested in many various scenarios. For example, combined use of vitamin D and metformin has chemo-

preventive functions for colorectal cancers in rat and mouse and maybe effective in treatment of patients with polycystic ovary syndrome. It is recently reported that in a mouse model of Type 2 DM, uncontrolled by metformin alone, additional vitamin D treatment could improve insulin sensitivity in skeletal muscles. Our findings demonstrate that combination of metformin and vitamin D down-regulate the HG-enhanced TRAIL expression in an additive manner. And we further found that combination of metformin and vitamin D could protect beta cell from TRAIL-mediated beta cell apoptosis. In addition, we also found the beneficial effects of metformin and vitamin D on the diabetic patients. To sum up, in my work, we discover a novel mechanism by which CTLs are involved in the progression of diabetes. It also establishes a new possible target of metformin and vitamin D treatment to protect beta cell from apoptosis.

There exist some drawbacks in our study. We listed them as follows: 1) We stimulated CTLs in medium with normal or high glucose for three days and TRAIL was upregulated in HG-cultured CTLs on day 3. We are not clear whether the HG-induced TRAIL expression is swift. To this end, we should test TRAIL expression after stimulation for 1 day and 2 days. 2) Whether HG-induced TRAIL upregulation in CTLs is stably maintained or transient after entering NG conditions. Blood glucose stability is important for Type 2 DM. Many factors influenced the stability of blood glucose such as age, sex, diet and diabetes history. Considering the unstable blood glucose, CTLs are much more prone to exposed to repeated fluctuations of glucose levels in their microenvironment. We therefore wondered whether the changes in CTL functions were

contingent on the acute presence of HG or NG or whether HG-induced TRAIL expression can be stably maintained when the cells enter NG microenvironments. To this end, we should subject CTLs that were stimulated in HG conditions to repeated restimulations in NG conditions. 3) HG-enhanced TRAIL expression in CTLs is regulated by ROS and PI3K/Akt/NFκB pathway, and metformin and vitamin D could diminish the TRAIL expression induced by HG. Based on these, whether metformin and vitamin D influence the PI3K/Akt/NFκB activity is unknown in this study. To examine this, we can test the PI3k activity using homogeneous time-resolved fluorescence (HTRF) and Akt activity by measuring Phosphorylation of the GSK-3α after stimulation of CTLs in presence of metformin and vitamin D for three days [213]. And for examination of NFκB activity, p-p65, p-IκBα, translocation of p65, and degradation of IκBα are all good markers for NFκB activation. 4) Our data found that TRAIL was increased in STZ-induced diabetic mice. *In vitro*, treatment of metformin and vitamin D could decrease the enhancement of TRAIL induced by HG in CTLs. However, due to the limitation of animal resource, we do not know whether metformin and vitamin D could have a similar effect on TRAIL regulation *in vivo*. This remains to be investigated. To this end, we can orally administer metformin and vitamin D to STZ-induced diabetic mice and test whether high blood glucose-induced TRAIL expression in diabetic mice can be ameliorated by metformin and vitamin D treatment, and whether metformin and vitamin D treatment can protect diabetic beta cell from apoptosis.

Our findings reported that high glucose levels can enhance CTL cytotoxicity. And it

provides new insights into how this is mediated. Our study show that high glucose levels lead to upregulation of TRAIL expression in CTLs and that promote enhanced apoptosis of pancreatic beta cells. The findings further show that ROS and the PI3K/Akt/NFκB axis is involved in the regulation of TRAIL expression. Metformin and vitamin D protect pancreatic beta cells from TRAIL-mediated apoptosis, which establish a potential benefit of to protect pancreatic beta cell of diabetic patients.

6. References

1. Netea, M.G., et al., *Innate and Adaptive Immune Memory: an Evolutionary Continuum in the Host's Response to Pathogens.* Cell Host Microbe, 2019. **25**(1): p. 13-26.
2. de Veer, M.J., J.M. Kemp, and E.N. Meeusen, *The innate host defence against nematode parasites.* Parasite Immunol, 2007. **29**(1): p. 1-9.
3. Zimmerman, L.M., L.A. Vogel, and R.M. Bowden, *Understanding the vertebrate immune system: insights from the reptilian perspective.* J Exp Biol, 2010. **213**(5): p. 661-71.
4. Riera Romo, M., D. Pérez-Martínez, and C. Castillo Ferrer, *Innate immunity in vertebrates: an overview.* Immunology, 2016. **148**(2): p. 125-39.
5. McInturff, J.E. and J. Kim, *The role of toll-like receptors in the pathophysiology of acne.* Semin Cutan Med Surg, 2005. **24**(2): p. 73-8.
6. Grubbs, H. and C.I. Kahwaji, *Physiology, Active Immunity*, in *StatPearls*. 2022, StatPearls Publishing Copyright © 2022, StatPearls Publishing LLC.: Treasure Island (FL).
7. Li, W., et al., *Roles of Mucosal Immunity against Mycobacterium tuberculosis Infection.* Tuberc Res Treat, 2012. **2012**: p. 791728.
8. Kalló, G., et al., *Chemical Barrier Proteins in Human Body Fluids.* Biomedicines, 2022. **10**(7).
9. Clark, G.J., et al., *The role of dendritic cells in the innate immune system.* Microbes and Infection, 2000. **2**(3): p. 257-272.
10. Geissmann, F., et al., *Development of monocytes, macrophages, and dendritic cells.* Science, 2010. **327**(5966): p. 656-61.
11. de Ruiter, K., et al., *A field-applicable method for flow cytometric analysis of granulocyte activation: Cryopreservation of fixed granulocytes.* Cytometry A, 2018. **93**(5): p. 540-547.
12. Hilligan, K.L. and F. Ronchese, *Antigen presentation by dendritic cells and their instruction of CD4+ T helper cell responses.* Cell Mol Immunol, 2020. **17**(6): p. 587-599.
13. Zhao, M., et al., *The Roles of Monocyte and Monocyte-Derived Macrophages in Common Brain Disorders.* Biomed Res Int, 2020. **2020**: p. 9396021.
14. Speer, C.P. and M. Gahr, *[The monocyte-macrophage system in the human].* Monatsschr Kinderheilkd, 1989. **137**(7): p. 390-5.
15. Hirayama, D., T. Iida, and H. Nakase, *The Phagocytic Function of Macrophage-Enforcing Innate Immunity and Tissue Homeostasis.* Int J Mol Sci, 2017. **19**(1).
16. Yunna, C., et al., *Macrophage M1/M2 polarization.* Eur J Pharmacol, 2020. **877**: p. 173090.
17. Gordon, S. and A. Plüddemann, *Tissue macrophages: heterogeneity and functions.* BMC Biol, 2017. **15**(1): p. 53.
18. Schuijs, M.J., H. Hammad, and B.N. Lambrecht, *Professional and 'Amateur' Antigen-Presenting Cells In Type 2 Immunity.* Trends Immunol, 2019. **40**(1): p. 22-34.

19. Roche, P.A. and K. Furuta, *The ins and outs of MHC class II-mediated antigen processing and presentation.* Nat Rev Immunol, 2015. **15**(4): p. 203-16.
20. Cooper, M.A., T.A. Fehniger, and M.A. Caligiuri, *The biology of human natural killer-cell subsets.* Trends Immunol, 2001. **22**(11): p. 633-40.
21. Myers, J.A. and J.S. Miller, *Exploring the NK cell platform for cancer immunotherapy.* Nat Rev Clin Oncol, 2021. **18**(2): p. 85-100.
22. Zwirner, N.W., C.I. Domaica, and M.B. Fuertes, *Regulatory functions of NK cells during infections and cancer.* J Leukoc Biol, 2021. **109**(1): p. 185-194.
23. Carnevalli, L.S., H. Ghadially, and S.T. Barry, *Therapeutic Approaches Targeting the Natural Killer-Myeloid Cell Axis in the Tumor Microenvironment.* Front Immunol, 2021. **12**: p. 633685.
24. Patra, T., R.B. Ray, and R. Ray, *Strategies to Circumvent Host Innate Immune Response by Hepatitis C Virus.* Cells, 2019. **8**(3).
25. Hubel, P., et al., *A protein-interaction network of interferon-stimulated genes extends the innate immune system landscape.* Nat Immunol, 2019. **20**(4): p. 493-502.
26. Chang, W.T., et al., *Spatiotemporal characterization of phagocytic NADPH oxidase and oxidative destruction of intraphagosomal organisms in vivo using autofluorescence imaging and Raman microspectroscopy.* J Am Chem Soc, 2010. **132**(6): p. 1744-5.
27. Bonilla, F.A. and H.C. Oettgen, *Adaptive immunity.* J Allergy Clin Immunol, 2010. **125**(2 Suppl 2): p. S33-40.
28. Mackay, C.R., W.L. Marston, and L. Dudler, *Naive and memory T cells show distinct pathways of lymphocyte recirculation.* J Exp Med, 1990. **171**(3): p. 801-17.
29. Huster, K.M., et al., *Selective expression of IL-7 receptor on memory T cells identifies early CD40L-dependent generation of distinct CD8+ memory T cell subsets.* Proc Natl Acad Sci U S A, 2004. **101**(15): p. 5610-5.
30. Joshi, N.S., et al., *Inflammation directs memory precursor and short-lived effector CD8(+) T cell fates via the graded expression of T-bet transcription factor.* Immunity, 2007. **27**(2): p. 281-95.
31. Homann, D., L. Teyton, and M.B. Oldstone, *Differential regulation of antiviral T-cell immunity results in stable CD8+ but declining CD4+ T-cell memory.* Nat Med, 2001. **7**(8): p. 913-9.
32. Razvi, E.S. and R.M. Welsh, *Programmed cell death of T lymphocytes during acute viral infection: a mechanism for virus-induced immune deficiency.* J Virol, 1993. **67**(10): p. 5754-65.
33. Murali-Krishna, K., et al., *Counting antigen-specific CD8 T cells: a reevaluation of bystander activation during viral infection.* Immunity, 1998. **8**(2): p. 177-87.
34. Devadiga, S., et al., *Dynamics of human B and T cell adaptive immune responses to Kyasanur Forest disease virus infection.* Sci Rep, 2020. **10**(1): p. 15306.
35. Dong, X., et al., *Discs large homolog 1 regulates B-cell proliferation and*

antibody production. Int Immunol, 2019. **31**(12): p. 759-770.
36. Koch, U. and F. Radtke, *Mechanisms of T cell development and transformation.* Annu Rev Cell Dev Biol, 2011. **27**: p. 539-62.
37. Yamano, T., et al., *Thymic B Cells Are Licensed to Present Self Antigens for Central T Cell Tolerance Induction.* Immunity, 2015. **42**(6): p. 1048-61.
38. Andersen, M.H., et al., *Cytotoxic T cells.* J Invest Dermatol, 2006. **126**(1): p. 32-41.
39. Fink, P.J. and M.J. Bevan, *Positive selection of thymocytes.* Adv Immunol, 1995. **59**: p. 99-133.
40. Hardardottir, F., J.L. Baron, and C.A. Janeway, Jr., *T cells with two functional antigen-specific receptors.* Proc Natl Acad Sci U S A, 1995. **92**(2): p. 354-8.
41. Sutherland, R.M., et al., *Cognate antigen engagement on parenchymal cells stimulates CD8(+) T cell proliferation in situ.* Nat Commun, 2017. **8**: p. 14809.
42. Petrova, G., A. Ferrante, and J. Gorski, *Cross-reactivity of T cells and its role in the immune system.* Crit Rev Immunol, 2012. **32**(4): p. 349-72.
43. Miceli, M.C. and J.R. Parnes, *The roles of CD4 and CD8 in T cell activation.* Semin Immunol, 1991. **3**(3): p. 133-41.
44. Li, Y., Y. Yin, and R.A. Mariuzza, *Structural and biophysical insights into the role of CD4 and CD8 in T cell activation.* Front Immunol, 2013. **4**: p. 206.
45. Clemente, T., et al., *In vivo assessment of specific cytotoxic T lymphocyte killing.* Methods, 2013. **61**(2): p. 105-9.
46. Jung, P., et al., *T cell stiffness is enhanced upon formation of immunological synapse.* Elife, 2021. **10**.
47. Zhao, R., et al., *Targeting the Microtubule-Network Rescues CTL Killing Efficiency in Dense 3D Matrices.* Front Immunol, 2021. **12**: p. 729820.
48. Yue, B., *Biology of the extracellular matrix: an overview.* J Glaucoma, 2014. **23**(8 Suppl 1): p. S20-3.
49. Jürgensen, H.J., et al., *Cellular uptake of collagens and implications for immune cell regulation in disease.* Cell Mol Life Sci, 2020. **77**(16): p. 3161-3176.
50. Najafi, M., B. Farhood, and K. Mortezaee, *Extracellular matrix (ECM) stiffness and degradation as cancer drivers.* J Cell Biochem, 2019. **120**(3): p. 2782-2790.
51. Salmon, H., et al., *Matrix architecture defines the preferential localization and migration of T cells into the stroma of human lung tumors.* J Clin Invest, 2012. **122**(3): p. 899-910.
52. Peng, D.H., et al., *Collagen promotes anti-PD-1/PD-L1 resistance in cancer through LAIR1-dependent CD8(+) T cell exhaustion.* Nat Commun, 2020. **11**(1): p. 4520.
53. Acuto, O. and D. Cantrell, *T cell activation and the cytoskeleton.* Annu Rev Immunol, 2000. **18**: p. 165-84.
54. Dupré, L., et al., *T Lymphocyte Migration: An Action Movie Starring the Actin and Associated Actors.* Front Immunol, 2015. **6**: p. 586.
55. Krummel, M.F., F. Bartumeus, and A. Gérard, *T cell migration, search strategies and mechanisms.* Nat Rev Immunol, 2016. **16**(3): p. 193-201.
56. Jacobelli, J., et al., *Confinement-optimized three-dimensional T cell amoeboid*

motility is modulated via myosin IIA-regulated adhesions. Nat Immunol, 2010. **11**(10): p. 953-61.
57. Schmidt, S. and P. Friedl, *Interstitial cell migration: integrin-dependent and alternative adhesion mechanisms.* Cell Tissue Res, 2010. **339**(1): p. 83-92.
58. Bromley, S.K., et al., *The immunological synapse.* Annu Rev Immunol, 2001. **19**: p. 375-96.
59. Trebak, M. and J.P. Kinet, *Calcium signalling in T cells.* Nat Rev Immunol, 2019. **19**(3): p. 154-169.
60. Zhou, X., et al., *A calcium optimum for cytotoxic T lymphocyte and natural killer cell cytotoxicity.* J Physiol, 2018. **596**(14): p. 2681-2698.
61. Kataoka, T., et al., *Estimation of pH and the number of lytic granules in a CD8+ CTL clone treated with an inhibitor of vacuolar type H(+)-ATPase concanamycin A.* Biosci Biotechnol Biochem, 1996. **60**(10): p. 1729-31.
62. Griffiths, G.M. and Y. Argon, *Structure and biogenesis of lytic granules.* Curr Top Microbiol Immunol, 1995. **198**: p. 39-58.
63. Clark, R. and G.M. Griffiths, *Lytic granules, secretory lysosomes and disease.* Curr Opin Immunol, 2003. **15**(5): p. 516-21.
64. Kurowska, M., et al., *Terminal transport of lytic granules to the immune synapse is mediated by the kinesin-1/Slp3/Rab27a complex.* Blood, 2012. **119**(17): p. 3879-89.
65. Krzewski, K., et al., *LAMP1/CD107a is required for efficient perforin delivery to lytic granules and NK-cell cytotoxicity.* Blood, 2013. **121**(23): p. 4672-83.
66. Pattu, V., et al., *In the crosshairs: investigating lytic granules by high-resolution microscopy and electrophysiology.* Front Immunol, 2013. **4**: p. 411.
67. Traore, D.A., et al., *Defining the interaction of perforin with calcium and the phospholipid membrane.* Biochem J, 2013. **456**(3): p. 323-35.
68. Stewart, S.E., et al., *Analysis of Perforin Assembly by Quartz Crystal Microbalance Reveals a Role for Cholesterol and Calcium-independent Membrane Binding.* J Biol Chem, 2015. **290**(52): p. 31101-12.
69. Smyth, M.J., et al., *Unlocking the secrets of cytotoxic granule proteins.* J Leukoc Biol, 2001. **70**(1): p. 18-29.
70. Trapani, J.A., *Granzymes: a family of lymphocyte granule serine proteases.* Genome Biol, 2001. **2**(12): p. Reviews3014.
71. Zeglinski, M.R. and D.J. Granville, *Granzymes in cardiovascular injury and disease.* Cell Signal, 2020. **76**: p. 109804.
72. Lieberman, J. and Z. Fan, *Nuclear war: the granzyme A-bomb.* Curr Opin Immunol, 2003. **15**(5): p. 553-9.
73. Masson, D., M. Zamai, and J. Tschopp, *Identification of granzyme A isolated from cytotoxic T-lymphocyte-granules as one of the proteases encoded by CTL-specific genes.* FEBS Lett, 1986. **208**(1): p. 84-8.
74. Nakajima, H., H.L. Park, and P.A. Henkart, *Synergistic roles of granzymes A and B in mediating target cell death by rat basophilic leukemia mast cell tumors also expressing cytolysin/perforin.* J Exp Med, 1995. **181**(3): p. 1037-46.
75. Velotti, F., et al., *Granzyme B in Inflammatory Diseases: Apoptosis,*

Inflammation, Extracellular Matrix Remodeling, Epithelial-to-Mesenchymal Transition and Fibrosis. Front Immunol, 2020. **11**: p. 587581.

76. Trapani, J.A., et al., *Perforin-dependent nuclear entry of granzyme B precedes apoptosis, and is not a consequence of nuclear membrane dysfunction.* Cell Death Differ, 1998. **5**(6): p. 488-96.
77. Lord, S.J., et al., *Granzyme B: a natural born killer.* Immunol Rev, 2003. **193**: p. 31-8.
78. Lee, J., et al., *Fas Ligand localizes to intraluminal vesicles within NK cell cytolytic granules and is enriched at the immune synapse.* Immun Inflamm Dis, 2018. **6**(2): p. 312-321.
79. Strasser, A., P.J. Jost, and S. Nagata, *The many roles of FAS receptor signaling in the immune system.* Immunity, 2009. **30**(2): p. 180-92.
80. Volpe, E., et al., *Fas-Fas Ligand: Checkpoint of T Cell Functions in Multiple Sclerosis.* Front Immunol, 2016. **7**: p. 382.
81. Jacquemin, G., S. Shirley, and O. Micheau, *Combining naturally occurring polyphenols with TNF-related apoptosis-inducing ligand: a promising approach to kill resistant cancer cells?* Cell Mol Life Sci, 2010. **67**(18): p. 3115-30.
82. Kichev, A., et al., *Tumor necrosis factor-related apoptosis-inducing ligand (TRAIL) signaling and cell death in the immature central nervous system after hypoxia-ischemia and inflammation.* J Biol Chem, 2014. **289**(13): p. 9430-9.
83. Ehrlich, S., et al., *Regulation of soluble and surface-bound TRAIL in human T cells, B cells, and monocytes.* Cytokine, 2003. **24**(6): p. 244-53.
84. Naval, J., et al., *Importance of TRAIL Molecular Anatomy in Receptor Oligomerization and Signaling. Implications for Cancer Therapy.* Cancers (Basel), 2019. **11**(4).
85. Szliszka, E., et al., *Targeting death receptor TRAIL-R2 by chalcones for TRAIL-induced apoptosis in cancer cells.* Int J Mol Sci, 2012. **13**(11): p. 15343-59.
86. Meng, R.D., et al., *The TRAIL decoy receptor TRUNDD (DcR2, TRAIL-R4) is induced by adenovirus-p53 overexpression and can delay TRAIL-, p53-, and KILLER/DR5-dependent colon cancer apoptosis.* Mol Ther, 2000. **1**(2): p. 130-44.
87. Ning, Q., et al., *TNF related apoptosis-inducing ligand and its receptors in ocular tumors.* Int J Ophthalmol, 2011. **4**(5): p. 552-7.
88. Johnstone, R.W., A.J. Frew, and M.J. Smyth, *The TRAIL apoptotic pathway in cancer onset, progression and therapy.* Nat Rev Cancer, 2008. **8**(10): p. 782-98.
89. Zhong, H.H., et al., *TRAIL-based gene delivery and therapeutic strategies.* Acta Pharmacol Sin, 2019. **40**(11): p. 1373-1385.
90. Palacios, C., et al., *The long and winding road to cancer treatment: the TRAIL system.* Curr Pharm Des, 2014. **20**(17): p. 2819-33.
91. Vaccarezza, M., G. Delbello, and G. Zauli, *A role of the TRAIL-TRAIL receptor system in the pathogenesis of diabetes.* Acta Biomed, 2007. **78 Suppl 1**: p. 262-7.
92. Lorz, C., et al., *The death ligand TRAIL in diabetic nephropathy.* J Am Soc

Nephrol, 2008. **19**(5): p. 904-14.
93. Lorz, C., et al., *Trail and kidney disease.* Front Biosci (Landmark Ed), 2009. **14**(10): p. 3740-9.
94. Forde, H., et al., *Serum OPG/TRAIL ratio predicts the presence of cardiovascular disease in people with type 2 diabetes mellitus.* Diabetes Res Clin Pract, 2022. **189**: p. 109936.
95. Wang, X., et al., *Role of Glucose Transporters in Drug Membrane Transport.* Curr Drug Metab, 2020. **21**(12): p. 947-958.
96. Wilde, L., et al., *Metabolic coupling and the Reverse Warburg Effect in cancer: Implications for novel biomarker and anticancer agent development.* Semin Oncol, 2017. **44**(3): p. 198-203.
97. Chapman, N.M., S. Shrestha, and H. Chi, *Metabolism in Immune Cell Differentiation and Function.* Adv Exp Med Biol, 2017. **1011**: p. 1-85.
98. Zhao, L., et al., *Reversal of Abnormal CD4+ T Cell Metabolism Alleviates Thyroiditis by Deactivating the mTOR/HIF1a/Glycolysis Pathway.* Front Endocrinol (Lausanne), 2021. **12**: p. 659738.
99. Yin, Y., et al., *Glucose Oxidation Is Critical for CD4+ T Cell Activation in a Mouse Model of Systemic Lupus Erythematosus.* J Immunol, 2016. **196**(1): p. 80-90.
100. Hamaidi, I. and S. Kim, *Sirtuins are crucial regulators of T cell metabolism and functions.* Exp Mol Med, 2022. **54**(3): p. 207-215.
101. Chang, C.H., et al., *Posttranscriptional control of T cell effector function by aerobic glycolysis.* Cell, 2013. **153**(6): p. 1239-51.
102. Ho, P.C., et al., *Phosphoenolpyruvate Is a Metabolic Checkpoint of Anti-tumor T Cell Responses.* Cell, 2015. **162**(6): p. 1217-28.
103. Lunt, S.Y. and M.G. Vander Heiden, *Aerobic glycolysis: meeting the metabolic requirements of cell proliferation.* Annu Rev Cell Dev Biol, 2011. **27**: p. 441-64.
104. Zhu, J., et al., *High Glucose Enhances Cytotoxic T Lymphocyte-Mediated Cytotoxicity.* Front Immunol, 2021. **12**: p. 689337.
105. Zou, H., et al., *High glucose distinctively regulates Ca(2+) influx in cytotoxic T lymphocytes upon target recognition and thapsigargin stimulation.* Eur J Immunol, 2020. **50**(12): p. 2095-2098.
106. Lushchak, V.I., *FREE RADICALS, REACTIVE OXYGEN SPECIES, OXIDATIVE STRESSES AND THEIR CLASSIFICATIONS.* Ukr Biochem J, 2015. **87**(6): p. 11-8.
107. Weinberg, F., et al., *Mitochondrial metabolism and ROS generation are essential for Kras-mediated tumorigenicity.* Proc Natl Acad Sci U S A, 2010. **107**(19): p. 8788-93.
108. Magnani, F. and A. Mattevi, *Structure and mechanisms of ROS generation by NADPH oxidases.* Curr Opin Struct Biol, 2019. **59**: p. 91-97.
109. D'Autréaux, B. and M.B. Toledano, *ROS as signalling molecules: mechanisms that generate specificity in ROS homeostasis.* Nat Rev Mol Cell Biol, 2007. **8**(10): p. 813-24.

110. Velarde, M.C., et al., *Mitochondrial oxidative stress caused by Sod2 deficiency promotes cellular senescence and aging phenotypes in the skin.* Aging (Albany NY), 2012. **4**(1): p. 3-12.
111. Redza-Dutordoir, M. and D.A. Averill-Bates, *Activation of apoptosis signalling pathways by reactive oxygen species.* Biochim Biophys Acta, 2016. **1863**(12): p. 2977-2992.
112. Jakubczyk, K., et al., *Reactive oxygen species - sources, functions, oxidative damage.* Pol Merkur Lekarski, 2020. **48**(284): p. 124-127.
113. Valko, M., et al., *Free radicals and antioxidants in normal physiological functions and human disease.* Int J Biochem Cell Biol, 2007. **39**(1): p. 44-84.
114. Bowler, R.P. and J.D. Crapo, *Oxidative stress in allergic respiratory diseases.* J Allergy Clin Immunol, 2002. **110**(3): p. 349-56.
115. Takahashi, K., et al., *Effect of Oxidative Stress on Cardiovascular System in Response to Gravity.* Int J Mol Sci, 2017. **18**(7).
116. Salim, S., *Oxidative Stress and the Central Nervous System.* J Pharmacol Exp Ther, 2017. **360**(1): p. 201-205.
117. Volpe, C.M.O., et al., *Cellular death, reactive oxygen species (ROS) and diabetic complications.* Cell Death Dis, 2018. **9**(2): p. 119.
118. Ceriello, A., *New insights on oxidative stress and diabetic complications may lead to a "causal" antioxidant therapy.* Diabetes Care, 2003. **26**(5): p. 1589-96.
119. Chen, X., et al., *Reactive Oxygen Species Regulate T Cell Immune Response in the Tumor Microenvironment.* Oxid Med Cell Longev, 2016. **2016**: p. 1580967.
120. Yang, Y., et al., *Reactive oxygen species in the immune system.* Int Rev Immunol, 2013. **32**(3): p. 249-70.
121. Chaudhri, G., et al., *Effect of antioxidants on primary alloantigen-induced T cell activation and proliferation.* J Immunol, 1986. **137**(8): p. 2646-52.
122. Sapra, A. and P. Bhandari, *Diabetes Mellitus*, in *StatPearls*. 2022, StatPearls Publishing Copyright © 2022, StatPearls Publishing LLC.: Treasure Island (FL).
123. Majid, U. and C. Argáez, *CADTH Rapid Response Reports*, in *Off-Loading Devices for People with Diabetic Neuropathic Foot Ulcers: A Rapid Qualitative Review*. 2020, Canadian Agency for Drugs and Technologies in Health
Copyright © 2020 Canadian Agency for Drugs and Technologies in Health.: Ottawa (ON).
124. Makaryus, A.N. and S.I. McFarlane, *Diabetes insipidus: diagnosis and treatment of a complex disease.* Cleve Clin J Med, 2006. **73**(1): p. 65-71.
125. Davies, T.T., et al., *Diabetes prevalence among older people receiving care at home: associations with symptoms, health status and psychological well-being.* Diabet Med, 2019. **36**(1): p. 96-104.
126. Dambha-Miller, H., et al., *Behaviour change, weight loss and remission of Type 2 diabetes: a community-based prospective cohort study.* Diabet Med, 2020. **37**(4): p. 681-688.
127. Thummadi, N.B., et al., *A graph centrality-based approach for candidate gene prediction for type 1 diabetes.* Immunol Res, 2021. **69**(5): p. 422-428.
128. Willcox, A., et al., *Analysis of islet inflammation in human type 1 diabetes.* Clin

Exp Immunol, 2009. **155**(2): p. 173-81.
129. Wicker, L.S., et al., *Type 1 diabetes genes and pathways shared by humans and NOD mice.* J Autoimmun, 2005. **25 Suppl**: p. 29-33.
130. Gagnerault, M.C., et al., *Pancreatic lymph nodes are required for priming of beta cell reactive T cells in NOD mice.* J Exp Med, 2002. **196**(3): p. 369-77.
131. Kurts, C., et al., *Constitutive class I-restricted exogenous presentation of self antigens in vivo.* J Exp Med, 1996. **184**(3): p. 923-30.
132. Le Saout, C., et al., *Memory-like CD8+ and CD4+ T cells cooperate to break peripheral tolerance under lymphopenic conditions.* Proc Natl Acad Sci U S A, 2008. **105**(49): p. 19414-9.
133. Hernández, J., et al., *Uncoupling of proliferative potential and gain of effector function by CD8(+) T cells responding to self-antigens.* J Exp Med, 2002. **196**(3): p. 323-33.
134. Coppieters, K., N. Amirian, and M. von Herrath, *Intravital imaging of CTLs killing islet cells in diabetic mice.* J Clin Invest, 2012. **122**(1): p. 119-31.
135. Unger, W.W., et al., *Islet-specific CTL cloned from a type 1 diabetes patient cause beta-cell destruction after engraftment into HLA-A2 transgenic NOD/scid/IL2RG null mice.* PLoS One, 2012. **7**(11): p. e49213.
136. Fousteri, G., et al., *Beta-cell Specific Autoantibodies: Are they Just an Indicator of Type 1 Diabetes?* Curr Diabetes Rev, 2017. **13**(3): p. 322-329.
137. Shirakawa, K., et al., *Obesity accelerates T cell senescence in murine visceral adipose tissue.* J Clin Invest, 2016. **126**(12): p. 4626-4639.
138. Navarro, J.F. and C. Mora, *Diabetes, inflammation, proinflammatory cytokines, and diabetic nephropathy.* ScientificWorldJournal, 2006. **6**: p. 908-17.
139. Abouzeid, S. and N. Sherif, *Role of alteration in Treg/Th17 cells' balance in nephropathic patients with Type 2 diabetes mellitus.* Electron Physician, 2015. **7**(8): p. 1613-8.
140. Kumar, N.P., et al., *Type 2 diabetes mellitus is associated with altered CD8(+) T and natural killer cell function in pulmonary tuberculosis.* Immunology, 2015. **144**(4): p. 677-86.
141. Bouillon, R., *How much vitamin D is needed for healthy bones?* J Intern Med, 2017. **282**(5): p. 461-464.
142. Urena-Torres, P. and J.C. Souberbielle, *Pharmacologic role of vitamin D natural products.* Curr Vasc Pharmacol, 2014. **12**(2): p. 278-85.
143. Zhang, Y., et al., *Association between vitamin D supplementation and mortality: systematic review and meta-analysis.* Bmj, 2019. **366**: p. l4673.
144. Chau, Y.Y. and J. Kumar, *Vitamin D in chronic kidney disease.* Indian J Pediatr, 2012. **79**(8): p. 1062-8.
145. Rutjes, A.W., et al., *Vitamin and mineral supplementation for maintaining cognitive function in cognitively healthy people in mid and late life.* Cochrane Database Syst Rev, 2018. **12**(12): p. Cd011906.
146. Charoenngam, N. and M.F. Holick, *Immunologic Effects of Vitamin D on Human Health and Disease.* Nutrients, 2020. **12**(7).
147. Aranow, C., *Vitamin D and the immune system.* J Investig Med, 2011. **59**(6): p.

881-6.
148. Martens, P.J., et al., *Vitamin D's Effect on Immune Function.* Nutrients, 2020. **12**(5).
149. Schardey, J., et al., *Vitamin D Inhibits Pro-Inflammatory T Cell Function in Patients With Inflammatory Bowel Disease.* J Crohns Colitis, 2019. **13**(12): p. 1546-1557.
150. Sheikh, V., et al., *Vitamin D3 inhibits the proliferation of T helper cells, downregulate CD4(+) T cell cytokines and upregulate inhibitory markers.* Hum Immunol, 2018. **79**(6): p. 439-445.
151. Vyas, S.P. and R. Goswami, *Calcitriol and Retinoic acid antagonize each other to suppress the production of IL-9 by Th9 cells.* J Nutr Biochem, 2021. **96**: p. 108788.
152. Vieira, I.H., D. Rodrigues, and I. Paiva, *Vitamin D and Autoimmune Thyroid Disease-Cause, Consequence, or a Vicious Cycle?* Nutrients, 2020. **12**(9).
153. Infante, M., et al., *Influence of Vitamin D on Islet Autoimmunity and Beta-Cell Function in Type 1 Diabetes.* Nutrients, 2019. **11**(9).
154. Starchl, C., M. Scherkl, and K. Amrein, *Celiac Disease and the Thyroid: Highlighting the Roles of Vitamin D and Iron.* Nutrients, 2021. **13**(6).
155. Bailey, C.J., *Metformin: historical overview.* Diabetologia, 2017. **60**(9): p. 1566-1576.
156. Pan, Q., et al., *Metformin: the updated protective property in kidney disease.* Aging (Albany NY), 2020. **12**(9): p. 8742-8759.
157. Driver, C., et al., *Cardioprotective Effects of Metformin.* J Cardiovasc Pharmacol, 2018. **72**(2): p. 121-127.
158. Ashinuma, H., et al., *Antiproliferative action of metformin in human lung cancer cell lines.* Oncol Rep, 2012. **28**(1): p. 8-14.
159. Podhorecka, M., B. Ibanez, and A. Dmoszyńska, *Metformin - its potential anti-cancer and anti-aging effects.* Postepy Hig Med Dosw (Online), 2017. **71**(0): p. 170-175.
160. Chen, X., et al., *Immunomodulatory and Antiviral Activity of Metformin and Its Potential Implications in Treating Coronavirus Disease 2019 and Lung Injury.* Front Immunol, 2020. **11**: p. 2056.
161. Ursini, F., et al., *Metformin and Autoimmunity: A "New Deal" of an Old Drug.* Front Immunol, 2018. **9**: p. 1236.
162. Sun, Y., et al., *Metformin ameliorates the development of experimental autoimmune encephalomyelitis by regulating T helper 17 and regulatory T cells in mice.* J Neuroimmunol, 2016. **292**: p. 58-67.
163. Fan, K.J., et al., *Metformin inhibits inflammation and bone destruction in collagen-induced arthritis in rats.* Ann Transl Med, 2020. **8**(23): p. 1565.
164. Qu, B., et al., *Docking of lytic granules at the immunological synapse in human CTL requires Vti1b-dependent pairing with CD3 endosomes.* J Immunol, 2011. **186**(12): p. 6894-904.
165. Bhat, S.S., et al., *Syntaxin 8 is required for efficient lytic granule trafficking in cytotoxic T lymphocytes.* Biochim Biophys Acta, 2016. **1863**(7 Pt A): p. 1653-

64.
166. Alter, G., J.M. Malenfant, and M. Altfeld, *CD107a as a functional marker for the identification of natural killer cell activity.* J Immunol Methods, 2004. **294**(1-2): p. 15-22.
167. Lorenzo-Herrero, S., et al., *CD107a Degranulation Assay to Evaluate Immune Cell Antitumor Activity.* Methods Mol Biol, 2019. **1884**: p. 119-130.
168. Elshal, M.F. and J.P. McCoy, *Multiplex bead array assays: performance evaluation and comparison of sensitivity to ELISA.* Methods, 2006. **38**(4): p. 317-23.
169. Lombardelli, L., et al., *Evaluation of Secreted Cytokines by Multiplex Bead-Based Assay (X MAP Technology, Luminex).* Methods Mol Biol, 2021. **2285**: p. 121-130.
170. Kim, Y. and D.W. Seol, *TRAIL, a mighty apoptosis inducer.* Mol Cells, 2003. **15**(3): p. 283-93.
171. Hull, R.L., et al., *High fat feeding unmasks variable insulin responses in male C57BL/6 mouse substrains.* J Endocrinol, 2017. **233**(1): p. 53-64.
172. Yang, W., et al., *Unspecific CTL Killing Is Enhanced by High Glucose via TNF-Related Apoptosis-Inducing Ligand.* Front Immunol, 2022. **13**: p. 831680.
173. Ou, D., et al., *TNF-related apoptosis-inducing ligand death pathway-mediated human beta-cell destruction.* Diabetologia, 2002. **45**(12): p. 1678-88.
174. Figueiredo, V.C., J.F. Markworth, and D. Cameron-Smith, *Considerations on mTOR regulation at serine 2448: implications for muscle metabolism studies.* Cell Mol Life Sci, 2017. **74**(14): p. 2537-2545.
175. Eruslanov, E. and S. Kusmartsev, *Identification of ROS using oxidized DCFDA and flow-cytometry.* Methods Mol Biol, 2010. **594**: p. 57-72.
176. Jo, E.S., et al., *Sulfur Compounds Inhibit High Glucose-Induced Inflammation by Regulating NF-κB Signaling in Human Monocytes.* Molecules, 2020. **25**(10).
177. Balwani, S., et al., *Regulation of NF-κB activation through a novel PI-3K-independent and PKA/Akt-dependent pathway in human umbilical vein endothelial cells.* PLoS One, 2012. **7**(10): p. e46528.
178. Jamka, M., et al., *The effect of vitamin D supplementation on insulin and glucose metabolism in overweight and obese individuals: systematic review with meta-analysis.* Sci Rep, 2015. **5**: p. 16142.
179. H, P., et al., *The impact of Vitamin D Replacement on Glucose Metabolism.* Pak J Med Sci, 2013. **29**(6): p. 1311-4.
180. Wei, Z., et al., *Vitamin D Switches BAF Complexes to Protect β Cells.* Cell, 2018. **173**(5): p. 1135-1149.e15.
181. Maddaloni, E., et al., *Vitamin D and Diabetes Mellitus.* Front Horm Res, 2018. **50**: p. 161-176.
182. Ferreira, G.B., et al., *Vitamin D3 Induces Tolerance in Human Dendritic Cells by Activation of Intracellular Metabolic Pathways.* Cell Rep, 2015. **10**(5): p. 711-725.
183. Gorchs, L., et al., *The vitamin D analogue calcipotriol promotes an anti-tumorigenic phenotype of human pancreatic CAFs but reduces T cell mediated*

immunity. Sci Rep, 2020. **10**(1): p. 17444.
184. Bajnok, A., et al., *The Distribution of Activation Markers and Selectins on Peripheral T Lymphocytes in Preeclampsia.* Mediators Inflamm, 2017. **2017**: p. 8045161.
185. Cibrián, D. and F. Sánchez-Madrid, *CD69: from activation marker to metabolic gatekeeper.* Eur J Immunol, 2017. **47**(6): p. 946-953.
186. Yang, S., et al., *The shedding of CD62L (L-selectin) regulates the acquisition of lytic activity in human tumor reactive T lymphocytes.* PLoS One, 2011. **6**(7): p. e22560.
187. Schumann, J., et al., *Differences in CD44 Surface Expression Levels and Function Discriminates IL-17 and IFN-γ Producing Helper T Cells.* PLoS One, 2015. **10**(7): p. e0132479.
188. Harith, H.H., M.J. Morris, and M.M. Kavurma, *On the TRAIL of obesity and diabetes.* Trends Endocrinol Metab, 2013. **24**(11): p. 578-87.
189. Gupta, S.S., J. Wang, and M. Chen, *Metabolic Reprogramming in CD8(+) T Cells During Acute Viral Infections.* Front Immunol, 2020. **11**: p. 1013.
190. da Rosa, P.M., et al., *High-glucose medium induces cellular differentiation and changes in metabolic functionality of oligodendroglia.* Mol Biol Rep, 2019. **46**(5): p. 4817-4826.
191. Thorens, B. and M. Mueckler, *Glucose transporters in the 21st Century.* Am J Physiol Endocrinol Metab, 2010. **298**(2): p. E141-5.
192. Zezina, E., et al., *Glucose transporter 1 in rheumatoid arthritis and autoimmunity.* Wiley Interdiscip Rev Syst Biol Med, 2020. **12**(4): p. e1483.
193. Macintyre, A.N., et al., *The glucose transporter Glut1 is selectively essential for CD4 T cell activation and effector function.* Cell Metab, 2014. **20**(1): p. 61-72.
194. Song, W., et al., *Solute carrier transporters: the metabolic gatekeepers of immune cells.* Acta Pharm Sin B, 2020. **10**(1): p. 61-78.
195. Hochrein, S.M., et al., *The glucose transporter GLUT3 controls T helper 17 cell responses through glycolytic-epigenetic reprogramming.* Cell Metab, 2022. **34**(4): p. 516-532.e11.
196. Amir Shaghaghi, M., et al., *The SLC2A14 gene, encoding the novel glucose/dehydroascorbate transporter GLUT14, is associated with inflammatory bowel disease.* Am J Clin Nutr, 2017. **106**(6): p. 1508-1513.
197. Triozzi, P.L., et al., *Circulating Immune Bioenergetic, Metabolic, and Genetic Signatures Predict Melanoma Patients' Response to Anti-PD-1 Immune Checkpoint Blockade.* Clin Cancer Res, 2022. **28**(6): p. 1192-1202.
198. Rizwan, H., et al., *High glucose augments ROS generation regulates mitochondrial dysfunction and apoptosis via stress signalling cascades in keratinocytes.* Life Sci, 2020. **241**: p. 117148.
199. Nikooie, R., D. Moflehi, and S. Zand, *Lactate regulates autophagy through ROS-mediated activation of ERK1/2/m-TOR/p-70S6K pathway in skeletal muscle.* J Cell Commun Signal, 2021. **15**(1): p. 107-123.
200. Zhang, D., et al., *High Glucose Intake Exacerbates Autoimmunity through Reactive-Oxygen-Species-Mediated TGF-β Cytokine Activation.* Immunity,

2019. **51**(4): p. 671-681.e5.
201. Berridge, M.J., *Vitamin D deficiency and diabetes.* Biochem J, 2017. **474**(8): p. 1321-1332.
202. von Essen, M.R., et al., *Vitamin D controls T cell antigen receptor signaling and activation of human T cells.* Nat Immunol, 2010. **11**(4): p. 344-9.
203. Zhou, Q., et al., *1,25(OH)(2)D(3) induces regulatory T cell differentiation by influencing the VDR/PLC-γ1/TGF-β1/pathway.* Mol Immunol, 2017. **91**: p. 156-164.
204. Chauss, D., et al., *Autocrine vitamin D signaling switches off pro-inflammatory programs of T(H)1 cells.* Nat Immunol, 2022. **23**(1): p. 62-74.
205. Miteva, M.Z., et al., *Vitamin D and Autoimmune Thyroid Diseases - a Review.* Folia Med (Plovdiv), 2020. **62**(2): p. 223-229.
206. Pierrot-Deseilligny, C. and J.C. Souberbielle, *Vitamin D and multiple sclerosis: An update.* Mult Scler Relat Disord, 2017. **14**: p. 35-45.
207. Sukharani, N., et al., *Association Between Rheumatoid Arthritis and Serum Vitamin D Levels.* Cureus, 2021. **13**(9): p. e18255.
208. Zai-Xing, Y., et al., *Preliminary clinical measurement of the expression of TNF-related apoptosis inducing ligand in patients with ankylosing spondylitis.* J Clin Lab Anal, 2008. **22**(2): p. 138-45.
209. Remuzgo-Martínez, S., et al., *Expression of osteoprotegerin and its ligands, RANKL and TRAIL, in rheumatoid arthritis.* Sci Rep, 2016. **6**: p. 29713.
210. Pagano, G., et al., *Metformin reduces insulin requirement in Type 1 (insulin-dependent) diabetes.* Diabetologia, 1983. **24**(5): p. 351-4.
211. Ma, R., et al., *Metformin and cancer immunity.* Acta Pharmacol Sin, 2020. **41**(11): p. 1403-1409.
212. Zou, W., et al., *Metformin attenuates high glucose-induced injury in islet microvascular endothelial cells.* Bioengineered, 2022. **13**(2): p. 4385-4396.
213. Sugita, H., et al., *A new evaluation method for quantifying PI3K activity by HTRF assay.* Biochem Biophys Res Commun, 2008. **377**(3): p. 941-5.

7. Publications

1. **Yang W**, Denger A, Diener C, Küppers F, Soriano-Baguet L, Schäfer G, Yanamandra AK, Zhao R, Knörck A, Schwarz EC, Hart M, Lammert F, Prates Roma L, Brenner D, Christidis G, Helms V, Meese E, Hoth M, Qu B. Unspecific CTL Killing Is Enhanced by High Glucose *via* TNF-Related Apoptosis-Inducing Ligand. *Frontiers in immunology.* **2022***, 13*, 831680.

2. Zhu J‡, **Yang W**†, Zhou X, Zöphel D, Soriano-Baguet L, Dolgener D, Carlein C, Hof C, Zhao R, Ye S, Schwarz EC, Brenner D, Prates Roma L, Qu B. High glucose Enhances Cytotoxic T lymphocyte-mediated Cytotoxicity. *Frontiers in immunology.* **2021***, 12*, 689337. (†**Equal contribution**)

3. Zhao R, Zhou X, Khan ES, Alansary D, Friedmann KS, **Yang W**, Schwarz EC, Del Campo A, Hoth M, Qu B. Targeting the microtubule-network rescues CTL killing efficiency in dense 3D matrices. *Frontiers in immunology.* **2021**, *12*, 729820.

4. Liu Y, Zhao R, Reda B, **Yang W**, Hannig M, Qu B. Profiling of cytokines, chemokines and growth factors in saliva and gingival crevicular fluid. *Cytokine.* **2021**, *142*, 155504.

5. Zou H, Yang W, Schwär G, Zhao R, Alansary D, Yin D, Schwarz EC, Niemeyer BA, Qu B. High glucose distinctively regulates Ca^{2+} influx in cytotoxic T lymphocytes upon target recognition and thapsigargin stimulation. *European Journal of Immunology.* **2020***, 50*, 2095-2098.

8. Acknowledgements

My sincere and hearty thanks go firstly to my supervisor Dr. Bin Qu for her constant guidance and help. Looking back on the past few years during my Ph.D. period, many scenes are still vivid in my mind. First of all, in terms of topics and academic guidance, I remember that from the moment I came to the lab, Dr. Qu taught us the relevant knowledge of immunology, taught us how to be a qualified scientific researcher and how to ensure the rigor of the experiment. During the Ph.D. period, Dr. Qu's support, encouragement, and spirit of exploration on the subject deeply touched me. When the subject encountered difficulties, Dr. Qu always encouraged us to made more persistence and tried different methods. Dr. Qu not only helped me a lot academically, but also cared deeply for our daily life. I remember that when I first arrived in Germany, Mr. Qu did his best to help in renting a house, applying for bank cards and telephone cards, and all kinds of trivial matters in life. In addition, Dr. Qu also gave us a lot of guidance in English learning. In short, without the guidance and support of Dr. Qu, the project and my thesis would not have been completed so quickly, and I would not have grown so fast.

My sincere appreciation also goes to another supervisor Prof. Dr. Markus Hoth for the constant supporting and guidance. As a supervisor, he is always being motivated, supportive, and encouraging. Dr. Hoth gave me kind encouragement and useful instruction all through my writing. Without his consistent supports, patience and guidance, my dissertation will not reach its current state.

I would like sincerely to express my thanks to Dr. Eva Schwarz, who is always

supportive and encouraging. She always keeps our lab work well.

My acknowledgements also go to the group of cell isolation and culture team, with special thanks to Carmen Haessig, Gertrud Schwaer, Cora Hoxha. My thanks also extend to our colleague Renping Zhao, Xiangda Zhou, Arne Knoerck and our secretary Regine Kaleja.

I am also grateful to our collaborators Prof. Dr. Leticia Prates Roma who support the diabetic mouse model. My sincere thanks also go to the microarray analysis group Andreas Denger, Caroline Diener, Martin Hart and Volhard Helms. I also express my appreciation to seahorse assay group Leticia Soriano-Baguet and Dirk Brenner. My cordial thanks also go to Frederic Kuppers and Grigorios Christidis who collected blood samples from diabetic patients and healthy individuals.

And finally, my warm gratitude also goes to my family and my friends who gave me much encouragement and financial support on my way to study.